State-to-State Vibrational Transfer in Atom–Molecule Collisions. Beams vs. Bulbs

DOUGLAS J. KRAJNOVICH and CHARLES S. PARMENTER*†

Department of Chemistry, Indiana University, Bloomington, Indiana 47405

DAVID L. CATLETT, JR.

Department of Chemistry, University of Minnesota, Minneapolis, Minnesota 55455

Received June 16, 1986 (Revised Manuscript Received October 6, 1986)

Contents

I. Introduction

By the standards of publication activity, interest in gas phase collisional vibrational energy transfer has been overwhelmingly on the side of 300 K thermal systems as opposed to the more precisely defined conditions of crossed molecular beams. The cause is elementary. With relatively small cross sections, vibrationally inelastic scattering has proven hard to follow at the low collision frequencies attainable in beams. The thermal vibrational relaxation studies, which we shall call "bulb" experiments, are by comparison easily accessible, even to the experimentalist only modestly equipped with laser excitation and suitable detection apparatus.

Historically, beam and bulb experimentalists have tended to represent almost separate cultures because of the wide distinctions between the experimental techniques, the molecular systems accessible for study, and the level of detail sought. Even the language of these workers is symptomatic of the separation. Beam people talk about "vibrationally inelastic scattering" while the bulb experimentalists discuss "vibrational energy transfer". We, in fact, retain this separation by using these distinct but synonomous terms in the beam and bulb sections of this review.

Developments in technology and experimental design are now bringing beams and bulbs closer together. Beams are being opened to vibrationally complex molecules that previously could be studied only in bulbs. In turn, bulb experiments are increasingly able to characterize state-to-state transfers in the single-collision domain commonly associated with beams. It is thus an appropriate time to set bulbs and beams side-by-side in a single review to display their complementarity.

The beam literature concerning vibrationally inelastic scattering is presently so small that it can be discussed conveniently in a single review. The discussion will show that virtually all beam experiments probe what happens as the result of a single collision between a structureless particle and a diatomic or polyatomic molecule in a known vibrational level (usually the zero-point level). By "structureless particle" we mean

† Alexander von Humboldt-Stiftung Preistrager at the Institut fur Physikalische und Theoretische Chemie, Technischen Universitat Munchen, D-8046 Garching, West Germany, 1986.

0009-2665/87/0787-0237$06.50/0

Douglas J. Krajnovich was born near Chicago, IL, in 1955. He received a B.S. degree in Chemistry from the University of Illinois, Urbana, in 1977, and a Ph.D. in Physical Chemistry from the University of California, Berkeley, in 1983. For the past 3 years he has been a postdoctoral research associate at Indiana University. He is presently employed at the IBM Almaden Research Center in San Jose, CA.

David L. Catlett, Jr., was born in Kansas City, KA, in 1959. He received his B.S. in Chemistry and Mathematics in 1980 from Illinois State University in Normal, IL. In 1985 he received his Ph.D. in Physical Chemistry from Indiana University under the supervision of Professor Parmenter. Presently he holds a postdoctoral position in the laboratory of Professor W. R. Gentry at the University of Minnesota. His research interests include rotationally and vibrationally inelastic scattering and the structure and dynamics of van der Waals molecules.

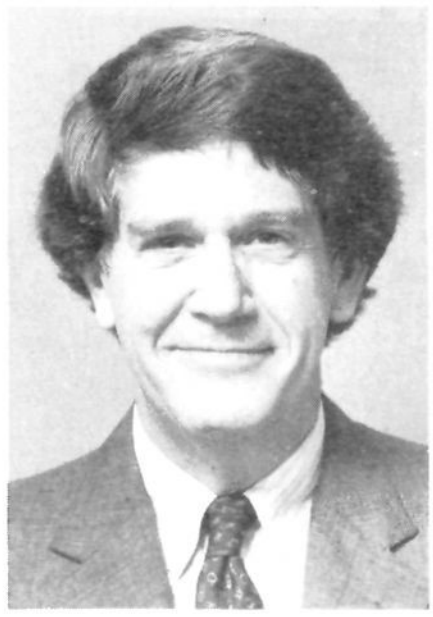

Charles S. Parmenter was born in 1933 in Philadelphia and completed his B.A. in chemistry at the University of Pennsylvania in 1955. Following a year of service as a technical representative with E. I. du Pont de Nemours and 2 years as a Lieutenant in the U.S. Air Force, he completed his Ph.D. study at the University of Rochester with W. A. Noyes, Jr. After a 2-year postdoctoral at Harvard with G. B. Kistiakowsky, he began, in 1964, his academic career at Indiana University where he is now a Professor of Chemistry. He has had visiting appointments at Cambridge University (Guggenheim Fellowship 1971–1972), the Joint Institute for Laboratory Astrophysics and the University of Colorado (JILA Fellowship, 1977–1978), Griffith University in Brisbane, Australia (Fulbright Fellowship, 1980), and the Technischen Universität München (Humboldt Stiftung Senior U.S. Scientist Award, 1986). He began his Indiana University research with the development of techniques for obtaining single vibronic level fluorescence spectra from large polyatomic molecules (using, in the early days, xenon arcs!). Those efforts have evolved into studies of the electronic spectroscopy of polyatomic molecules, intramolecular dynamics, photodissociations, light scattering from particulates, and collisional energy transfer processes involving electronic, vibrational, and rotational energies. The work is described in over 80 publications.

either an atom (atomic ion) or a stiff diatomic whose vibrational frequency is too high to influence the outcome of the scattering process. Thus, beam workers have mainly explored how energy is transferred between the vibrational degree(s) of freedom of a diatomic or polyatomic molecule and the relative translational motion of the collision pair. We shall refer to these processes as T ↔ V transfers, even when both the initial and final states may be vibrationally excited. (A more restrictive use of the term T ↔ V transfer has sometimes been used in the bulb literature.)

The bulb literature is far too voluminous to encompass in a single review. We focus in this review on a set of bulb experiments that most closely complements the T ↔ V explorations of beams. That set happens to involve studies of T ↔ V transfers in collisions of electronically excited (S_1) polyatomic molecules with atoms or stiff diatomics. The experimental advantages of these studies allow measurements of absolute rate constants for many single-collision state-to-state transfers from a selection of initial S_1 vibrational levels. Some of the polyatomics, with nine to thirty-six vibrational degrees of freedom, are large by the usual standards for state-resolved vibrational energy transfer studies. As such, they provide a uniquely detailed experimental view of collisional T ↔ V transfer in vibrationally complex systems.

Two other distinct classes of vibrational energy transfer studies lie intermediate to the S_1 polyatomic bulb experiments and the beam investigations. The first is comprised of explorations of vibrational relaxation in the very low energy collisions of an expanding supersonic jet. In a sense, these are low-temperature "bulb" experiments. The second is concerned with the flow of vibrational energy that accompanies the vibrational predissociation of a van der Waals complex between, say, a rare gas atom and an S_1 polyatomic molecule. When discussed from the point of view of T ↔ V transfers, this is a "half-collision" involving a complex of highly specific geometry. Critical reviews of these areas would add substantially to the length of the present review, and for this reason they are not attempted. An exception concerns the very low collision energy experiments (and theory) for the He + I_2* system, for which a limited discussion appears at the end of the crossed beam comments in section III.

The organization of this paper is as follows. In sec-

tion II, the kinds of quantities that are traditionally measured in beams and bulbs are briefly reviewed and compared. Section III contains a fairly comprehensive discussion of the existing crossed beam results on vibrationally inelastic scattering. A number of excellent reviews of the crossed beam work have been given by Faubel and Toennies over the past 10 years.[1-5] There are definitely regions of overlap between our section III and these earlier reviews. However, since the early reviews all contain extensive discussions of pure rotationally inelastic scattering in addition to vibrationally inelastic scattering, we felt that it might be useful to "pull out" the more limited vibrational information, bring it up to date, and present it together in one place.

In section IV, the S_1 polyatomic studies are discussed. An extended summary of a subset of these results was given by Rice[6] in 1981. Rice uses the term "collision-induced intramolecular energy transfer" to describe these studies. We shall not employ this oxymoron, since, in our opinion, it tends to obscure the similarity between these atom–polyatomic collision processes and other T ↔ V energy transfer processes. An introduction to some of the S_1 polyatomic work has also been given by Parmenter.[7] For discussion of recent bulb work in the ground electronic state see the reviews by Smith[8,9], Weitz and Flynn,[10] and others.[11-14]

Our review concludes in section V with a discussion of theoretical approaches to the vibrational energy transfer problem. There are two reasons why the theory section is at the end rather than the beginning. First, we prefer to avoid a prolonged detour at the outset from our main emphasis, which is experimental work. Second, we are not qualified to review comprehensively and critically the recent theoretical literature. Rather, we have tried to review the theory from an experimentalist's perspective, with an emphasis on theoretical approaches with three-dimensional applications to experimental systems or results. More detailed and/or rigorous theoretical discussions occur in the 1979 review volume, *Atom-Molecule Collision Theory*,[15] and in more recent reviews by Secrest,[16a] Schatz,[16b] and Billing.[17]

The three main sections of this review are fairly "modular" and need not be read sequentially. Experimentalists who are not too familiar with the crossed beam world might benefit from at least skimming through section V before reading section III, since the latter makes frequent references to theoretical calculations and models.

II. Experimental Measurements in Beams and Bulbs: Expectations vs. Reality

Suppose we want to study the vibrationally inelastic scattering of an atom A with a diatomic or polyatomic molecule B. The ideal inelastic scattering experiment would consist of (i) preparing B in a known initial quantum state, B(i), where the index i covers electronic, vibrational, and perhaps also rotational quantum numbers; (ii) studying isolated bimolecular encounters of A and B(i) at a well-defined center-of-mass (c.m.) collision energy E_T^i; (iii) measuring the c.m. angular distribution of scattered molecules for each energetically allowed inelastic channel, A + B(i) + E_T^i → A + B(f) + E_T^f, where f and E_T^f denote the final quantum numbers of B and the final c.m. translational energy.

In the jargon of scattering theory, such angular distributions are referred to as differential cross sections. For a given inelastic channel, $i \rightarrow f$, the c.m. differential cross section may be written as

$$\frac{d\sigma_{i\rightarrow f}(\theta;E_T^i)}{d\omega} \tag{1}$$

where $d\omega$ is the unit of solid angle in the c.m. coordinate system and θ is the c.m. scattering angle ($\theta = 0°$ corresponds to "forward" scattering, $\theta = 180°$ to "backward" scattering). The ideal experiment, then, would measure the state-to-state differential cross section (1) for transitions between a variety of initial states i to all final states f, all as a function of the initial collision energy E_T^i. (Note that the differential cross section is normalized per unit solid angle. To get the total scattered intensity as a function of θ, the differential cross section must be weighted by $2\pi \sin \theta$.)

If the inelastic signal is not resolved as a function of scattering angle, one is left with the integral state-to-state cross section $\sigma_{i\rightarrow f}$ (which is still a function of E_T^i):

$$\sigma_{i\rightarrow f}(E_T^i) = \int \frac{d\sigma_{i\rightarrow f}(\theta;E_T^i)}{d\omega}\, d\omega \tag{2}$$

If the final states f are not resolved, one has the total inelastic cross section for initial state i at collision energy E_T^i:

$$\sigma_i^{tot}(E_T^i) = \sum_f \sigma_{i\rightarrow f}(E_T^i)\ . \tag{3}$$

Finally, if the collision energy is not well-defined, one must average the relevant cross section over the initial distribution of E_T^i. In particular, what one measures in a bulb experiment is an average of $v\cdot\sigma_{i\rightarrow f}$ or $v\cdot\sigma_i^{tot}$ over a Boltzmann distribution of collision velocities, v, at a particular temperature T:

$$k_{i\rightarrow f}(T) = \langle v\cdot\sigma_{i\rightarrow f}(E_T^i)\rangle_{Boltz} \tag{4a}$$

$$k_i^{tot}(T) = \sum_f \langle v\cdot\sigma_{i\rightarrow f}(E_T^i)\rangle_{Boltz} \tag{4b}$$

The quantities in eq 4 are the usual bulb state-to-state and total inelastic rate constants. In this article, we are mainly interested in state-to-state measurements. Therefore, experiments that *only* measure quantities of the type (3) or (4b) will not be considered.

In comparing the value of vibrational energy transfer measurements in beams and bulbs, several factors should be considered: (i) the extent of averaging involved in the measurements; (ii) the flexibility provided in the choice of systems to study; (iii) the flexibility provided in the choice of initial vibrational level; (iv) whether or not, for a given initial vibrational level, all possible final levels are probed experimentally.

Traditionally, beam people have tried to obtain very detailed information of the type (1) or (2), but have been limited in their choices of systems to study by experimental resolution and signal-to-noise constraints. For example, there have only been two measurements so far of state-resolved vibrationally inelastic differential cross sections in neutral collision systems (section III.C.4). In contrast, bulb people have been able to tackle a wider variety of complicated chemical systems using the high sensitivity and resolution of modern laser spectroscopic techniques, but they have had to content

themselves with highly averaged information of the type (4). There is also a big difference between beam and bulb experiments in the choice of initial vibrational level: while most crossed beam experiments so far have involved no "active" preparation of the initial vibrational level (that is, only vibrational excitation out of the zero-point vibrational level has been studied), nearly all bulb experiments have explored vibrational energy transfer to and from vibrationally excited molecules. Regarding the final point (iv) mentioned above, most crossed beam experiments performed so far have allowed all (or nearly all) of the possible final vibrational levels to be probed experimentally. (In the case of the so-called "energy-change" experiments, the final vibrational levels are not always well-resolved, but none are "missing" from the data; see section III). In bulb experiments, on the other hand, it is not always true that all possible final levels are probed experimentally. For example, experiments relying on infrared fluorescence to identify final vibrational levels usually only probe a subset of the possible final levels. In this regard, bulb studies of vibrational energy transfer in *excited* electronic states have a particular advantage, in that *all* vibrational levels in an excited electronic state give rise to electronic fluorescence (section IV).

Clearly, those experiments with the least amount of averaging will be most sensitive to the details of the forces responsible for T $\leftrightarrow$ V transfer in molecular collisions. Therefore, one experimental goal must be to extend the range of vibrationally inelastic differential and integral cross section measurements, not only in terms of the number and types of systems studied, but also in terms of studying inelastic scattering of vibrationally excited molecules. Presumably, such studies must be done in crossed molecular beams.[18] But, it is unlikely that the beam people will ever put the bulb people out of business. For vibrationally complex polyatomic molecules, the first results and insights into the collisional vibrational energy flow will usually be obtained in a bulb. Hopefully, it will then become possible to extend some of these studies to a crossed beam environment. Bulbs will also continue to serve as a testing ground for new laser state preparation and detection techniques that might eventually be carried over to crossed beam experiments.

III. Crossed Molecular Beam Studies of Vibrationally Inelastic Scattering

Of the three main types of scattering processes (elastic, inelastic, and reactive) it is probably still fair to say that the least is known experimentally about inelastic scattering. (For example, in a recent monograph on molecular beam scattering,[19] only 8 pages are devoted to inelastic scattering). The main reason for this is simple. Since the elastic cross section is usually orders of magnitude larger than either the inelastic or reactive cross section, the detector in a scattering experiment must be capable of distinguishing a small inelastic or reactive signal from a huge elastic background signal. In reactive scattering, this difficulty is readily overcome, since the reaction products differ chemically from the reagents. The "universal" mass spectrometer detectors of modern crossed molecular beam machines[20] can usually be used to monitor one of the products of a chemical reaction without elastic intereference. However, in inelastic scattering, the "product" has the same chemical identity as the "reagent". To distinguish inelastic from reactive scattering, the detector must be quite sophisticated. It must be capable of *either*: (i) resolving the change in relative translational energy that accompanies each inelastic transition ("energy-change" method), *or* (ii) probing the internal quantum state distribution of the scattered molecules directly ("state-change" method). Both of these methods have been used extensively in crossed beam experiments.

A. Energy-Change Experiments (Ions)

In principle, the energy-change method is the most general approach to the study of state-to-state inelastic scattering. The ability to measure differential cross sections, and thereby selectively probe different regions of the potential energy surface, is inherent to the method. However, from a practical point of view, the energy-change method is difficult to implement, especially in the case of vibrationally inelastic scattering. In many systems of interest, the vibrationally inelastic cross sections are exceedingly small at thermal collision energies, while at higher collision energies it is difficult to achieve the energy resolution needed to distinguish inelastic from elastic scattering. In many systems it is also difficult to separate the rotational and vibrational contributions to the inelastic scattering.

So far, practically all studies of vibrationally inelastic scattering by the energy-change method have employed ions, since ions are much easier than neutrals to energy select and analyze, and since ions can be detected with near unit efficiency. The first such ion scattering experiments were done more than 15 years ago. Since then, an impressive body of data has been built up on collisions of atomic ions (H^+, D^+, Li^+,...) with a wide variety of diatomic, triatomic, and larger polyatomic molecules. Much less is known about vibrationally inelastic scattering of neutral atoms from molecular ions, mainly because of the experimental difficulties associated with forming an intense beam of molecular ions in a well-defined electronic and vibrational state.[21a] There is no question that these experimental difficulties are being gradually overcome. The last 10 years have seen a steady increase in the number of studies of state-selected molecular ions using photoionization methods (especially coincidence methods[21b]), ion traps, and tunable visible and UV light sources. Most of this work, however, has been in areas outside of the scope of this review. Therefore, we shall concentrate in this section on atomic ion–neutral molecule inelastic scattering.

Although the forces responsible for inelastic scattering in ion–molecule systems are often different from (and simpler than) those involved in neutral systems, the fundamental problem of relating the experimentally observed inelastic scattering to the microscopic forces giving rise to the inelastic transitions is the same in both cases. As we shall see, many of the same questions arise in the ion scattering experiments as in the neutral experiments to be discussed later. Similar theoretical approaches have been applied to both classes of systems.

Our primary goal in this section is to leave the reader with a mental picture of what a "typical" vibrationally inelastic scattering event looks like in the different systems under study. But we have also tried to explain "how" the experiments were done, and we have tried to examine critically both the experimental results and their theoretical interpretation. We assume that the reader is acquainted with velocity vector diagrams, the transformation between laboratory and center-of-mass coordinate systems, and simple concepts from classical scattering theory (the defection function, rainbow scattering, etc.). If not, he/she is referred to one of several simple introductions to the subject.[19,22-24]

1. $H^+ + H_2$

The H^+–H_2 system is extremely simple, consisting of only three heavy particles and two electrons. Reasonably accurate ab initio calculations of the potential energy surface for this system were carried out in the early 1970's. Therefore, when trying to reproduce experimental scattering results on this system, it should be possible to judge the merits of various dynamical approximations without additional complications caused by imperfect knowledge of the potential energy surface.

One drawback of the H^+–H_2 system, from the standpoint of an inelastic scattering experiment, is that the system is reactive. Also, charge transfer can occur at collision energies greater than 1.8 eV. Fortunately, the rearrangement reaction only becomes important at energies below about 2 eV, and at higher energies the charge-transfer cross section is much smaller than the inelastic cross section. Therefore, at collision energies greater than 3 eV, inelastic processes dominate, and the scattering can be considered to occur on a single adiabatic potential energy surface corresponding to the ground electronic state of the system.

Vibrational excitation in $H^+ + H_2$ collisions was first studied by Doering and co-workers[25] at Johns Hopkins University, and by Udseth, Giese, and Gentry[26] at the University of Minnesota. Both groups used a scattering cell for the target gas and electrostatic analyzers to resolve the proton energy loss spectrum. The Johns Hopkins group worked at high collision energies, where all of the inelastically scattered ions are confined to a small angular range about the incident ion beam direction. They measured absolute integral cross sections for vibrational excitation (up to $v = 4$) in H^+, $D^+ + H_2$ collisions at collision energies between 100 and 1500 eV. In contrast, the Minnesota group used a rotatable detector with a wide angular travel to measure vibrationally state-resolved differential cross sections for the $H^+ - H_2$, HD, D_2 systems at much lower collision energies (4–21 eV). In discussing the experimental results, it is important to distinguish between the vibrationally state-resolved differential cross section, $[d\sigma(\theta)/d\omega]_v$, and the so-called vibrational transition probabilities, $P_v(\theta)$, defined by

$$P_v(\theta) = [d\sigma(\theta)/d\omega]_v / \sum_v [d\sigma(\theta)/d\omega]_v.$$

$[d\sigma(\theta)/d\omega]_v$ represents the number of particles scattered per unit solid angle into final vibrational level v, as a function of the c.m. scattering angle θ (measured with respect to the incident ion beam direction). $P_v(\theta)$, on the other hand, represents the *fraction* of those particles scattered by angle θ that end up in vibrational level v, i.e., the vibrational transition probabilities (*including* the elastic channel) sum to unity at each θ.

For $H^+ + H_2$ collisions at $E_{cm} = 10$ eV, the Minnesota group[26] found that the vibrational transition probabilities from $v = 0$ to $v = 1$–4 increased monotonically with scattering angle between $\theta = 5$ and 22°, which includes the range up to the classical rainbow angle. The elastic ($v = 0$) differential cross section shows a well-resolved rainbow and the usual steep increase at small scattering angles, with some small-angle undulations superimposed. Although a rainbow maximum can still be seen in the $v = 1$ and $v = 2$ differential cross sections (shifted slightly to larger angles), the inelastic differential cross sections are reasonably flat between 5 and 20°. Therefore, the increase in the vibrational transition probabilities with increasing scattering angle is mainly due to the rapid fall-off of the elastic cross section, rather than to a real increase in the inelastic differential cross section. At angles larger than the rainbow angle, both the elastic and inelastic differential cross sections fall off steeply, so most of the inelastic scattering in this system is probably accounted for by the angular range covered in these experiments.

For the same collision energy and scattering angle, Udseth, Giese, and Gentry[26] found that the vibrational transition probabilities for the different isotopes scaled in the order $D_2 > HD > H_2$. However, the isotopic differences disappeared when the transition probabilities were weighted by the transition energies; that is, the average energy transfer is approximately independent of the isotopic composition of the molecule. This result is difficult to reconcile with any model of the energy transfer process which assumes that the proton interacts with only one atom in the target molecule. Rather, it appears that the main effect of the passing proton is to temporarily withdraw electron density from the H_2 bond, resulting in bond extension and concomitant vibrational excitation.

This "bond dilution" mechanism was given a secure footing in 1974 when Giese and Gentry[27] applied their DECENT model to this system. The assumptions underlying the DECENT model are discussed in section V.C. By performing 3-dimensional classical trajectory calculations on the ab initio H^+–H_2 potential energy surface and invoking the DECENT prescription for calculating the quantum vibrational transition probabilities, Giese and Gentry were able to satisfactorily reproduce the gross features of the inelastic scattering in this system. Individual trajectories showed clearly the weakening and stretching of the H_2 bond as the proton passed by. All initial molecular orientations were found to contribute comparably to the vibrational excitation.

The DECENT model also predicted that substantial rotational excitation should occur in this system. Although the resolution of the Minnesota group's apparatus was insufficient to resolve rotational transitions, Giese and Gentry found that they obtained much better agreement with the DECENT calculations if they first corrected their measured vibrational transition probabilities for contributions from underlying, unresolved rotational transitions. (As the following discussion will show, this improved agreement was probably fortuitous.)

Not content with this level of understanding, Linder and co-workers at Kaiserslautern University embarked on an ambitious program to *simultaneously* resolve rotational and vibrational transitions in low-energy $H^+ + H_2$ collisions. In their apparatus, two 127° electrostatic selectors were used in series to sharply define both the energy and angular spread of the incident H^+ beam, and a second pair of selectors was used to scan the energy loss spectrum. The scattering cell used by earlier workers was replaced here by a skimmed nozzle beam of H_2, to reduce the spread in collision energies and improve the overall angular resolution of the apparatus. The first results from this apparatus were published by Schmidt et al.[28] in 1976. In subsequent papers,[29-32] the Kaiserslautern group reported detailed measurements at several collision energies (E_{cm} = 4.67, 6, 10, 15.3, 20 eV). At 4.67 and 6 eV, pure rotational excitation[29,30,32] is the dominant process. (In fact, at 4.67 eV, the average $J = 1 \rightarrow 7$ rotational transition probability of ortho-hydrogen is about the same as the $v = 0 \rightarrow 1$ transition probability summed over all final rotational states.) At energies above about 7 or 8 eV, vibrational excitation becomes dominant. The most detailed study of simultaneous vibrational and rotational excitation was performed at 10 eV,[31] to allow comparison with Giese and Gentry's most detailed calculations at the same energy. The overall agreement between experiment and the DECENT calculations, summarized in Figure 6 of ref 31, is quite good, especially considering that no adjustable parameters were used in the DECENT calculations, and considering that the experimental and calculated cross section data are normalized at a single point. However, the experimental vibrationally-state-resolved differential cross sections for v = 1–3 (summed over final rotational states) do not fall off as rapidly as the calculated cross sections in the rainbow region, and some quantum undulations in the experimental cross sections are seen that are not encountered for by the semiclassical DECENT model. The DECENT model also underestimates slightly the vibrational inelasticity, but the prediction of a Poisson distribution of final vibrational states agrees nicely with the experimental results. Interestingly, the pattern of rotational excitation was measurably higher for the vibrationally inelastic (v = 1) as compared to the vibrationally elastic (v = 0) channel.

The quantum undulations in the vibrationally inelastic differential cross sections were addressed in the quantal scattering calculations of Schinke and McGuire.[34] In their calculations, the rotational motion was treated using the infinite-order sudden approximation, but the vibrational motion was treated exactly by solving the close-coupled radial equations (VCC/IOS treatment). The Giese–Gentry-fit potential energy surface was used. Even though the shapes and positions of the undulations in the elastic and inelastic differential cross sections were reproduced quite well by the calculations, the amount of vibrational excitation was still underestimated (by about 30% in the case of v = 1), just as it was in the DECENT calculations. This discrepancy was resolved in 1980, when Schinke, Dupuis, and Lester[35] recomputed the ground state potential surface for the H_3^+ system, including configuration interaction (CI) effects. Significant differences were found between the new CI potential and the Giese–Gentry potential, particularly in the regions corresponding to small and large H_2 bond separations. When Schinke, Dupuis, and Lester[35] reran the scattering calculations of Schinke and McGuire on the new potential surface, excellent agreement was obtained with all of the experimental results at 10 eV collision energy as shown in Figure 1. Similar agreement was obtained at 4.67 and 6 eV; the rotational excitation is significantly less on the new surface.[36]

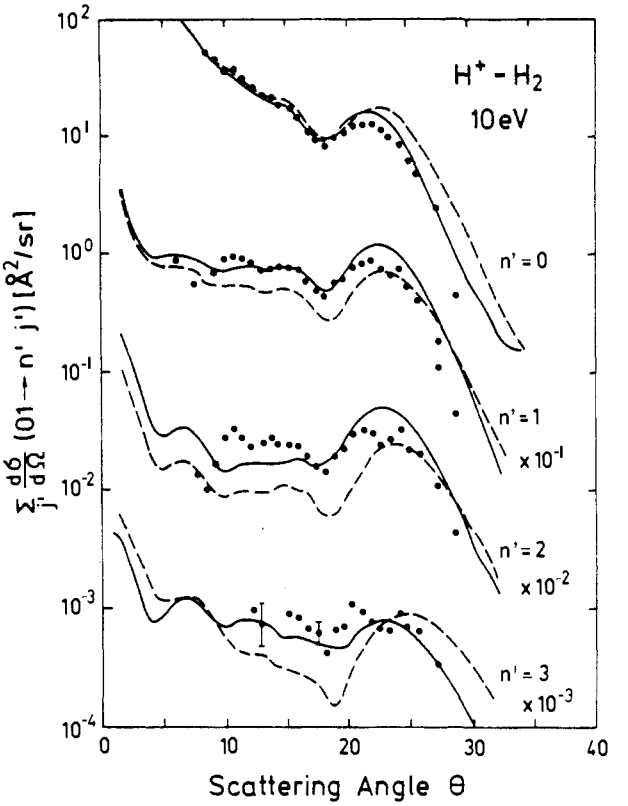

Figure 1. Differential cross sections (summed over final rotational levels) for $n = 0 \rightarrow n' = 0$, 1, 2, and 3 vibrational transitions in $H^+ + H_2$ scattering at E_{cm} = 10 eV. ● experimental measurements of Hermann, Schmidt, and Linder (ref 31); --- VCC/IOS quantal scattering calculations performed by Schinke and McGuire on the Gentry-Giese-fit potential energy surface (ref 34); — VCC/IOS calculations performed by Schinke, Dupuis, and Lester on an improved H^+–H_2 potential surface (ref 35). Each set of theoretical curves was normalized to the experimental data at a single point. Reproduced with permission from ref 35. Copyright 1980 American Institute of Physics.

As far as we know, the DECENT calculations have not been repeated using the new CI surface. In retrospect, it appears that the original DECENT calculations predicted too much rotational excitation and too little vibrational excitation. Most likely, the agreement between experiment and the DECENT model would improve significantly if the new potential surface were used for the trajectory calculations.

The experiments at E_{cm} = 15.3 and 20 eV resolved vibrational, but not rotational states.[32] At these higher energies, semiclassical scattering calculations using the so-called "impact parameter" approximation[32,37] agreed reasonably well with experiment at angles smaller than the rainbow angle. The impact parameter approximation has also been used successfully to explain the observation of glory-type oscillations in the forward inelastic differential cross section at c.m. energies between 15 and 120 eV.[38]

2. $Li^+ + H_2$

Because of their closed shell electronic configuration, low electron affinity, and low reactivity, Li^+ ions make excellent projectiles for inelastic scattering studies. Since the first excited electronic state of Li^+ is at 66 ev, Li^+ ions formed in a thermal source are known to be in the ground electronic state. Therefore, at collision energies below the charge transfer threshold (typically 5–10 eV), the scattering occurs on a single potential energy surface corresponding to the ground electronic state of the interacting system, and only rotational and vibrational inelastic transitions are possible.

In 1973, David, Faubel, and Toennies[39] reported measurements of differential cross sections for resolved vibrational transitions in the Li^+–H_2 system at c.m. collision energies between 2 and 9 eV. These workers used a time-of-flight (TOF) method to measure the energy loss spectra of the inelastically scattered ions. Deflection plates were used to chop the Li^+ beam into short bursts, which were then focused onto the axis of an intense, sharply collimated H_2 target molecular beam. The detector consisted of a long drift tube with an electron multiplier at the end. A time-to-amplitude converter and pulse-height analyzer were used to measure ion flight time distributions at different angles, which were then converted to energy loss spectra using the known length of the drift tube. In this apparatus, both the ion beam and drift tube axis were at right angles to the target beam, the detector was stationary, and scattering at different angles was measured by rotating the ion beam source in the plane perpendicular to the target beam.

Due to the large projectile:target mass ratio in the Li^+–H_2 system, the kinematics are much less favorable for resolving inelastic transitions than in the case of H^+–H_2. Neglecting the small H_2 beam velocity compared to that of the Li^+ beam, it is easy to see that the c.m. for this system lies $^7/_9$ of the way along the Li^+ beam velocity vector. Therefore, in the laboratory coordinate system, all of the inelastically scattered Li^+ ions are confined to a narrow cone, ± 16° about the incident Li^+ direction. David et al. performed measurements at c.m. collision energies of 3.65, 5.54, and 8.8 eV, and at lab angles between 3° and 16°. At each lab angle, ions scattered in the forward and backward c.m. directions both arrive at the detector. At all energies, the inelastic scattering was swamped by elastic scattering in the forward direction and could not be resolved. In the backward direction, even though elastic scattering still dominates, vibrationally inelastic transitions up to $v = 4$ were resolved in the TOF spectra. The data were analyzed to obtain relative vibrational transition probabilities for $v = 0$–4 as a function of c.m. scattering angle between $\theta = 130$–167°. At each energy and scattering angle, the vibrational transition probabilities fall off monotonically as v increases, but it appears that the fall-off is not as rapid as one would calculate for a Poisson distribution. No strong angular dependence of the transition probabilities was observed over the accessible range of scattering angles.

A lot of additional work has been done on this system.[40–43] Most of it has been directed toward resolving rotationally inelastic transitions in forward scattering at much lower collision energies, where comparison with nearly exact quantal scattering calculations is possible. The most detailed measurements of the rotationally inelastic scattering, at $E_{cm} = 0.6$ eV, were reported by Faubel and Toennies[42] in 1979. Faubel and co-workers also obtained improved results on the vibrationally inelastic scattering at $E_{cm} = 3.6$ eV.[43] Although most of this improved data has not been published, it confirms the results of David et al.[39] at least up to $v = 3$. The $v = 0 \rightarrow 4$ transition probabilities may have been overestimated by David et al., because of underlying rotation excitation.

Both SCF-[44] and CI-type[45] calculations of the Li^+–H_2 potential energy surface were reported in the early 1970s. While the isotropic part of the H^+–H_2 potential is strongly bound by 3.5 eV, the spherically averaged Li^+–H_2 potential has a well depth of only 0.17 eV. Therefore, while most of the vibrationally inelastic scattering in the H^+–H_2 system involves fairly large impact parameters, forward scattering angles, and the attractive part of the potential, vibrationally inelastic transitions in the Li^+–H_2 system are induced mainly by small impact parameter collisions with the repulsive wall, leading to backward c.m. scattering. Another important difference between the H^+–H_2 and Li^+–H_2 potentials is that the latter is much more anisotropic. [For Li^+–H_2 separations around 2 Å (in the vicinity of the minimum of the spherically averaged potential), the v_0 and v_2 terms in the Legendre series expansion of the interaction potential are roughly equal in magnitude and opposite in sign.] This strong anisotropy leads not only to very efficient rotationally inelastic scattering, but also to an intimate coupling between the vibrational and rotational degrees of freedom in the vibrationally inelastic scattering.

This coupling was demonstrated very clearly when Gentry and Giese[46] applied their DECENT model to the Li^+–H_2 system. Trajectories were run on Lester's SCF potential surface[44] at c.m. collision energies of 3.65 and 5.54 eV, to allow comparison with the experimental results of David et al.[39] (The highest collision energy, 8.8 eV, was not studied in detail, since some trajectories were found to "escape" the well-characterized regions of the ab initio potential energy surface.) In these trajectory calculations, all scattering at c.m. angles larger than 130° resulted from initial impact parameters less than 0.5 Å. By performing calculations using both the spherically averaged and full anisotropic potentials, Gentry and Giese[46] found that the anisotropic potential gave ~6× more vibrational excitation (on the average) than the spherically averaged potential. This enhancement was traced to a particular class of trajectories in which the H_2 molecule is "deoriented by about 15° from the orientation which would result in an approximately collinear configuration during the period of strong interaction." Interestingly, in exactly collinear collisions, although the force acting on the oscillator is large, the force acts symmetrically over the H_2 vibrational period resulting in little net vibrational excitation. (In other words, the interaction time is sufficiently long that the H_2 molecule is able to follow the driving force adiabatically). However, if the H_2 molecule is deoriented slightly, then as the bond is initially compressed by the incoming proton, the H_2 molecule rotates away from the collinear configuration; this turns off the driving force while the H_2 bond is still compressed and results in large vibrational excitation.

The quantitative agreement between the DECENT

calculations and the experimental results is not as good for Li^+-H_2 as it was for H^+-H_2. At E_{cm} = 3.65 eV, the DECENT model correctly predicts the $v = 1$ transition probability, but the higher vibrational transition probabilities are underestimated (the discrepancy is about a factor of 2 for the $v = 0 \rightarrow 2$ transition and a factor of 4 for the $v = 0 \rightarrow 3$ transition). The DECENT calculations fare better at 5.54 eV, however.

Other scattering calculations have also had trouble reproducing the experimental transition probabilities. Unfortunately, the very best calculations (using the exact quantum mechanical close-coupling scheme[47] and the classical S-matrix theory[48]) are available only at 1.2 eV or lower, where the vibrational transition probabilities are too small to measure experimentally. A full close-coupling calculation at 3.6 eV was attempted by Schaefer and Lester in 1975, but since the results were not converged they were never published.[49] Approximate quantal scattering calculations at 5.54 and 8.8 eV were reported by Schinke[50] in 1978. These calculations were performed using the infinite-order sudden (IOS) approximation for the H_2 rotational motion (see section V.A.). The IOS approximation is expected to have a rough time in the Li^+-H_2 system, because of the high anisotropy of the potential energy surface and the rotation–vibration coupling discussed earlier.[51] In fact, Schinke found that his IOS calculations underestimated all of the vibrational transition probabilities by a factor of six or more (except the $v = 0 \rightarrow 1$ transition probability at 8.8 eV, which was only a factor of two low). The inferior results of these quantal scattering calculations (as compared to the DECENT model calculations) is probably due to the neglect of rotation–vibration coupling in the IOS approximation.

A quasiclassical trajectory study of Li^+-H_2 scattering at 3.6 eV was published by Barg, Kendall, and Toennies.[52] In their paper, results are presented only for the $v = 0 \rightarrow 0,1$ transitions. Good agreement with experiment was obtained. However, Schinke[50] quotes additional (unpublished) trajectory results by Barg that are said to underestimate the higher vibrational transitions very strongly.

We conclude that the humble Li^+-H_2 system is not yet fully understood. Quasiclassical, semiclassical, and approximate quantal scattering calculations have all failed to reproduce the experimental vibrational transition probabilities in detail.[53] It is not clear to what extent these failures are due to dynamical approximations, or to shortcomings in the ab initio potential energy surface. We should note, however, that significant discrepancies between theory and experiment have also been observed in the pure rotationally inelastic scattering at 0.6 eV.[42] Exact quantal scattering calculations are possible at this energy, so the residual discrepancies must be attributed to the potential surface.

These observation reveal the need for another round of theoretical efforts on the Li^+-H_2 system. They also inspire humility as we proceed to more and more complicated systems in the remainder of this review.

3. Other Ion–Diatomic Molecule Systems

The energy-change techniques described in the last two subsections have all been applied to diatomics heavier than H_2. The molecules studied include N_2, CO, NO, O_2, HCl, and HF, but the bulk of the work has focused on the isoelectronic molecules N_2 and CO.

Udseth, Giese, and Gentry[54] used their apparatus to study the small-angle scattering of protons from N_2, CO, HCl, and HF at collision energies between 10 and 30 eV. Large proton energy losses were observed in collisions with HCl and HF. Due to the large vibrational spacings in these molecules, it was possible to attribute most of the energy loss to rotational excitation of the diatomic molecules. In contrast, no energy loss was observed with N_2, and only a small energy loss was observed in the case of CO. Udseth et al.[54] could not clearly distinguish CO rotational excitation from $v = 0 \rightarrow 1$ vibrational excitation because the energy resolution of their apparatus was comparable to a CO vibrational quantum. They concluded that the small excitation energy for CO was probably rotational, since they expected the probability of vibrational excitation to be similar for N_2 and CO.

Higher resolution studies by two independent groups[55,56] have shown that proton collisions actually excite more vibrational energy in CO than in N_2. Krutein and Linder[55] (at Kaiserslautern) used an apparatus similar to the one used for the high resolution H^+-H_2 experiments to study proton scattering from N_2, CO, and NO at E_{cm} = 30 eV. Proton energy loss spectra were measured at various angles out to and just beyond the rainbow angle (which is approximately 10° at E_{cm} = 30 eV). These data were used to derive vibrationally-state-resolved differential cross sections and vibrational transition probabilities as a function of scattering angle. Both $v = 1$ and $v = 2$ excitation of CO and NO were observed, but only $v = 1$ excitation could be detected in N_2. In the H^+–CO system, the $v = 1$ and $v = 2$ transition probabilities were found to increase monotonically with increasing scattering angle. However, as was the case in H^+-H_2, this trend mainly reflects the more rapid fall-off of the vibrationally elastic differential cross section and not a real increase in the inelastic differential cross sections with increasing scattering angle. In fact, there is very little elastic or inelastic scattering at angles larger than the rainbow angle. Similar trends were evidently observed for the other systems, although less extensive data is presented.

Although the angular dependence of the inelastic scattering in these systems is similar to that observed in H^+-H_2, the magnitude of the vibrational energy transfer is much smaller. For H^+-H_2 scattering at E_{cm} = 20 eV, and angles close to the rainbow angle, vibrational transition probabilities of 0.35, 0.15, and 0.05 were observed for the $v = 1,2$, and 3 levels of H_2, respectively;[32] this corresponds to an average vibrational energy transfer of $\langle \Delta E_{vib} \rangle$ = 0.44 eV, or ~2% of the available energy. In contrast, for H^+–CO rainbow scattering at E_{cm} = 30 eV, Krutein and Linder[55] observed vibrational transition probabilities of 0.18 and 0.05 for $v = 1$ and 2, corresponding to $\langle \Delta E_{vib} \rangle$ = 0.07 eV, or 0.25% of the available energy. The average vibrational energy transfer was slightly higher for NO, and about 2× lower for N_2. Krutein and Linder also estimated the extent of rotational excitation from the slight broadening of their energy loss peaks. They concluded that both the rotational and vibrational inelasticity increase in the order N_2, CO, NO.

Before considering the "mechanism" of the vibrationally inelastic scattering in these systems, we shall first review the results of a second set of high resolution

experiments performed by Gianturco, Gierz, and Toennies[56] at Goettingen. Although these experiments were performed at a lower collision energy than those of Krutein and Linder, there appear to be some discrepancies between the two sets of results that cannot be simply explained just on the basis of the difference in collision energy.

The Goettingen group used a time-of-flight apparatus similar to the one used for the Li^+-H_2 experiments to study proton scattering from N_2, CO, NO, and O_2 at E_{cm} = 10 eV. Since, for a given potential, the product of collision energy and rainbow angle is roughly constant, the rainbow occurs at approximately 30° in this experiment. Time-of-flight measurements were performed at four angles between 5° and 20°. The relative vibrational transition probabilities, P_v, were obtained by fitting the inelastic peaks in the time-of-flight spectra to a set of Gaussian functions. The average vibrational energy transfer at each angle was calculated from

$$\langle \Delta E_{vib} \rangle = \hbar\omega \sum_v v \cdot P_v$$

The average rotational energy transfer, $\langle \Delta E_{rot} \rangle$, was then obtained by subtracting $\langle \Delta E_{vib} \rangle$ from the observed average *total* energy transfer, $\langle \Delta E_{tot} \rangle$. Since $\langle \Delta E_{tot} \rangle$ can be obtained from a direct integration of the time-of-flight spectrum, this is expected to be a reliable procedure.

Gianturco et al.[56] observed that (i) the vibrational transition probabilities for N_2, CO, and NO increase monotonically with scattering angle over the angular range studied; (ii) only $v = 1$ is excited in N_2, whereas both $v = 1$ and 2 are excited in CO and NO; (iii) the amount of vibrational energy transfer increases in the order N_2, CO, NO with $\langle \Delta E_{vib} \rangle$ being 2–3× higher for CO than for N_2 at most angles. These results agree qualitatively with those of Krutein and Linder.[55] The main "discrepancy" between the two sets of results is that the vibrational transition probabilities obtained by Gianturco et al. at 10 eV are larger (by roughly a factor of two) than those obtained by Krutein and Linder at 30 eV (when comparison is made at the same value of the "reduced" scattering angle, $E_{cm} \cdot \theta$, to account for the shift of the rainbow angle with collision energy). This trend is opposite to the "normal" trend observed in the H^+-H_2 and Li^+-H_2 systems, where the vibrational transition probabilities increase monotonically with increasing collision energy. Although there is no reason to doubt the validity of either set of results, it would be reassuring to check for systematic errors by collecting data at several collision energies on a single apparatus.

The analysis of Gianturco et al. also indicates that, for N_2, CO, and NO, the amount of rotational excitation is comparable to or larger than the amount of vibrational excitation at all scattering angles. The amount of rotational excitation was found to increase in the order NO, CO, N_2. This ordering is opposite to that obtained by Krutein and Linder. In this instance, the analysis of Gianturco et al. should be more reliable, since it does not depend on an interpretation of the somewhat uncertain broadening and shifts of the inelastic peaks. Thus, it appears that there is no correlation between the average rotational excitation and the permanent dipole moment of the diatomic molecule in these systems.

Compared to the other three systems, H^+-O_2 shows considerably greater vibrational excitation. Gianturco et al. suggest that a charge transfer mechanism may be responsible for this "anomalous" vibrational excitation of O_2.[57] Charge transfer may also play a role in the H^+–NO system, since the ionization potentials of both NO and O_2 are less than that of the H-atom.

Here we will restrict our attention to the H^+-N_2,CO systems, where the scattering presumably is electronically adiabatic. In some respects these systems resemble the simpler H^+-H_2 system. All three systems are characterized by a deep attractive potential well (ϵ = 3.5 eV for H^+-H_2, ϵ = 5–6 eV for both H^+-N_2 and H^+–CO in the minimum-energy configuration), and nearly all of the vibrationally inelastic scattering occurs at angles smaller than the rainbow angle where the attractive part of the potential dominates. However, the valence interactions responsible for the large vibrational excitation in the H^+-H_2 system are not expected to play such an important role in the H^+-N_2,CO systems, since the N–N and C–O bond lengths hardly change upon protonation. (The equilibrium N–N bond distance decreases from 1.0977 Å in the free molecule[58] to 1.0947 Å in the HNN^+ molecular ion.[59] The C–O bond distance decreases from 1.1283 Å in the free molecule[58] to 1.1071 Å in the HCO^+ ion.[60] While the bond contraction is larger for CO than for N_2, it is smaller than the amplitude of the zero-point vibrational motion in both cases.)

Although the H^+-N_2 and H^+–CO interaction potentials have been accurately characterized in the vicinity of the minimum-energy, linear configuration by ab initio methods, calculations at the many geometries needed to map the full potential energy surface are not yet available. Therefore, no realistic scattering calculations have been performed on these systems, and we must content ourselves with a few qualitative observations.

The most striking experimental result in need of an explanation is the higher vibrational excitation observed in CO compared to N_2. Although the interaction of the proton charge with the small permanent dipole moment of CO may have something to do with this difference, the fact that CO has a large dipole moment derivative may be even more important. The results on ion–polyatomic molecule scattering, to be discussed shortly, have lent support to a very simple model in which the vibrationally inelastic transitions are viewed as "spectroscopic" transitions induced by the time-dependent electric field generated by the passing ion. Although the evidence is not as compelling here as it is in some of the polyatomic systems, the higher vibrational excitation observed in the infrared-active CO molecule is at least qualitatively consistent with this simple picture. (Recent theoretical work by Richards[61] also supports this conclusion, although Richards' approach is strictly valid only in the region of very small scattering angles.)

Scattering of Li^+ ions from N_2 and CO was also studied by the Goettingen group. Reasonably accurate potential energy surfaces are available for these systems.[62] The attractive interactions are about an order-of-magnitude weaker in Li^+-N_2,CO than in H^+-N_2,CO, so the Li^+ collisions are expected to be much more impulsive (just as Li^+-H_2 collisions are more impulsive than H^+-H_2 collisions.) While the Li^+-N_2,CO interactions are also highly anisotropic (the v_0 and v_2

terms in the potential are both attractive and comparable in magnitude), rotation–vibration coupling is expected to be less important in these systems than in $Li^+–H_2$, because of the much longer rotational periods of N_2 and CO compared to H_2.

The first experimental results on these systems, at E_{cm} = 4.23 and 7.07 eV, were published by Böttner, Ross, and Toennies[63] in 1976. At each energy, Böttner et al. measured time-of-flight spectra at laboratory angles of 30°, 35°, and 40°, corresponding to c.m. angles of θ = 37°, 43°, and 49°, respectively (for elastic scattering). For comparison, the c.m. rainbow angle is expected to be approximately 7° at E_{cm} = 4.23 eV, and 4° at E_{cm} = 7.07 eV. For $Li^+–N_2$ at 4.23 eV, Böttner et al. observed a single energy-loss peak in the time-of-flight distributions which they attributed to rotationally inelastic scattering. For Li^+–CO at the same energy, a bimodal energy-loss distribution was observed at the larger angles, with the second hump occurring in the position expected for $v = 0 \rightarrow 1$ excitation of CO. At E_{cm} = 7.07 eV, bimodal energy-loss distributions were observed for both N_2 and CO; Böttner et al.[63] assigned the higher-energy-loss peaks to v = 1 excitation of N_2, and to v = 1 and v = 2 excitation of CO.

While these assignments appeared quite sensible at the time, subsequent theoretical[64] and experimental[65] work has shown that most of the energy transfer in these systems is actually due to rotationally inelastic scattering. This result was conclusively demonstrated by Gierz, Toennies, and Wilde[65] in 1984. By increasing the target beam density and sacrificing resolution, Gierz et al. were able to extend the measurements of Böttner et al. to much larger scattering angles. Measurements were performed at E_{cm} = 8.4 and 16.8 eV for $Li^+–N_2$, and at E_{cm} = 7.3 and 15.3 eV for Li^+–CO. In the case of $Li^+–N_2$, one low-energy-loss and one high-energy-loss peak were observed in the time-of-flight spectra. In Li^+–CO, although a bimodal energy-loss distribution was observed at small scattering angles (in agreement with the data of Böttner et al.), one low- and two high-energy-loss peaks were observed at larger scattering angles. These observations were reproduced by classical trajectory calculations[65] assuming impulsive energy transfer between the Li^+ ions and the cigar-shaped diatomic molecules. The high-energy-loss peaks are associated with the so-called "rotational rainbow" phenomenon, which was actually discovered[64a] in connection with theoretical attempts to reproduce the data of Böttner et al. We shall not discuss rotational rainbow theory here.[66] However, we note that two high-energy-loss peaks are observed for CO, as opposed to one for N_2, because different amounts of momentum are transfered depending on whether the Li^+ ion strikes the carbon or oxygen end of the CO molecule (more momentum is transfered to the carbon end). The low-energy-loss peak in each case results from near central collisions.

Gierz et al.[65] concluded from their trajectory calculations that probably 70–80% of the total energy transfer goes into rotation. Unfortunately, the accompanying vibrational excitation cannot be clearly distinguished from the more predominant rotational energy loss features.

Finally, we note recent work by Hege and Linder[67] on the forward inelastic scattering of H^- ions from H_2, N_2, and O_2. The mechanism of vibrational excitation in these cases involves transient charge transfer from H^- to an antibonding orbital of the target molecule, resulting in a bond-stretching force during the collision. The transient charge-transfer mehanism in $H^–H_2$ was found to be less efficient than the bond dilution mechanism in $H^+–H_2$ at producing vibrational excitation. However, more vibrational excitation was observed in $H^–N_2$ than in $H^+–N_2$ collisions.

4. Ion–Polyatomic Molecule Systems

A number of fascinating studies of vibrationally inelastic scattering of atomic ions from polyatomic target molecules have been reported. Protons, deuterons, and alkali ions (mainly Li^+) have been used as projectiles, and the target molecules include the triatomics CO_2 and N_2O, the spherical top molecules CH_4, CF_4, and SF_6, and a number of small fluorohydrocarbons.[68] The existence of many vibrational degrees of freedom in polyatomic molecules raises a number of new questions, including the following: How mode-selective is the vibrational excitation? Does the pattern of vibrational excitation depend on collision energy and scattering angle? To what extent can the vibrationally inelastic scattering be understood in terms of the properties of the isolated molecule, and to what extent are more subtle details of the ion–molecule interaction potential important? Do anharmonic couplings between vibrational modes influence the pattern of vibrational excitation? All of these questions have been answered (sometimes qualitatively, sometime more quantitatively) by the scattering experiments.

Before reviewing the experimental results in detail, we offer a few summary observations to provide perspective. First, a surprising degree of mode selectivity has been observed in some of the ion–polyatomic molecule systems. The mode selectivity is higher with H^+ or D^+ projectiles than with alkali ion projectiles. Second, both the pattern and the magnitude of the vibrational excitation can be strong functions of the collision energy and scattering angle. Third, as mentioned in the preceding subsection, many of the experimental results can be rationalized using a simple model in which the vibrationally inelastic transitions are viewed as "spectroscopic transitions" induced by the electric field of the passing ion. In this view, the intramolecular properties of the polyatomic molecule (dipole moment derivatives, polarizability, etc.) mainly determine the inelastic scattering. However, a quantitative description of the experimental results, particularly at large scattering angles, requires that the details of the ion–molecule interaction potential (including the short-range repulsive interactions) be taken explicitly into account. Finally, there is no strong evidence that intramolecular anharmonic couplings are important in determining the vibrational excitation patterns.

CO_2 and N_2O. In 1977 Krutein and Linder[69] reported results on state-to-state vibrationally inelastic scattering in the $H^+–CO_2$ system. The CO_2 vibrational levels will be referred to using the usual labels, (v_1, v_2, v_3), where v_1, v_2, and v_3 are the number of quanta in the symmetric stretching mode (ν_1 = 1338 cm^{-1} = 0.166 eV), the doubly degenerate bending mode (ν_2 = 667 cm^{-1} = 0.083 eV), and the asymmetric stretching mode (ν_3 = 2349 cm^{-1} = 0.291 eV), respectively. Krutein and Lin-

der performed measurements at three c.m. collision energies (14.7, 28.8, and 48.9 eV) and at c.m. scattering angles between 0° and the rainbow region. For reference, the rainbow angle is approximately 18°, 9°, and 5.5° at E_{cm} = 14.7, 28.8, and 48.9 eV, respectively. (The small difference between laboratory and c.m. scattering angles in this system is less than the experimental angular resolution and can be ignored.)

Krutein and Linder[69] observed strong variations in the pattern of CO_2 vibrational excitation as a function of collision energy and scattering angle. In the small-angle region near $\theta = 0°$, (010) bending-mode excitation is the dominant inelastic process. Some (001) asymmetric stretch excitation is also observed at $\theta = 0°$, and this becomes relatively more important at the higher collision energies. At larger scattering angles, the pattern of vibrational excitation changes dramatically. At the lowest collision energy, 14.7 eV, mainly the fundamental modes of CO_2 are excited; the (001) and (100) transition probabilities increase monotonically with the scattering angle, while the (010) transition probability is nearly independent of angle. Eventually, the transition probabilities assume the order $P_{001} > P_{100} > P_{010}$. [Note: although the (100) and (020) levels are nearly degenerate and are mixed by a strong Fermi resonance, the different angular dependence of the 0.083 and 0.170 eV energy loss peaks suggests that the latter is mainly due to the symmetric stretch component of the (100)/(020) Fermi resonance pair.] At the two higher collision energies, asymmetric stretch excitation accounts for nearly all of the large-angle inelastic scattering, especially in the rainbow region. Both the fundamental and first two overtones of the asymmetric stretch are observed. Krutein and Linder present differential cross sections for the (001), (002), and (003) inelastic transitions at E_{cm} = 28.8 eV. All three roughly follow the shape of the elastic differential cross section, including rainbow structure, but the inelastic cross sections fall off less rapidly with scattering angle. At $\theta = 9°$, the ratio of (000):(001):(002):(003) differential cross sections is approximately 1.0:0.9:0.6:0.2. A weaker series of (10 υ_3) excitation peaks is also observed in the energy loss spectra at 28.8 eV, but little or no evidence for bending excitation can be seen in the rainbow region.

More detailed measurements of the forward ($\theta = 0 \pm 0.5°$) inelastic scattering of H^+ and D^+ from CO_2 were reported by Bischof et al.[70] in 1982. One purpose of this work was to separate "time effects" from "interaction effects" in the vibrationally inelastic scattering. Since most of the inelastic scattering at $\theta = 0°$ is due to large impact parameter collisions, only the longest-range part of the interaction potential, the charge–dipole interaction, should be important. The interaction is, of course, identical for H^+ and D^+, and the nature of the interaction should remain the same over a wide range of collision energies. Thus, any differences between H^+ and D^+ scattering at the same collision energy may be attributed to the different interaction times of the two ions.

The vibrational coupling is mainly due to the linear terms in the usual Taylor series expansion of the dipole moment operator:

$$\mu = \sum_k \frac{\partial \mu}{\partial Q_k} Q_k$$

The absence of symmetric stretch excitation in the forward inelastic scattering is readily understood since this motion give a vanishing dipole derivative. Although the asymmetric stretch has a larger dipole moment derivative than the bend, the lower frequency bending vibration is favored on energetic grounds. A simple Born approximation calculation predicts a (010):(001) ratio of about 3:1 in the forward direction. Bischof et al.[70] found that the (010):(001) ratio for both H^+ and D^+ projectiles actually converged to the Born approximation result at the highest collision energies. As the collision energy was lowered, the (010):(001) ratio increased (in agreement with the earlier results of Krutein and Linder), and the ratio was always higher for D^+ than for H^+ at the same collision energy. But when Bischof et al. plotted the *same* data as a function of the relative collision *velocity*, the H^+ and D^+ ratios fell on the same smooth curve, demonstrating that the duration of the collision is crucial in determining the pattern of forward inelastic scattering in this system. Bischof et al.[70] and Richards[61] were able to reproduce the observed velocity dependence of tne (010):(001) ratio in forward inelastic scattering using a variant of the semiclassical forced-oscillator model with only charge–dipole vibrational coupling. Besides the dominant (010) and (001) excitation, Bischof et al.[70] also observed many weak overtones and combination levels in the forward inelastic scattering, as illustrated in Figure 2. A detailed analysis of the forces responsible for these weak excitations has not been attempted.

The interactions responsible for H^+–CO_2 inelastic scattering at larger scattering angles, particularly in the rainbow region, are clearly more involved than just a charge–dipole interaction. The most interesting result at large angles is the dominance of asymmetric stretching excitation over bending excitation. Krutein and Linder[69] suggested that a valence interaction similar to the $H^+ + H_2$ "bond dilution" mechanism might be responsible for this behavior. Ab initio calculations on the protonated CO_2 species[71] lend some support to this idea. According to theory, the minimum energy geometry has H^+ bonded to one of the oxygens (with a C–O–H bond angle of 117°), and the C–O bond adjacent to the proton is predicted to undergo a 0.06 Å expansion while the other C–O bond undergoes a 0.04 Å contraction. It is easy to see how this could result in selective excitation of the asymmetric stretch in the inelastic scattering experiment. [The Goettingen group has recently obtained evidence for a sizeable contribution of charge-transfer intermediates to the observed ν_1-mode excitation in H^+–CO_2 collisions (J. P. Toennies, private communication).]

The forward inelastic scattering of H^- ions from CO_2 has also been studied by Hege and Linder.[67] The results are very similar for H^-–CO_2 and H^+–CO_2, confirming that the vibrational excitation in forward scattering is mainly due to the long-range dipole interaction in both cases.

Most of the remaining work to be discussed has been carried out by the Goettingen group using pulsed ion beams and time-of-flight (TOF) methods.

In 1977, Eastes, Ross, and Toennies[72] reported measurements of Li^+ scattering from CO_2 and N_2O at c.m. collision energies between 2.8 and 6.9 eV. The effective potential well depth is ~0.5 eV for these systems (much

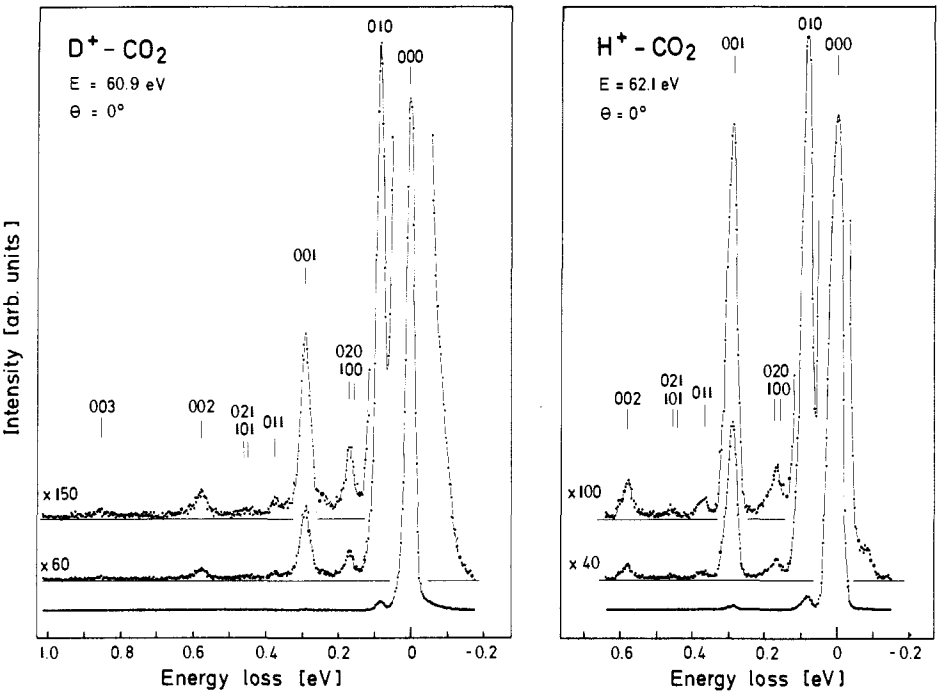

Figure 2. Energy loss spectra for D^+–CO_2 and H^+–CO_2 forward inelastic scattering at $E_{cm} \approx 60$ eV (Bischof et al., ref 70). Excitation of the (010) bending mode dominates in both cases. However, the relative peak intensities are significantly different in the two spectra because of interaction time effects. Reproduced with permission from ref 70. Copyright 1982 Institute of Physics.

smaller than in H^+–CO_2) and leads to a c.m. rainbow angle of only 9° at $E_{cm} = 4.7$ eV. Eastes et al. were able to resolve inelastic from elastic scattering only at angles larger than the rainbow angle. The experimental results clearly show more inelastic scattering in Li^+–CO_2 collisions than in Li^+–N_2O collisions under the same conditions of collision energy and scattering angle. Howver, the vibrationally inelastic peaks are not nearly as well resolved in the present data as in the H^+–CO_2 results discussed earlier. Except for two partially resolved inelastic peaks in the Li^+–CO_2 TOF spectra, which are probably due to (010) and (020)/(100) vibrational excitation, the assignment of the inelastic scattering is ambiguous. Eastes et al.[72] concluded that practically all of the inelastic scattering was due to vibrational excitation, since only a minor broadening of the elastic peak due to rotational excitation was observed in the TOF spectra. This conclusion should be scrutinized carefully. The most recent results on Li^+–N_2,CO scattering, discussed earlier, show that impulsive rotational energy transfer accounts for >70% of the total energy transfer in these systems. If anything, we would expect rotational energy transfer to be even more important in CO_2 and N_2O since they present more "extended" ellipsoidal targets to the Li^+ projectile. Perhaps the greater inelasticity observed in Li^+–CO_2 compared to Li^+–N_2O is also related to differences in the rotational, rather than vibrational, energy transfer. Additional experimental and theoretical work is needed on these systems.

CH_4, CF_4, and SF_6. A clearer picture emerges from an extensive body of work on the scattering of Li^+, H^+, and D^+ ions from the spherical top molecules CH_4, CF_4, and SF_6. All combinations except D^+–CH_4 have been studied experimentally. Spherical top molecules were chosen, in part, to minimize the complications caused by rotational energy transfer. As it turns out, the system with the largest propensity for rotationally inelastic scattering, Li^+–CH_4, was chosen first for study. Consequently, vibrational structure in the Li^+–CH_4 TOF spectra measured by Eastes et al.[73] is not very well resolved. Eastes et al.[73] used a statistical model to explain the apparent lack of selectivity in the CH_4 vibrational excitation. Subsequent theoretical calculations by Ellenbroek and Toennies, to be discussed shortly, suggest that the vibrational excitation in Li^+–CH_4 collisions may actually be highly selective, but hard to observe experimentally due to an unexpectedly large contribution from rotationally inelastic scattering. Therefore, we shall not discuss the Li^+–CH_4 results further.

After this experience with CH_4, the first results on Li^+ and H^+ scattering from SF_6 molecules came as a pleasant surprise. The TOF spectra measured by Ellenbroek, Gierz, and Toennies[74] showed a series of reasonably well-resolved, equally-spaced peaks, indicating that one vibrational mode is mainly contributing in each case. SF_6 has two infrared active vibrational modes, ν_3 and ν_4 (both triply degenerate), with ν_3 being the strongest. The Li^+–SF_6 TOF results were fit very well assuming a Poisson distribution in the ν_4 mode (although the infrared-inactive ν_2 mode, which has a similar frequency to ν_4, could not be ruled out). The H^+–SF_6 results could only be fit by assuming ν_3-mode excitation. The distribution in this case appeared not to agree so well with a Poisson distribution, but later results[75] showed that this was an artifact caused by some "blast through" of the tails of the unscattered primary ion beam. In fact, the vibrational distribution is close to Poisson in both cases. The preferential excitation of the lower frequency ν_4 mode by the "slower" Li^+ ions was originally attributed to an interaction-time effect by Ellenbroek, Gierz, and Toennies.[74] This interpretation has been criticized by Linder and coworkers,[70] who argue that specific details of the interaction should dominate time effects in the range of

scattering angles explored by the Li^+–SF_6 measurements.

Most of the experimental results on ion scattering from CH_4, CF_4, and SF_6 are summarized in a 1982 paper by Ellenbroek et al.[75] The experiments were performed at c.m. collision energies in the range 4–10 eV, and most of the TOF spectra were measured at c.m. scattering angles between 5° and 15°. Since the spherically averaged potentials for the $H^+(D^+)$–CH_4, $-CF_4$, $-SF_6$ systems have fairly deep wells (ϵ = 3.6–3.8 eV), the rainbow angles are large (θ_{RB} = 25°–30° at E_{cm} = 10 eV). Therefore, all of the H^+,D^+ TOF data pertains to scattering angles much less than the rainbow angle, where the inelastic scattering should be mainly determined by the long-range part of the interaction potential. The much smaller well depths (ϵ = 0.38–0.50 eV) of the spherically averaged Li^+–CH_4, $-CF_4$, $-SF_6$ potentials, on the other hand, result in smaller rainbow angles (θ_{RB} = 8° at E_{cm} = 10 eV, increasing to 20° at E_{cm} = 4 eV). Since some of the Li^+ TOF spectra were measured in the rainbow region, the Li^+ results are expected to show a greater sensitivity to the short-range potential, especially the repulsive part of the potential.

Ellenbroek et al.[75] analyzed each TOF spectrum using a procedure similar to that described earlier. First the average total energy transfer, $\langle \Delta E_{tot} \rangle$, was obtained by a direct integration of the TOF spectrum. Then, vibrational transition probabilities, $P(0 \rightarrow n)$, were found for the single vibrational mode that best fit the structure in the TOF spectrum, and the "mode-selective" vibrational energy transfer was calculated from

$$\langle \Delta E_{vib} \rangle = \hbar \omega_k \sum_n n \cdot P(0 \rightarrow n)$$

The difference between $\langle \Delta E_{tot} \rangle$ and $\langle \Delta E_{vib} \rangle$, referred to as the residual energy transfer $\langle \Delta E_{res} \rangle$ by Ellenbroek et al.,[75] represents rotational excitation as well as unresolved vibrational excitation in other vibrational modes. The smaller $\langle \Delta E_{res} \rangle$, the higher the degree of mode selectivity.

In all three molecules, only the triply degenerate ν_3 and ν_4 modes are infrared-active. In each case also the ν_3 mode has the highest frequency and the largest dipole moment derivative. By far the best resolved TOF spectra were obtained for H^+,D^+ scattering from CF_4, where ν_3 excitation clearly dominates. At E_{cm} = 9.7 eV and θ_{cm} = 10°, the average ν_3 vibrational excitation energy was determined to be $\langle \Delta E_{vib} \rangle$ = 0.25 eV for both H^+ and D^+ projectiles, or 2.6% of the available energy. $\langle \Delta E_{vib} \rangle$ was observed to increase monotonically with scattering angle over the range studied. Although differential cross sections were not reported in this work, we assume that the inelastic differential cross sections actually decrease with increasing scattering angle. The ν_3 mode also appears to be excited very selectively in H^+,D^+–SF_6 collisions. The SF_6 spectra are not as well resolved, however, because of the lower ν_3 frequency in SF_6 compared to CF_4. The average ν_3 vibrational excitation energy is similar for CF_4 and SF_6 at the same collision energy and scattering angle.

The Li^+–CF_4 results were best fit by assuming mainly ν_2 excitation at E_{cm} = 3.8 and 4.7 eV, and mainly ν_3 excitation at E_{cm} = 9.5 eV. The Li^+–SF_6 results at E_{cm} = 4.4 and 6.4 eV were best fit assuming mainly ν_4 excitation, and measurements at higher energies were not reported.

The H^+–CH_4 system, like Li^+–CH_4, exhibits more complicated behavior, and the analysis of the data is much less certain. In an early low-resolution study, Gentry, Udseth, and Giese[76] observed a large average excitation energy of ~1.8 eV in H^+–CH_4 collisions at E_{cm} = 20 eV, θ_{cm} = 10°; since the ionization potential of CH_4 is less than that of H, these authors postulated that an intermediate charge transfer mechanism, involving "surface hopping" between the $H^+ + CH_4$ and $H + CH_4^+$ potential energy surfaces, might be responsible for the large observed energy transfer. At E_{cm} = 9.2 eV, θ_{cm} = 10°, Ellenbroek et al.[75] observed a much lower energy transfer of 0.14 eV, so the importance of intermediate charge transfer at this lower collision energy is not clear. (The Goettingen group also studied H^+–CH_4 inelastic scattering at E_{cm} = 20 eV and obtained results in good agreement with those of Gentry, Udseth, and Giese (J. P. Toennies, private communication; M. Noll, Ph.D. Thesis, Goettingen, 1985). The collision energy dependence of the average CH_4 excitation energy suggests that there may be a sharp threshold for the $H^+ + CH_4 \rightarrow H + CH_4^+$ charge-transfer channel.) In any case, it is clear that a single vibrational mode does not stand out prominently in H^+–CH_4 and Li^+–CH_4 inelastic scattering.

A detailed semiclassical model for the vibrational excitation of spherical top molecules by ions was developed by Ellenbroek and Toennies[77] in connection with the above experimental work. Their model involves an extension of the usual forced-oscillator theory to polyatomic molecules, with the polyatomic normal modes treated as independent harmonic oscillators. As in the DECENT model, the quantum vibrational transition probabilities are calculated using the reduced classical energy transfer and the classical-quantal correspondence principle, and the reduced classical energy transfer into each polyatomic normal mode is calculated "exactly" by running trajectories on a realistic potential energy surface. If the driving force on each normal vibrational mode is only a function of time, then the quantum vibrational transition probabilities should be given by a simple product of Poisson distributions, one for each mode. In particular, the probability of exciting n_k quanta in mode k with no quanta in any other modes is given by

$$P[0 \rightarrow (0,...,n_k,...,0)] = \frac{1}{n_k!} \epsilon_k^{n_k} e^{-\epsilon_k} \prod_{l \neq k} e^{-\epsilon_l}$$

where $\epsilon_k = \Delta E_k / \hbar \omega_k$ is the reduced classical energy transfer into mode k, and similarly for the ϵ_l's. If mode k is exclusively excited, all of the ϵ_l are zero and a simple Poisson distribution results. If several modes are excited, the dominant mode k should still appear as a Poisson distribution but with all transition probabilities reduced by a constant factor. If mode k is degenerate, the above formula still holds, but ΔE_k now represents the sum of the classical energy transfers into each of the degenerate components.

Ellenbroek and Toennies[77] included both long-range and short-range interactions in their model. The long-range potential, $V_{long}(R)$, was expanded in terms of the electric field produced by the ion at the molecule (i.e., a multipole expansion). The main vibrational coupling terms in $V_{long}(R)$ involve the derivatives of the dipole moment, quadrupole moment, and polarizability with respect to the normal vibrational coordinates. The

short-range potential, $V_{short}(R)$, was approximated by a sum of exponentially repulsive interactions between the ion and the $N-1$ outer atoms of the spherical top molecule. Note that $V_{short}(R)$ depends on both the molecular orientation and (in a rather complicated way) on the vibrational normal coordinates. Additional spherically symmetric $1/R^8$ repulsive and $1/R^6$ attractive terms were added to the potential to fit the location and depth of the potential well. (These extra terms in themselves do not lead to vibrational excitation, but they affect the course of the ion trajectories and thereby influence the electric field and the vibrational coupling.) As far as possible, independent experimental data was used to fix the parameters in the long-range and short-range potentials.

With the interaction potential specified, it is a straightforward task to integrate the classical equations of motion. To save computation time, Ellenbroek and Toennies[77] only considered scattering in a σ_v plane of the XY_4 and XY_6 molecules (by symmetry, no out-of-plane forces are generated in this plane). However, all impact parameters and angles of approach within this plane were considered. The main results of the trajectory calculations are the energy transfer into each vibrational mode, and into rotation, as a function of the final c.m. scattering angle.

For the $H^+(D^+)$–CF_4, SF_6 systems, the calculations predict that more than 90% of the transferred energy is deposited in the ν_3 mode, in excellent agreement with the experiments. For $H^+(D^+)$–CH_4, although the total calculated energy transfer agrees nicely with experiment, there is not a strong preferential excitation of a single vibrational mode. The calculations predict that the largest amount of energy should be transferred to the ν_1 mode by the induced polarizability (Raman) term in the long-range potential. Ellenbroek and Toennies[77] found that the short-range part of the potential was unimportant in the H^+,D^+ systems over the range of energies and scattering angles explored by the experiments.

For all of the Li^+ systems, on the other hand, the short-range repulsive interactions were important to include in the scattering calculations, especially at angles larger than the rainbow angle. The repulsive forces result in more rotational excitation and less mode-selective vibrational excitation. For Li^+–CH_4 collisions at E_{cm} = 3.8 eV, the theoretical calculations predict roughly equal amounts of excitation energy in ν_2, ν_3, ν_4, and rotation, with a smaller contribution from ν_1. In contrast, the experimental TOF data at this energy were fit assuming mainly ν_2 excitation. At least part of this discrepancy can be explained as follows: since the ν_2 mode is lowest in frequency, the reduced classical energy transfer $\epsilon_2 = \Delta E_2/\hbar\omega_2$ is largest for it; therefore ν_2 gives the largest peak in the theoretical TOF spectra. However, it must be acknowledged that the single-mode fits to some of the less well-resolved TOF spectra involve quite a bit of ambiguity and are probably not unique. For Li^+–CF_4 collisions at E_{cm} = 9.4 eV, experiment and theory agree that ν_3 excitation dominates. But again, the calculated mode selectivity is not as great as was assumed in the fits to the experimental TOF data (e.g., at $\theta_{cm} = 20°$, ν_3 accounts for 42% of the total energy transfer, according to the theory).

Unfortunately, the discussion of the theoretical Li^+–SF_6 results in ref 77 is confusing. According to the tables, ν_3 and ν_4 are preferentially excited at all collision energies studied, and while ν_4 is slightly favored at 4.4 eV, ν_3 becomes dominant at higher collision energies. (Recall that the experimental TOF results, available only at 4.4 and 6.4 eV, were fit assuming ν_4 excitation, although ν_2 excitation could not be ruled out due to its similar vibrational frequency). However, Ellenbroek and Toennies[77] later claim that their theory "yields a predominant contribution from the ν_2 mode and not from the ν_4 mode," and that "the other long-range optical coupling terms and to a small extent the short-range repulsive coupling shift the energy transfer to the ν_2 mode." (The results given in the tables of ref 77 are, in fact, correct (J. P. Toennies, private communication).)

Compared to the other systems, the Li^+–CH_4 system is by far the most anisotropic, and the long-range potential alone fails completely to describe the experimental results. This anisotropy, combined with the large CH_4 rotational constant, leads to a surprisingly large amount of rotational excitation. For example, at E_{cm} = 4.9 eV and $\theta_{cm} = 20°$, the calculated rotational excitation energy is just over half of the total excitation energy of 0.84 eV. The vibrational excitation energy of 0.41 eV is mainly deposited in the two lowest frequency vibrational modes of CH_4, ν_2 and ν_4, according to the model calculations. These results argue strongly against the statistical model used by Eastes et al.[73] and explain why so little structure was observed in the experimental TOF distributions for this system.

Overall, the agreement between experiment and the semiclassical model calculations of Ellenbroek and Toennies[77] is satisfying. The model is attractive from an intuitive standpoint because it is easy to identify the main sources of the vibrational coupling in the multipole expansion of the ion–molecule interaction potential (although some might argue that a multipole expansion is not really valid at the rather small interaction distances involved in some of the scattering experiments).

Additional work on ion scattering from CF_4 and SF_6 has been reported by the Goettingen group.[78-80] By running the target beam without a skimmer, the sensitivity of the apparatus was greatly improved and it became possible to detect energy-loss contributions from trajectories probing the repulsive part of the interaction potential. Noll and Toennies[78] studied H^+–CF_4 scattering at E_{cm} = 18.3 eV and c.m. scattering angles between 5° and 14° (all less than the rainbow angle, expected at 20°). They found that each TOF spectrum could be fit with two Poisson distributions, each involving only the ν_3 mode. The first (lower ΔE) distribution is the same as that observed in the earlier work; this distribution shows an increasing energy loss with increasing scattering angle. The second (higher ΔE) distribution shows an energy loss nearly independent of scattering angle. A typical TOF spectrum is shown in Figure 3. ν_3 overtone levels up to $v = 10$ are clearly observed, with some partially resolved but not uniquely assignable structure at even higher energy transfers! Similar results have also been observed in high-energy H^+–SF_6 collisions.[79] At small scattering angles, there are three contributions from the classical deflection function, two corresponding to close-in, small impact parameter collisions, and one corresponding to larger impact parameter, grazing collisions. With the help of trajectory calculations, Toennies and co-work-

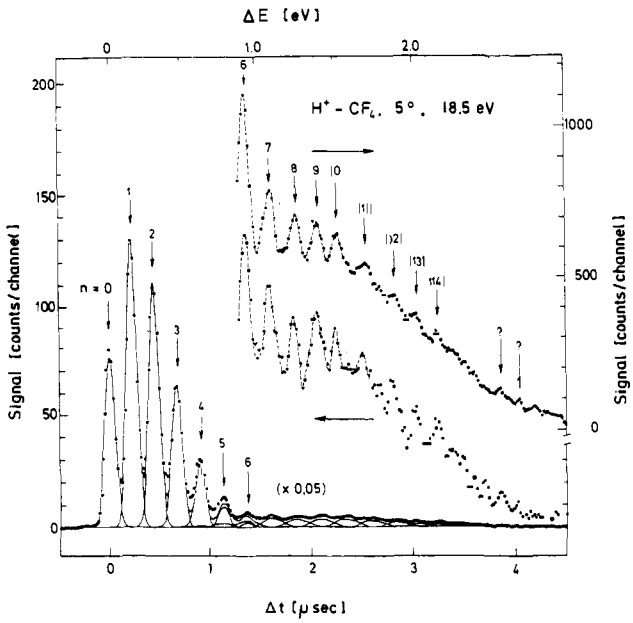

Figure 3. High-resolution time-of-flight spectra for proton inelastic scattering from CF_4 molecules at a laboratory collision energy of 18.5 eV and a lab scattering angle of 5° (Noll and Toennies, ref 78; Gierz, Noll, and Toennies, ref 79). Longer flight times correspond to larger energy transfers from the proton to the CF_4. The middle spectrum at the right is a 20× blow-up of the lower spectrum and represents a single 6-h measurement, while the upper spectrum is the average of 8 6-h measurements. Excitation of up to 10 quanta in the ν_3 mode of CF_4 is clearly observed. Reproduced with permission from ref 79. Copyright 1985 American Institute of Physics.)

ers[78-79] were able to attribute the large ΔE and small ΔE Poisson distributions to the close-in and grazing collisions, respectively. Impulsive energy transfer is not important due to the small H^+:F mass ratio. The trajectory calculations showed that, in many of the small impact parameter collisions, the protons actually passed between the outer F atoms of the CF_4 and SF_6 molecules.

Evidence for impulsive energy transfer has been observed, however, in Na^+–CF_4 collisions at large scattering angles. Gierz et al.[80] performed low-resolution TOF measurements on this system at c.m. collision energies between 4–24 eV and at laboratory scattering angles between 20°–70°. Two peaks were seen in each TOF spectrum. The first peak with smaller energy loss was assigned to mode-selective vibrational excitation. However, the second peak could not be explained by any interaction of the Na^+ ion with the entire CF_4 molecule. A simple kinematic analysis[80] showed that the second peak was due to Na^+ elastic scattering from single F atoms in the CF_4 molecule. (This behavior is similar to that described previously for Li^+–N_2, CO collisions.) Of course, the collision is not really elastic. The energy is initially transferred to just one F atom, which then bangs into the rest of the molecule, exciting it vibrationally and rotationally. At the larger collision energies and scattering angles, this impulsive mechanism transfers more than enough energy to dissociate the CF_3–F bond.

Fluorohydrocarbons. In a recent study, Gierz, Noll, and Toennies[81] have shown that the phenomenon of mode-selective vibrational excitation is not unique to highly symmetrical molecules such as CO_2, CF_4, and SF_6. Gierz et al. compared the inelastic scattering of protons from the fluorohydrocarbon molecules CH_4, CH_3F, CH_2F_2, CHF_3, CF_4, C_2H_4, C_2H_3F, $C_2H_2F_2$, C_2HF_3, C_2F_4, and C_2F_6. All of the molecules have at least one strong IR-active mode (a C–F stretch in most cases) with a mode energy of 110–160 meV (900–1300 cm^{-1}). For each system, TOF spectra were measured at several scattering angles between 5° and 20° at a c.m. collision energy of 9.8 eV. Not surprisingly, the results on CH_4, C_2H_4, and the slightly fluorinated molecules are complicated; although several peaks and/or shoulders are observed in the energy loss distributions, the assignments are somewhat uncertain. In contrast, the energy loss distributions for the highly fluorinated molecules show three or more regularly spaced maxima with a spacing characteristic of one or more C–F stretching (or C–F–H deformation) modes. The relative magnitudes of the measured energy transfers correlate well with absolute IR intensities (in cases where these are known). While it is unlikely that proton inelastic scattering is going to replace more conventional methods of vibrational spectroscopy, the scattering technique is extremely interesting and hopefully will be extended to a wider variety of polyatomic molecules.

B. Energy-Change Experiments (Neutrals)

The first detailed studies of state-to-state rotationally inelastic scattering by the energy-change method were reported in 1977. Since then, an enormous amount of experimental and theoretical work has been done in this area. The systems for which state-resolved rotationally inelastic differential cross sections are available include He + HD,[82] Ne + HD,[83] Ne + D_2,[84] Ar + D_2,[85] HD + HD,[86] HD + D_2,[87] H_2 + D_2,[88] He + N_2,[89,90] He + CO,[89] He + O_2,[91] and He + CH_4.[89,92] Differential energy loss distributions (without rotational state resolution) have also been reported for a large number of systems. The early work has been thoroughly reviewed by Loesch.[93] Systems that have been studied since 1980 include Ar + CO,O_2,[94] Ar + Cl_2,[95] D_2 + CO,[96] Xe + CO_2,[97] Ne + CH_4,[98] Ar + CH_4,[99] He + NH_3,[100] and Ar,Kr + SF_6.[101]

In contrast, very little work on vibrationally inelastic scattering in neutral systems by the energy-change method has been reported, and none of this work has been at the "state-to-state" level. Part of the problem has to do with the small cross sections for vibrational excitation at experimentally attainable collision energies and the lower detection sensitivity of the energy-change method for neutrals. Therefore, the problem of distinguishing vibrational from rotational excitation (already nonnegligible in many of the ion scattering experiments) is aggravated even further in neutral energy-change experiments.

Energy-change studies of vibrational and rotational deexcitation of hot KBr molecules by a variety of collision partners were performed by Fisk and co-workers[102] in the 1970's using a "triple-beam" arrangement. Beams of K atoms and Br_2 molecules were first crossed to generate rotationally and vibrationally hot KBr molecules by chemical reaction. Part of the KBr product beam was then crossed with a third molecular beam containing the energy-transfer partner, and the angular and velocity distributions of the scattered KBr molecules were measured using a rotatable surface ionization detector and velocity selector. Direct T →

V,R excitation of alkali halide molecules by rare gas atoms was also studied extensively in the 1970's.[103] The energy transfer in these systems is extremely facile. At hyperthermal collision energies, efficient collision-induced dissociation of the alkali halide molecules into ion pairs occurs.[104]

The most ambitious attempt so far to apply the energy-change method to vibrational excitation in a neutral system was reported by Eccles et al.[105] in 1984. These workers chose to study Ar scattering from SF_6 molecules, originally in the hope that the probability of rotational excitation would be minimized for the octahedral SF_6 molecule. More recent results have shown, however, that the Ar–SF_6 interaction potential is quite anisotropic, so there is still a lot of rotational excitation in this system.

The apparatus used by Eccles et al.[105] involves a novel design in which two nozzles and skimmers are mounted in a common source chamber, which is connected by a rotating seal to a large, stationary diffusion pump. The skimmed molecular beams of Ar and SF_6 crossed at 90° in the main vacuum chamber, and scattered SF_6 molecules were detected in the plane of the molecular beams by a differentially pumped, ultrahigh vacuum mass spectrometer. The laboratory scattering angle was varied by rotating the common source chamber about the interaction zone while the detector remained fixed. TOF distributions of the scattered molecules were measured using a standard technique.

To enhance the probability of vibrationally inelastic scattering, Eccles et al.[105] used the seeded beam method to achieve hyperthermal collision energies. For 1% mixtures of SF_6 in He and H_2 carrier gas (and nozzle temperatures around 500 K), terminal SF_6 beam velocities of 2.04×10^5 and 2.45×10^5 cm/s, respectively, were obtained. The Ar beam was run pure at room temperature and had a most probable velocity of 5.6×10^4 cm/s. Thus, the c.m. Ar–SF_6 collision energies were 0.73 and 1.05 eV for the He-seeded and H_2-seeded SF_6 beams.

It turns out (accidentally) that the kinematics of the SF_6–Ar system are similar to those of the Li^+–H_2 system discussed earlier. Thus, all of the SF_6 elastic and inelastic scattering is confined to a fairly narrow cone, ±20° about the incident SF_6 beam direction, and at each laboratory scattering angle both forward and backward c.m. scattering are observed. Angular and TOF distributions were measured over the entire range of accessible scattering angles. A typical TOF spectrum obtained at $E_{cm} = 0.73$ eV is shown in Figure 4. For comparison, a TOF spectrum for Xe–Ar scattering measured at approximately the same collision energy and scattering angle is also shown. (Since the masses of SF_6 and Xe are similar, so are the kinematics.) In the case of the Xe–Ar elastic scattering the c.m. forward and backward peaks are clearly separated. In the SF_6–Ar scattering, the forward and backward peaks merge into a single broad peak indicating considerable inelastic scattering.

The entire set of data at each collision energy was transformed into the c.m. system to obtain the total (sum over all final states) differential cross section and the fractional average excitation energy, $\Delta E/E_{cm}$, as a function of c.m. scattering angle. The results at the two collision energies were similar. The total differential cross sections were found to decrease by about a factor

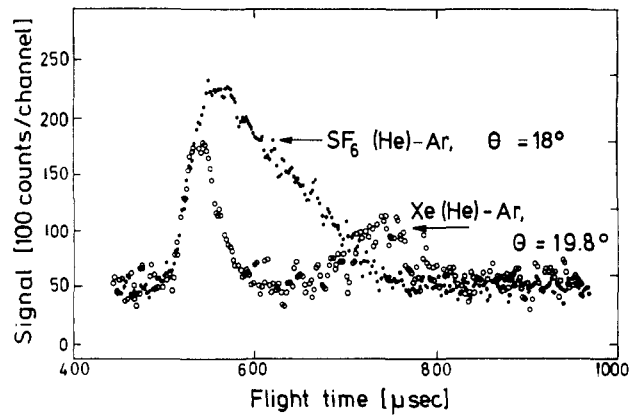

Figure 4. Time-of-flight spectra for SF_6–Ar and Xe–Ar scattering under nearly identical conditions of collision energy and scattering angle (Eccles et al., ref 105). In each system, the heavier species was detected using an ultrahigh vacuum mass spectrometer. Both SF_6 ($m = 146$) and Xe ($m = 131$) were seeded in He to achieve collision energies around 0.7 eV. In the Xe–Ar elastic scattering, the forward and backward c.m. peaks are clearly separated. In the SF_6–Ar scattering, the forward and backward peaks merge into one, indicating considerable inelastic scattering. Reproduced with permission from ref 105. Copyright 1984 North-Holland Physics Publishing.

of 50 between $\theta_{cm} = 20°$ and 180°, while $\Delta E/E_{cm}$ increased from a minimum of about 10% at $\theta_{cm} = 20°$ to a maximum of ~40% at $\theta_{cm} = 140°$. Beyond this there was a definite drop to $\Delta E/E_{cm} = 30\%$ at $\theta_{cm} = 180°$. It is not possible, solely on the basis of the experimental results, to determine the relative importance of rotational and vibrational excitation.

Motivated by the experimental work, Billing[106] carried out a detailed semiclassical study of the energy transfer in Ar + SF_6 collisions at $E_{cm} = 1$ eV. The potential energy surface was represented as the sum of an intramolecular part (the vibrational force field of the isolated SF_6 molecule as determined from spectroscopy) and an intermolecular part (determined empirically from transport properties and low-energy differential cross section data[101]). Billing made an approximate fit to the intermolecular potential in terms of additive Ar–F interactions, in order to extract the normal mode dependence, and then he expanded the potential up to second-order in the vibrational normal coordinates. Anharmonic terms in the intramolecular potential were neglected, partly because they would be very expensive to include in the calculation, and partly because they were not expected to be very important anyway for vibrational excitation from the ground vibrational state. With these approximations, three-dimensional classical trajectories were integrated to obtain the rotational and vibrational energy transfer as a function of scattering angle. Quantum vibrational transition probabilities were derived from the classical energy transfers in the usual way.

Billing[106] obtained excellent, quantitative agreement with the experimental fractional excitation energy over the entire range of scattering angles. His results show that ΔE_{rot} and ΔE_{vib} are nearly equal over a wide angular range, with ΔE_{rot} dominating slightly at scattering angles less than 70° and ΔE_{vib} dominating at angles greater than 130°. The calculations indicate that ΔE_{vib} increases monotonically with increasing scattering angle, becoming almost constant for $\theta_{cm} > 130°$. The small

drop in the total energy transfer at the largest scattering angles is entirely due to a decrease in ΔE_{rot}. The vibrational excitation is predicted to be highly mode-selective, with the lowest frequency ν_6 mode soaking up at least 80% of ΔE_{vib} at all angles; the second lowest frequency mode, ν_5, receives about half of the remaining vibrational energy, although (ν_5, ν_6) combination levels are more probable than ν_5 overtones, according to theory. This high selectivity for the two lowest frequency modes seems somewhat surprising, in view of the fact that the highest and lowest frequency modes of SF_6 differ in frequency by less than a factor of three.

The interplay between theory and experiment, demonstrated here for the Ar + SF_6 system, is very encouraging. It is clear that in most energy-change experiments on neutral systems, it will not be possible to unambiguously resolve rotational and vibrational excitation, so help from theory is necessary and welcome. At the same time, experimental measurements of the total energy transfer as a function of scattering angle provide a very useful check on the theory.

C. State-Change Experiments

Although only a handful of crossed beam studies of vibrationally inelastic scattering using state-change methods have been reported so far, this field is ripe with opportunities and is developing very rapidly. Several powerful techniques have already been devised and implemented, and many other exciting possibilities are just on the horizon and remain to be explored. In this area more than any other, opportunities exist to combine some of the traditional advantages of the bulb and beam worlds to study state-to-state vibrationally inelastic scattering at an ever-increasing level of detail.

1. Early Work on LiF and LiH

The first (to our knowledge) crossed molecular beam study of vibrationally inelastic scattering using a state-specific detection method was reported by Mariella, Herschbach, and Klemperer[107] in 1974. In this study, a thermal LiF beam at ~1100 K was crossed at 90° by an effusive (or nearly effusive) target molecular beam, and LiF molecules scattered at a laboratory angle of 20° were analyzed by electric resonance spectroscopy. The relative populations of LiF molecules in the level $v = 0$–3, $J = 1$, $M_J = 0$ were obtained by monitoring the $M_J = 0 \rightarrow 1$ Stark transitions, which occur at slightly different frequencies for each vibrational level. Strictly speaking, this is not a state-to-state experiment, since the initial vibrational level of LiF is not uniquely defined. Nevertheless, by comparing the relative vibrational populations after scattering to the initial 1100 K Boltzmann distribution, it was possible to obtain some qualitative information on the relative efficiencies of various target gases at vibrationally relaxing LiF.

Some results on vibrationally inelastic scattering of another alkali-containing molecule, LiH, were reported by Dagdigian[108] in 1980. In this work, partial cross sections were measured for $v = 0 \rightarrow v = 1$ excitation of LiH by various collision partners. A molecular beam of LiH was generated by passing H_2 through a reservoir of molten Li at ~1400 K and expanding the mixture through an orifice. The H_2 also served as a carrier gas and helped to accelerate the LiH to hyperthermal collision energies. The LiH beam then passed through a collimator and entered a scattering cell containing the collision partner. The c.m. collision energy was between 0.7–0.8 eV for each collision partner. The LiH vibrational frequency of 1360 cm^{-1} corresponds to an excitation energy of 0.169 eV.

The populations of individual LiH levels were probed 4.6 cm downstream from the collimator (still inside the scattering cell) by exciting fluorescence in the $A^1\Sigma^+$–$X^1\Sigma^+$ band system with a tunable N_2-pumped dye laser. By measuring the LiH $v = 0$ and $v = 1$ populations as a function of the scattering cell pressure, Dagdigian[108] arrived at lower limits to the integral $v = 0 \rightarrow 1$ excitation cross sections, which he denotes by σ_+ in his paper. The σ_+ values were all quite small: for HF, HCl, DCl, HBr, and SO_2 collision partners, the values fell in the range 0.03–0.10 Å^2, while for Ar, C_2H_4, CH_3Cl, and CH_2Cl_2 the σ_+ values were too small to measure reliably (< 0.01 Å^2). Unfortunately, the relationship between these σ_+ values and the true integral cross sections is not clear. The reason the σ_+ values represent lower limits to the true cross sections has to do with the geometry of the detection in the beam-gas experiment. Assuming that the length of the laser excitation zone viewed by the photomultiplier tube is the same in the present experiment as in earlier work by Dagdigian and co-workers[109] (~0.9 cm), then it is easy to see that most of the detected molecules have been scattered through laboratory angles <20°. The kinematics are also rather unfavorable from the standpoint of measuring integral cross sections in a beam-gas geometry, since LiH is lighter than all of the target molecules. Therefore, it would not be too surprising if most of the LiH inelastic collisions led to scattering angles too large to be seen in the above experiment.

2. $T \rightarrow V$ Excitation of CO_2

Fenn and co-workers[110,111] have performed some interesting measurements on the following process,

$$M + CO_2(000) \rightarrow M + CO_2(001)$$

where M = N_2, O_2, and Ar. In these experiments, slightly collimated molecular beams of CO_2 and the collision partner were crossed at hyperthermal collision energies and the CO_2 asymmetric stretch excitation was detected "simply" by monitoring the (001) → (000) spontaneous emission at 4.3 μm using a sensitive InSb detector. Actually, any ($v_1v_2v_3$) level with $v_3 = 1$ would contribute to the IR fluorescence signal. Therefore, what is really measured in this experiment is the cross section for exciting one quantum in the asymmetric stretch (irrespective of what happens in the symmetric stretching and bending modes).

Ryali et al.[110] performed measurements over a wide range of collision energies, from just above the 0.29 eV threshold energy to approximately 1.5 eV (still low compared to ion scattering experiments, but rather high for such light neutral collision systems). This wide range of collision energies was made possible by exploiting the seeded beam technique in combination with simple nozzle heating. Dilute mixtures of the colliding species in helium or hydrogen carrier gas and/or nozzle temperatures up to 1600 K were used to achieve the highest collision energies. CO_2 vibrational excitation by the light carrier gases was not energetically possible

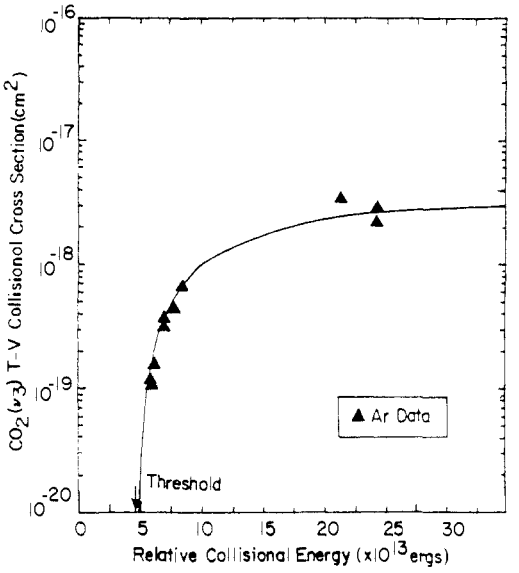

Figure 5. Kinetic energy dependence of the $CO_2(\nu_3)$ T → V excitation cross section in Ar + CO_2 collisions (Ryali et al., ref 110). The cross sections were obtained by monitoring the $CO_2(\nu_3)$ IR fluorescence at 4.3 μm. Reproduced with permission from ref 110. Copyright 1982 American Institute of Physics.

over the range studied. Ordinarily, the two molecular beams collided "head on", but some measurements were also taken in a 90° geometry.

While this experiment is conceptually very simple, its practical implementation turned out to be exceedingly difficult. As the authors note in the introduction to their paper,[110] "... the cross sections turned out to be relatively small so that the experiment became an excercise in extracting a whisper of a signal from a loud cacophony of noise." Nevertheless, some useful data was obtained on the CO_2 (ν_3) excitation cross section as a function of collision energy for all three collision partners. The data for Ar is shown in Figure 5. The cross section increases sharply just above the threshold, then appears to level off to a value around 0.03 Å^2 at the highest collision energies. The N_2 data looks similar, but the cross section for N_2 is 2–3× higher at the highest collision energies. The O_2 data is only available for a few energies just above threshold, where it behaves almost identically to N_2.

VenKateshan, Ryali, and Fenn[111] later repeated the N_2–CO_2 measurements with the addition of a Fourier transform infrared (FTIR) spectrometer to resolve the CO_2(001) rotational distribution. For collision energies in the range 0.4–0.7 eV, the CO_2(001) molecules were found to have a non-Boltzmann rotational distribution; by making a two-temperature fit to the data, VenKateshan et al. concluded that 90% of the excited molecules could be characterized by a rotational temperature of 340 K while the remaining 10% had a lower rotational temperature of about 64 K. The significance of this result is not clear. Although the CO_2(000) molecules are cooled to very low temperatures in the nozzle beam expansion, it is likely that many of these molecules suffer rotationally inelastic collisions with target beam molecules before undergoing the (000) → (001) vibrationally inelastic transition. Therefore, the measured (001) rotational distribution probably does not reflect the rotational energy transfer involved in just the vibrationally inelastic step. In the course of this work, the possibility of the near-resonant process

$$N_2\ (v = 1) + CO_2\ (000) \rightarrow N_2\ (v = 0) + CO_2\ (001)$$

was carefully considered, since at the higher nozzle temperatures an appreciable fraction of the N_2 molecules are in $v = 1$. From the magnitude of the observed cross sections, and the fact that no CO_2 (001) was detectable below the 0.29 eV T → V excitation threshold, VenKateshan et al.[111] concluded that the V–V process was not contributing.

Collisional excitation of CO_2(001) by N_2 and Ar has also been studied by Rahbee[112] using a similar setup. Rahbee used a circular variable filter instead of an FTIR spectrometer to obtain some low-resolution spectral information. For N_2–CO_2 collisions at E_{cm} = 1.3 eV, Rahbee deduced a (001) rotational temperature of 1000 ± 100 K. Again, it is not clear how much of the rotational excitation accompanies or precedes the vibrationally inelastic transition. The absolute vibrational excitation cross sections measured by Rahbee[112] are roughly a factor of two lower than those measured by Fenn and co-workers[110] (although both groups agree that N_2 collisions are 2–3× more effective than Ar collisions at exciting CO_2 (001) at the same collision energy). This level of agreement is very good for two independent measurements, considering the difficulties associated with an absolute determination of the beam number densities and the infrared detection sensitivity.

Some interesting theoretical calculations have been reported by Billing and Clary[113] in connection with the above experimental results. Billing and Clary first calculated Ar–CO_2 interaction energies at the SCF level for 45 geometries (including some nonequilibrium CO_2 geometries). They fit these ab initio points to a sum of pair-wise exponential repulsions between the HF atom and the three atoms in CO_2. Using this interaction potential and a realistic intermolecular potential for CO_2 (including cubic and quartic anharmonic terms), they then calculated cross sections for various (000) → ($v_1v_2v_3$) vibrational transitions as a function of collision energy using a three-dimensional classical path approach. Their theoretical cross section for $v_3 = 1$ excitation (summed over all contributing v_1 and v_2), at a collision energy of 1 eV, is two orders of magnitude below the experimental result.

The reason for this large discrepancy is not clear. It would seem unlikely that the experimental cross sections are grossly in error, since similar numbers have been obtained on two apparatus. On the other hand, the theoretical model used by Billing and Clary[113] is quite sophisticated and has given good results on other systems. More recent theoretical work on rare gas–CO_2 collisions has been reported,[114] but it does not address the above discrepancy.

3. T → V Excitation of I_2, Aniline, and p-Difluorobenzene

A more sensitive and general method of measuring the collision energy dependence of T → V excitation cross sections has been developed by Giese, Gentry, and co-workers at Minnesota. So far, the Minnesota group has studied vibrational excitation in collisions of He atoms with I_2, aniline, and *p*-difluorobenzene. (All studies involve excitation from the zero-point vibra-

tional level.) A brief summary of this work has been given recently by Gentry.[115]

A distinguishing feature of the Minnesota group's apparatus is that the collision energy can be continuously adjusted by varying the intersection angle between two independently rotatable molecular beam sources. Both beam sources incorporate the very fast electromechanical valves pioneered at Minnesota,[116] and are differentially pumped to keep the pressure in the main scattering chamber low during high repetition rate operation. The occurrence of vibrationally inelastic scattering in the crossing zone of the two pulsed molecular beams is detected using laser-induced fluorescence (LIF). Unlike Dagdigian's experiment,[108] where only forward-scattered molecules contributed to the LIF signal, in the present apparatus the pulsed laser beam passes directly through a small, well-defined scattering volume so that molecules scattered into all c.m. angles contribute to the LIF signal. Since pulsed LIF is a number density (rather than a flux) detector, it is not necessarily true that molecules scattered into all c.m. angles will contribute *equally* to the LIF signal. However, for experiments involving the scattering of a heavy molecule from a light atom or molecule, the final laboratory velocity of the heavy molecule will depend only weakly on its final quantum state and c.m. scattering angle. In such cases, the difference between number density and flux distributions can be neglected.

If the above condition is met, and if the relevant spectroscopic and photophysical data are known (e.g., Franck–Condon factors and fluorescence quantum yields), then it is possible to convert the measured LIF signals into (relative) total cross sections for the various vibrationally inelastic transitions observed. Since it is very difficult to determine absolute values of the vibrational excitation cross sections in this type of experiment (due to uncertainty in both the beam number densities and the overall efficiency of the fluorescence excitation and detection), Gentry and co-workers usually normalized the relative cross sections for the various transitions to a single value called the "attenuation cross section" σ_a, which essentially represents the total cross section for inelastic scattering of the primary beam molecules by the target beam at a particular high value of the collision energy. Usually, σ_a is expected to be on the order of the gas kinetic cross section.

First results from this apparatus, on $v = 0 \rightarrow 1$ excitation in He + I_2 collisions, were reported by Hall et al.[117] in 1983. In a follow-up paper,[118] detailed measurements were presented on the collision energy dependences of the $v = 0 \rightarrow 1, 2, 3$ excitation cross sections. The population in each vibrational level was probed by exciting fluorescence on a suitable (v', v'') transition in the $B0_u^+ \leftarrow X^1\Sigma_g^+$ band system of I_2 (where v' and $v'' = v$ are the vibrational quantum numbers in the upper and lower electronic states, respectively). In order to distinguish the very small collision-induced populations in $v > 0$ from residual hot-band populations, it was essential in these experiments to generate an extremely cold beam of I_2. By expanding a dilute mixture of I_2 in hydrogen carrier gas from a 0.6-mm diameter nozzle, Hall et al.[118] were able to achieve an initial (non-Boltzmann) $v = 0{:}1{:}2{:}3$ population ratio of $1{:}2 \times 10^{-4}{:}4 \times 10^{-6}{:}<5 \times 10^{-7}$. The initial rotational temperature was estimated to be between 1–2 K. By subtracting the LIF signals obtained with the He target beam ON and OFF, Hall et al. obtained the collision-induced LIF spectra shown in Figure 6. Note that the I_2 vibrational quantum of 213 cm^{-1} (in the ground electronic state) corresponds to an excitation energy of 26 meV. From data such as these, it was possible to construct the collision energy dependence of each state-to-state cross section.

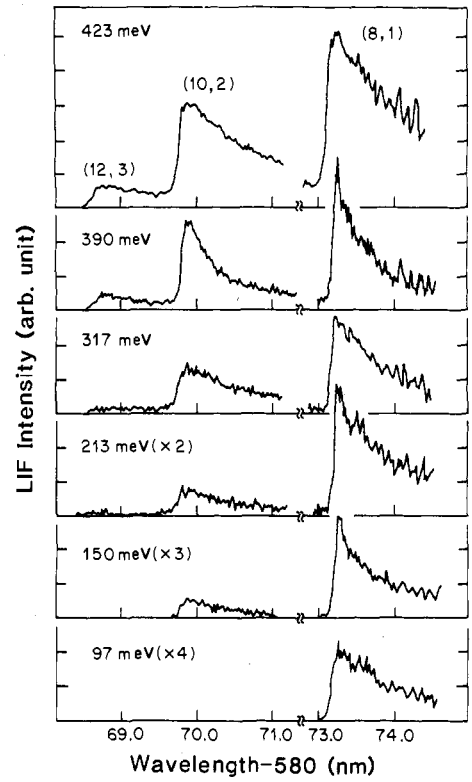

Figure 6. Collision-induced LIF spectra for the He + I_2 system at six well-defined collision energies (Hall et al., ref 118). The collision-induced populations in the $v'' = 1$, 2, and 3 levels of $I_2(X)$ were probed by exciting fluorescence in the vicinity of the (v',v'') = (8,1), (10,2), and (12,3) bandheads of the I_2 B–X band system. Reproduced with permission from ref 118. Copyright 1984 American Institute of Physics.

The most interesting result emerging from this study is that the $v = 0 \rightarrow 1$, 2, and 3 excitation cross sections appear to exhibit linear, quadratic, and cubic dependences, respectively, on the collision energy above threshold. Hall et al.[118] show that this result can be understood in the context of the semiclassical forced harmonic oscillator theory if (i) the average reduced classical energy transfer, $\epsilon = \Delta E/\hbar\omega$, is small, and (ii) the energy transfer ΔE is proportional to the c.m. collision energy E_{cm}. Condition (i) is certainly satisfied in this system, since the $v = 0 \rightarrow 1$ excitation cross section at $E_{cm} = 400$ meV is roughly 200× smaller than the total $v = 0$ attenuation cross section. (If the attenuation cross section σ_a is set equal to the gas kinetic cross section of ~45 Å^2, then the experimental vibrational excitation cross sections at $E_{cm} = 400$ meV work out to be σ ($0 \rightarrow 1$) = 0.18 Å^2, σ ($0 \rightarrow 2$) = 0.011 Å^2, and σ ($0 \rightarrow 3$) = 0.0010 Å^2.) Condition (ii) should also hold quite well, since the energy transfer is expected to be fairly impulsive in He + I_2 collisions. (Recall that a classical treatment of impulsive energy transfer in one dimension leads to an exact linear dependence of the energy transfer on the collision energy.[119] An approximately

linear dependence is also expected in three dimensions, although the constant of proportionality will, in general, be much smaller). With these assumptions, it is easy to see that the semiclassical Poisson distribution for the vibrational transition probabilities,

$$P(0 \rightarrow v) = \epsilon^v e^{-\epsilon}/v!$$

leads to the observed collision energy dependence of the vibrational excitation cross sections,

$$\sigma(0 \rightarrow v) \propto E_{cm}{}^v$$

The actual magnitudes of the experimental cross sections are, however, much smaller than those predicted by the simple 1-D classical impulsive formulas. Additional evidence that the dynamics are somewhat more subtle is that less vibrational excitation has been observed in $D_2 + I_2$ collisions as compared to $He + I_2$ collisions.[115,120] An impulsive model would predict identical results in both systems, since the fractional energy transfer in impulsive A + BC collisions depends only on the relative mass combination. Hall et al.[120] have also reported measurements on $H_2 + I_2$ collisions. In this system, an unexplained "kink" is observed in the $v = 0 \rightarrow 1$ excitation cross section about 100 cm^{-1} above threshold.

The I_2 experiments performed so far do not provide any information on the angular distribution of the inelastically scattered molecules. Such measurements are possible, if the LIF detection is performed at some point removed from the scattering volume. The Minnesota group fashioned their apparatus to allow the possibility of differential cross section measurements in the future. The practical difficulty, of course, is that much higher detection sensitivity is required to perform differential as opposed to integral cross section measurements.

Additional information on the $He + I_2$ scattering dynamics is provided by some quantal scattering calculations performed by Schwenke and Truhlar[121] in connection with the above experimental work. These calculations were performed using the infinite-order sudden approximation for the I_2 rotational motion, a full close coupling treatment of the vibrational motion (VCC/IOS), and an approximate HeI_2 potential energy surface derived from both ab initio and empirical results. The calculations predict that the differential cross section for each vibrationally inelastic channel (summed over final rotational levels) should increase monotonically with increasing scattering angle. The shapes of the calculated differential cross sections were not too sensitive to collision energy. A plot of the integral vibrational excitation cross sections as a function of the initial I_2 orientation angle showed that collinear collision geometries are strongly favored in this system, although a small secondary maximum was also observed for perpendicular approach geometries. The collision energy dependence of the calculated integral state-to-state cross sections agreed reasonably well with experiment (the absolute agreement being within about a factor of two).

More complicated (and therefore interesting!) possibilities arise in atom-polyatomic molecule collisions. Thus far, the Minnesota group has studied vibrational excitation in two large polyatomics, aniline[122] and *p*-difluorobenzene,[123] both in collisions with He atoms. Vibrational energy transfer in the excited S_1 electronic states of these molecules has been studied extensively in bulbs, as will be discussed in section IV. The work at Minnesota, on the other hand, involves vibrational excitation from the zero-point vibrational level of the ground electronic state S_0. The vibrational excitation in S_0 was detected by using $S_1 \leftarrow S_0$ LIF.

Preliminary results on the He + aniline system were reported by Liu et al.[122] By seeding ~0.1 torr aniline in 14–17 atm of helium carrier gas, primary beam rotational temperatures on the order of 1 K were achieved. The total attenuation cross section of the aniline beam due to the He target beam was measured at the peak of the rotational contour of the $S_1 \leftarrow S_0$ origin. The relative cross sections for exciting different vibrational modes were determined by tuning the laser to known $S_1 \leftarrow S_0$ hot-band transitions (usually sequence transitions) and subtracting the LIF signals obtained with the He target beam ON and OFF; these difference signals were then normalized to the total attenuation cross section. For this preliminary work, the population in each S_0 vibrational level was probed at just one or two positions on the rotational contour of its respective hot-band transition; that is, full collision-induced LIF spectra were not recorded. Therefore, although the measurements reveal the propensities in the mode-to-mode energy transfer, the cross sections cannot be taken quantitatively until the details of the rotational state distributions are explored more fully.

The $S_1 \leftrightarrow S_0$ band system in aniline has been characterized fairly thoroughly in absorption and fluorescence studies.[124] The $-NH_2$ inversion mode, denoted I, is extremely anharmonic in the ground electronic state. The inversion potential exhibits a double minimum, with a barrier of approximately 500 cm^{-1} at the planar configuration. The angle between the benzene ring and the $-NH_2$ group is 42° in S_0. The energies of the first three excited inversion levels, I_1, I_2, and I_3, are 41, 422, and 700 cm^{-1}, respectively. (We will follow the usual convention of denoting vibrational quantum numbers in the ground and excited electronic states by subscripts and superscripts to the mode label, respectively.) The inversion mode is much less anharmonic in S_1, and the I^1 vibrational energy is 337 cm^{-1}. Therefore, the $I^1{}_1$ sequence transition occurs 296 cm^{-1} to the blue of the $S_1 \leftarrow S_0$ origin. The two next lowest S_0 vibrational modes are (following Varsanyi's notation[125]) 10b and 15, with vibrational frequencies of 217 and 390 cm^{-1}, respectively. Mode 10b is an out-of-plane bending vibration of the entire $-NH_2$ group against the ring. Mode 15 is an in-plane bending vibration involving mainly the $-NH_2$ group and the adjacent carbon atom. A strong sequence transition 40 cm^{-1} to the red of $0^0{}_0$, denoted $T^1{}_1$ by Chernoff and Rice[124], is almost certainly due to one (or possibly both) of these modes, but a definitive assignment has not been made spectroscopically.

The range of collision energies covered by Liu et al.[122] was 20–220 meV, or approximately 150–1800 cm^{-1}. There are (at least) 11 aniline fundamental vibrations below 1300 cm^{-1}. Five of these (I, 10b, 4, 16a, 16b) are out-of-plane modes while the other six (1, 6a, 12, 13, 15, 18a) are in-plane modes. Liu et al. probed with high sensitivity for excitation in each of these modes except 4, 16a, and 16b. (Modes 4 and 16b could not be probed using LIF because vibronic transitions involving these

modes have not been assigned. Sequences involving 16a are known, however, so it is unclear why this mode was not probed.) Collision-induced vibrational excitation was only observed in two vibrational modes, I_1 and T_1 (as monitored at the I^1_1 and T^1_1 sequence transitions). It was possible to unambiguously assign T_1 to mode 10b, since the observed threshold energy for T_1 excitation agreed closely with that of mode 10b, rather than with that of the higher frequency mode 15. This is the first time that a sequence transition has been assigned on the basis of the collision energy dependence of a T → V excitation cross section!

The collision energy dependence of the 10b excitation cross section was "unremarkable", increasing linearly above threshold at first and then leveling off at the highest collision energies. The behavior of the I_1 excitation cross section was refreshingly different, in that it increased steadily as the collision energy was lowered. This trend continued down to the lowest value of the collision energy attainable in the experiment, about 150 cm^{-1}, which is still 3–4× higher than the I_1 threshold. The same qualitative trend was observed whether the laser was tuned to probe low-J or high-J I_1 rotational levels, but the increase at low collision energies was more pronounced for the low-J levels. The reason for the unusual collision energy dependence of the I_1 excitation cross section is not yet clear, but presumably is related to the fact that the inversion mode in S_0 aniline is a very atypical vibrational mode (involving as it does a very low frequency, large amplitude, anharmonic motion). It is also quite remarkable that no excitation was observed in any of the low frequency in-plane modes. As we shall see, a similar preference for out-of-plane modes has been observed in S_1 bulb studies of vibrational energy flow in aromatic molecules. Evidently, mode geometry is more important than mode frequency in determining the pattern of vibrational excitation.

Most recently, Hall, Giese, and Gentry[123] have reported measurements of vibrational excitation of S_0 *p*-difluorobenzene (*p*DFB) in collisions with He. *p*DFB was chosen in part because a large body of data exists on both collision-indued and collision-free vibrational energy transfer in the S_1 electronic state of this molecule. Most of this work has been done in bulbs and will be discussed in detail later. However, the main qualitative conclusion emerging from the S_1 experiments is that both the collision-induced and collision-free vibrational energy flows in *p*DFB are strongly influenced by the lowest frequency vibrational mode, ν_{30}, which is an out-of-plane, in-phase bend of both F atoms relative to the benzene ring. The reason for the special activity of ν_{30} in the S_1 studies is not yet clear, and may involve a combination of several effects, including anharmonic mixing, Coriolis vibrational–rotational mixing, and centrifugal vibrational–rotational mixing.[126]

Hall et al.[123] found that mode 30 is also dominant in vibrational excitation from the zero-point level of the ground electronic state. The vibrational frequency of mode 30 is 157.5 cm^{-1} in S_0 (as compared to 119.7 cm^{-1} in S_1). Both $v = 1$ and $v = 2$ excitation in mode 30 were observed, as shown in Figure 7. (These transitions were detected by exciting fluorescence on the 30^1_1 and 30^2_2 sequence transitions.) Hall et al. searched carefully for evidence of collisional excitation of six other relatively

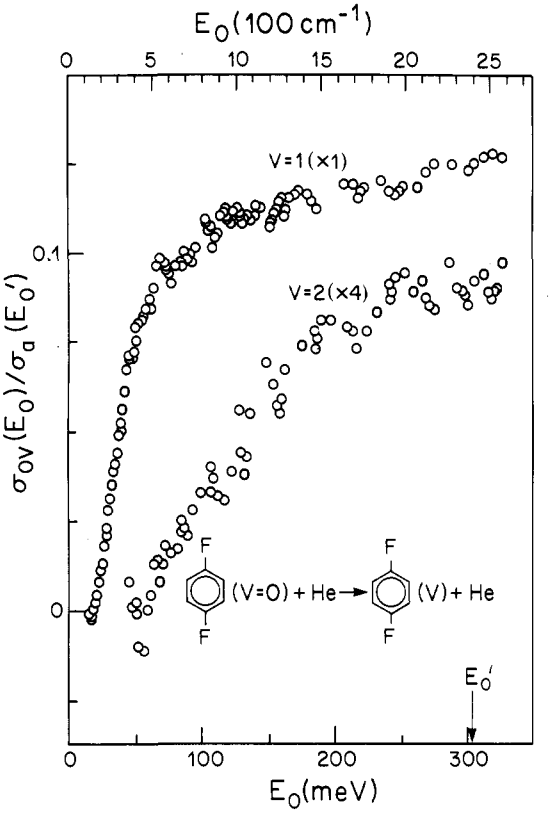

Figure 7. Kinetic energy dependence of cross sections for exciting the 30_1 and 30_2 levels of S_0 *p*DFB in collisions with He (Hall, Giese, and Gentry, ref 123). The cross sections are normalized to the attenuation cross section $\sigma_a(E_0')$, which is expected to fall in the range 20–50 Å^2. Reproduced with permission from ref 123. Copyright 1985 American Institute of Physics.

low-frequency vibrational modes (including both in-plane and out-of-plane modes) and found none. An important feature of this experiment is that the pDFB molecules start out very cold rotationally (with an estimated rotational temperature of 1.2 K). This implies that the special activity of mode 30 in the vibrational excitation of S_0 *p*DFB is not due to level-mixing alone. The linear dependence of the $0_0 \rightarrow 30_1$ excitation cross section near threshold also suggests that the collisions leading to mode 30 excitation are mainly impulsive. Hall et al. conclude that the important properties of mode 30 are simply its low frequency and large amplitude (and to a lesser extent, the fact that it is an out-of-plane mode).

4. Differential Cross Sections for Na_2–Rare Gas Scattering

There are only two examples so far of differential cross section measurements for state-to-state vibrationally inelastic scattering in a neutral collision system. Both involve Na_2. The first is the elegant study of $v = 0 \rightarrow 1$ excitation in Na_2–Ar collisions by Pritchard, Kinsey, and co-workers[127] at MIT using the so-called "angular distribution from the Doppler shift," or ADDS, technique. In this experiment, beams of Na_2 and Ar were crossed at 90°. Upstream of the collision zone, a single-frequency dye laser was used to pump the $A^1\Sigma_u^+$ ($v' = 9, j = 6$) ← $X^1\Sigma_g^+$ ($v'' = 0, j = 7$) transition in Na_2, thereby depleting the population in the $v = 0, j = 7$ level

of the ground electronic state. A second single-frequency dye laser, directed to intersect the Na_2–Ar collision volume along the relative velocity vector (20° with respect to the Na_2 beam in this case), was then used to measure the populations in the various final Na_2 levels by exciting fluorescence on suitable A–X transitions. By performing a double subtraction of the LIF signals obtained with the pump laser ON and OFF and with the Ar target beam ON and OFF, it was possible to isolate the component of the signals due only to collisions of Ar atoms with Na_2 molecules in the initial level $v_i = 0$, $j_i = 7$.

The unique feature of this experiment is that, since the analysis laser is parallel to the relative velocity vector, there is a 1:1 correspondence between the c.m. scattering angle and the Doppler shift for each probed transition. By making measurements with sub-Doppler resolution, the MIT group[127] succeeded in mapping out state-to-state differential cross sections for dozens of rotationally inelastic and vibrationally–rotationally inelastic transitions originating out of $v_i = 0$, $j_i = 7$:

$$Na_2(v_i = 0, j_i = 7) + Ar \rightarrow Na_2(v_f, j_f) + Ar$$

Recall that the differential cross section is defined as the number of scattered particles per unit solid angle. In the ADDS technique, for each c.m. scattering angle θ, all azimuthal angles are sampled simultaneously. This would seem to introduce a sin θ weighting factor to the differential cross sections. However, for a constant analysis laser bandwidth $\Delta\nu$, the $\Delta\theta$ angular resolution of the ADDS method goes as $1/\sin\theta$. [This is easy to see. The resolution is worse for θ near 0 or π, since a first order change in θ leads to no change in the velocity component along the relative velocity vector and hence no change in the Doppler shift. The resolution is best for θ near $\pi/2$, where a first order change in θ produces a first order change in the Doppler shift.] Therefore, the sin θ and $1/\sin\theta$ factors cancel, and the ADDS signal is directly proportional to the usual differential cross section.

A few of the state-to-state differential cross sections measured by Serri et al.[127] are shown in Figure 8, where the solid lines correspond to vibrationally elastic scattering and the dashed lines correspond to $\Delta v = 1$ vibrationally inelastic scattering. The qualitative shapes of the differential cross section curves are similar for the $\Delta v = 0$ and $\Delta v = 1$ channels for the same Δj. In both cases, the peak in the differential cross section shifts to larger angles as Δj increases. This is a manifestation of the rotational rainbow phenomenon. Although the $\Delta v = 0$ differential cross section is always larger than the $\Delta v = 1$ cross section (for the same Δj), the difference becomes smaller at large scattering angles, reflecting the increasing probability of vibrational excitation in small impact parameter collisions. Serri et al.[127] also observed $v = 0 \rightarrow 2$ inelastic scattering, but the maximum $\Delta v = 2$ signal was at least 5× lower than the maximum $\Delta v = 1$ signal.

These data pertain to a c.m. collision energy of approximately 0.3 eV (2400 cm^{-1}), which is 15× higher than the Na_2 vibrational quantum of 158 cm^{-1}. At this energy, the Na_2–Ar interaction is strongly repulsive, and classical mechanics is expected to provide a reasonable approximation to the dynamics. A simple model involving classical scattering of point particles from a hard ellipse in two dimensions was used successfully by Serri,

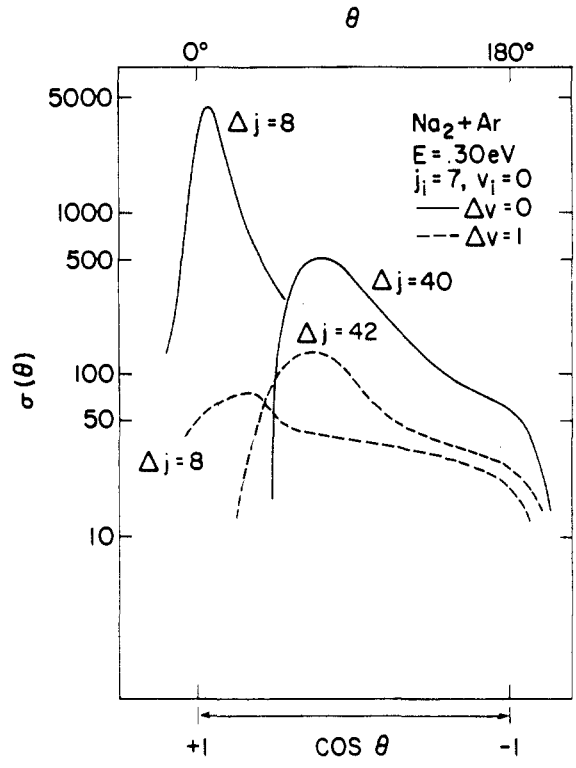

Figure 8. Differential cross sections for vibrationally elastic ($\Delta v = 0$) and vibrationally inelastic ($\Delta v = 1$) scattering in the Na_2–Ar system at $E_{cm} = 0.30$ eV, for different values of the rotational quantum number change Δj (Serri et al., ref 127). These data pertain to the initial level $v_i = 0$, $j_i = 7$. Reproduced with permission from ref 127. Copyright 1981 American Institute of Physics.

Bilotta, and Pritchard[128] to account for the main features of the experimental results. The vibrational excitation was assumed simply to be proportional to the square of the component of the momentum transfer along the major axis of the ellipse.

The main shortcoming of the ADDS technique is its poor angular resolution near $\theta = 0°$ and 180°. A variant of ADDS has been developed at MIT in which the analysis laser intersects the collision volume perpendicular to the relative velocity vector. This technique, denoted "perpendicular ADDS," or PADDS,[129] is complementary to ADDS in that it provides the best resolution at $\theta = 0°$ and 180° and the worst resolution at $\theta = 90°$. With PADDS, however, there is no longer a 1:1 correspondence between Doppler shift and scattering angle, and an integral transform is required to recover the differential cross section from the Doppler profile. (Actually, the integral transform only yields the sum of the differential cross sections at θ and $(\pi-\theta)$, with $0 < \theta < \pi/2$.) Changes of collision energy are much simpler using PADDS, since the technique is insensitive to the orientation of the relative velocity vector in the plane perpendicular to the laser beam. So far, PADDS has only been applied to rotationally inelastic scattering.[130]

A similar pump modulation/LIF detection technique has been developed by Bergmann and co-workers at Kaiserslautern to measure differential cross sections for rotationally and vibrationally inelastic transitions in the Na_2–rare gas systems. But instead of using ADDS to obtain the angular distributions of scattered molecules, the Kaiserslautern group built a LIF detector that is

rotatable about the collision zone.[131] To maintain the critical alignment of the analysis laser beam as the detector is rotated, these workers use a single optical fiber to couple the analysis laser to the detector, and a fiber optic bundle to carry the fluorescence outside the main vacuum chamber. In systems with favorable kinematics, this experimental arrangement is capable of higher angular resolution than the Doppler shift techniques. Since the differential cross sections are measured in the laboratory coordinate system, however, a center-of-mass to laboratory transformation is required before the data can be compared (or fit) to calculated c.m. differential cross sections.

Very recently, the Kaiserslautern group (Gottwald et al.[132]) reported differential cross section measurements for $(v_i = 0, j_i = 9) \rightarrow (v_f = 1, j_f)$ transitions in He + Na_2 collisions at E_{cm} = 90 meV. The measurements were performed with a constant laboratory angular resolution of ±0.6°. But because of particularly unfavorable kinematics in this system, the c.m. angular resolution is much worse—between 10 and 30 times worse, depending on the value of θ_{cm}. (The resulting c.m. angular resolution is comparable to what was achieved in the Na_2–Ar system using ADDS.[127])

Not surprisingly, the experimental results are qualitatively similar in the Na_2–He and Na_2–Ar systems. In both cases, the $\Delta v = 1$ differential cross section peaks in the backward direction. The theoretical description of Na_2–He inelastic scattering in ref 132, however, goes well beyond the hard ellipse model of Serri, Bilotta, and Pritchard.[128] Gottwald et al.[132] performed VCC/IOS quantal scattering calculations on a fully ab initio potential energy surface. State-to-state differential cross sections were calculated and transformed into the laboratory frame to allow comparison with the experimental results. While the overall agreement between theory and experiment was very good (on the order of 25%), some additional features were observed in the calculated cross sections that were not quite resolved experimentally. In particular, an unusual oscillatory structure was observed in the calculated vibrationally inelastic differential cross sections (in addition to the usual rainbow and supernumerary rainbow structure); it was traced to the fact that the vibrational transition amplitude vanishes for a specific approach angle between Na_2 and He.

The "extra" oscillatory structure was most pronounced for rotational–vibrational transitions originating out of the $j_i = 0$ rotational level. Unfortunately, Gottwald et al.[132] had to restrict their measurements to the $j_i = 9$ rotational level (since this level had the largest thermal population under the operating conditions of their beam source). With further improvements in sensitivity and angular resolution, it should become possible to verify the detailed predictions of the quantal scattering calculations for $j_i = 0$, and perhaps also to refine the ab initio Na_2–He potential energy surface.

5. Inelastic Scattering of Vibrationally Excited $I_2(B)$ Molecules

All of the experiments discussed so far have involved vibrational excitation out of the zero-point vibrational level of the ground electronic state. These experiments have already produced some exciting results, and data on a wide variety of systems is sure to follow. These data, in conjunction with increasingly sophisticated theoretical calculations, should lead to rapid advances in our understanding of T → V excitation processes in neutral collision systems.

There remains the challenge of extending the crossed beam studies to molecules prepared initially in excited vibrational levels. Such studies have been performed routinely in bulbs using a variety of double resonance and pump–probe techniques.

Most bulb studies of vibrational energy transfer in the ground electronic state have employed an infrared pump and an IR fluorescence probe. This IR pump–probe method was used by Polanyi and co-workers[133] in a crossed beam experiment to study pure rotationally inelastic scattering in HF–rare gas collisions. In principle, this technique could also be used to study vibrationally inelastic scattering, but the smaller cross sections for V ↔ T transfers and the relatively low sensitivity of IR detectors would make this a very difficult experiment.

Many bulb studies have also been performed in excited electronic states, using a visible or UV light source to pump initial vibrational levels in the excited electronic state and resolved visible/UV fluorescence detection to identify the final levels populated in single collisions. As will be discussed in detail in the following section, this optical pump-dispersed fluorescence probe technique offers several advantages over its infrared counterpart.

At Indiana University, we have begun to explore the possibility of studying vibrationally inelastic scattering of electronically excited molecules having relatively long fluorescence lifetimes and high fluorescence quantum yields. To demonstrate this technique, we have studied collisions of He atoms with I_2 molecules in the $B0_u^+$ electronic state (hereafter designated I_2*). The first observations of collisional energy transfer in the B-state of molecular iodine were made by Franck and Wood[134] 75 years ago. Since then, the iodine problem has captured the imagination of many workers. In particular, we mention the beautiful series of bulb measurements by Brown, Klemperer, Steinfeld, and co-workers[135] in the 1960's and early 70's. Because of this rich history, we thought it would be both fun and informative to study He + I_2* vibrationally inelastic scattering in a crossed molecular beam experiment.

In our study, pulsed molecular beams of He and I_2 were generated in two differentially pumped source chambers using commercially available solenoid valves. The two beams crossed at a fixed intersection angle of 90° in a well-defined collision volume approximately 5 mm on a side. In the plane of the molecular beams, a pulsed dye laser was used to pump some of the I_2 molecules in the collision volume to a specific v' level of the B electronic state. Since the fluorescence lifetimes in the B-state of I_2 are fairly long (e.g., τ_f = 1.7 μs for v' = 35), the electronically excited molecules have a reasonable chance of suffering a vibrationally inelastic collision with the He target beam before they fluoresce. Fluorescence was collected along the axis perpendicular to the collision plane and imaged into a 1.7-m monochromator. Total (undispersed) fluorescence was detected along another axis and used for normalization purposes. By subtracting the dispersed fluorescence signals obtained with the He target beam ON and OFF, it is easy to isolate the effects due to rotationally and

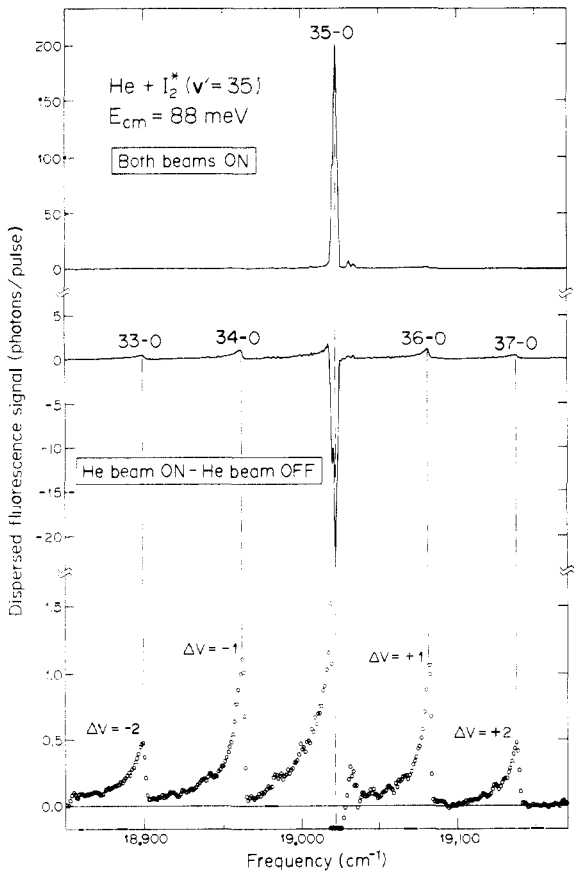

Figure 9. Crossed beam data for inelastic scattering of He atoms from electronically and vibrationally excited I_2 molecules. The I_2 molecules were initially prepared in the $v' = 35$ level of the $B0_u^+$ electronic state by pumping near the 35–0 bandhead. The top panel shows a small portion of the dispersed fluorescence spectrum measured with both beams running (spectrometer resolution: 1.4 cm^{-1} FWHM). The middle panel shows the difference between the spectra obtained with the He target beam ON and OFF. The $v' = 35$ level is depleted by inelastic collisions and new vibrational levels appear. The positive-going part of the difference spectrum is displayed again in the bottom panel, this time as a three-point sliding average of the raw experimental points (Parmenter and co-workers, unpublished results).

vibrationally inelastic scattering in the excited electronic state. Although collisional quenching of the I_2 B-state is known to occur, vibrational energy transfer is more probable than quenching for light collision partners such as He. To a first approximation, then, the effects of quenching can be neglected, and the inelastic scattering can be considered to occur on a single adiabatic potential energy surface.

Some results on He + I_2* ($v' = 35$) scattering at a c.m. (translational) collision energy of 88 meV (710 cm^{-1}) are shown in Figure 9. In this experiment, the pump laser was tuned about 2 cm^{-1} to the red of the (35,0) bandhead. Rotational levels between $J' = 8$–13 in $v' = 35$ were mainly excited. The top panel of the figure shows a small portion of the dispersed fluorescence spectrum obtained with both molecular beams running. The spectrometer resolution was 1.4 cm^{-1} FWHM. The spectrum in the middle panel represents the difference between the spectra obtained with the target beam ON and OFF. The initially pumped levels are depleted by inelastic collisions, giving a dip in the subtracted spectrum at the position of (35,0).[136] Rotationally inelastic scattering within $v' = 35$ and vibrationally inelastic scattering to the levels $v' = 33$, 34, 36, and 37 show up as positive signals in the subtracted spectrum. The positive-going signals are shown more clearly in the bottom panel of Figure 9, where the points now represent a 3-point sliding average of the raw data.

To a good approximation, the raw fluorescence intensities in Figure 9 give directly the relative transition probabilities, since the Franck–Condon factors for all of the (v', 0) transitions probed are the same within 15% and since the fluorescence quantum yield does not vary much over this range of v' levels. Thus, the probabilities of the $\Delta v = \pm 1$ transitions are very nearly equal, as are those of the $\Delta v = \pm 2$ transitions. It is also clear that vibrationally inelastic scattering competes much more effectively with pure rotationally inelastic scattering here than in the ground electronic state studies of Hall et al. Additional measurements covering a wider frequency range were performed at lower spectrometer resolution. V → T transitions up to $\Delta v = -7$ and T → V transitions up to $\Delta v = +7$ were clearly resolved. In the $\Delta v = +7$ transition, 52% of the initial translational energy is transformed into additional vibrational energy of the anharmonic I_2 oscillator. Multiquantum transitions were also observed when $v' = 25$ and $v' = 15$ were initially pumped.

So far measurements have only been performed at a single collision energy. With minor modifications to the apparatus, it should be possible to map out the collision energy dependence of each state-to-state cross section. Such data would provide an interesting complement to the T → V excitation cross sections already measured by Hall et al.[118] in the ground electronic state. In the future this technique may also provide detailed information on rotationally and vibrationally inelastic scattering in vibrationally complex polyatomic molecules.[137]

Added Note: As mentioned in the Introduction, we reluctantly decided *not* to include critical discussions of very-low-energy collisional relaxation or van der Waals molecule vibrational predissociation in this review, mainly because of a desire to keep the article to a manageable length. However, in response to the suggestions of two reviewers, we include a few comments here on the role of very-low-energy collisions in He + I_2* vibrational relaxation.

There is evidence from at least three experimental groups[276–278] that the cross section for I_2* vibrational relaxation is substantially larger at very low collision energies than at thermal collision energies. The evidence was inferred from studies of collisional effects in He/I_2 free jet expansions using the optical pump-dispersed fluorescence probe technique.

For example, Russell, DeKoven, Blazy, and Levy[276] used a cw dye laser to pump the $v' = 25$ level of I_2* in a high pressure, cw He/I_2 expansion. The local translational temperature at the point of excitation was estimated to be 0.14 K. Despite the low frequency of collisions in the beam, significant emission was observed from the $v' = 24$ and 23 levels in addition to $v' = 25$. Russel et al. used a kinetic model to analyze their data and concluded (i) that the cross section for $\Delta v = -1$ collisional relaxation was on the order of several hundred Å^2 (as compared to the geometric $He–I_2$ collision cross section of about 20 Å^2); and (ii) that the $\Delta v = -1$:$\Delta v = -2$ cross section ratio was approximately 6:1. (For comparison, the $\Delta v = -1$:$\Delta v = -2$ branching ratio

is approximately 30:1 in vibrational predissociation of the He···I_2 van der Waals molecule.)

Similar studies have been performed on the $v' = 14$, 16, and 28 levels by Sulkes, Tusa, and Rice[277] and on the $v' = 43$ level by Baba and Sakurai.[278] All workers agree that the vibrational relaxation cross section is large at very low collision energies (although perhaps not as large as estimated by Russell et al.[276]). However, there appears to be some disagreement concerning the importance of multiquantum transitions in the low-energy relaxation process. The experiments of Sulkes et al.[277] involved pulsed dye laser excitation of a cw molecular beam. By comparing emission spectra measured during different time "windows" following the excitation pulse, Sulkes et al. concluded that nearly all of the relaxation in low-energy He–I_2* collisions is due to sequential $\Delta v = -1$ processes. Baba and Sakurai,[278] on the other hand, insist that single-collision, multiquantum transitions must be included in the kinetic model in order to fit their $v' = 43$ relaxation data.

It should be emphasized that there is considerable uncertainty concerning both the magnitude of the vibrational relaxation cross section and the range of He–I_2 collision energies probed in the above experiments. The uncertainty is caused by imprecise knowledge of the bulk flow velocity, the random velocity of molecules, the local temperature, and the number density of molecules in the expanding free jet as a function of distance from the nozzle. The usual procedure has been to estimate the various parameters of the mixed He/I_2 expansion using the well-known continuum flow formulas for isentropic expansion of a pure monatomic gas (see, for example, Figure 1 of ref 277). This procedure will always *underestimate* the true distribution of He–I_2 collision energies at a given point in the expansion, because it neglects the phenomenon of "velocity slip" in mixed beam expansions.[279] (It is also probably incorrect to assume that the I_2 mole fraction is the same at all points in the expansion.[280])

In general, when a heavy species is seeded in a light carrier gas, the bulk flow velocity of the heavy species will lag behind that of the carrier gas. At the same time, the velocity dispersion of the light species increases (relative to that of a pure light beam) at the expense of a narrowing in the velocity distribution of the heavy species. Both of these effects will tend to increase the average energy of heavy–light collisions in the expansion. It is important to recognize that even a very small velocity slip (i.e., one that might be considered "negligible" from the standpoint of the bulk flow velocity) can still have a significant impact on the distribution of heavy–light collision energies *within the beam*. The importance of velocity slip in mixed He/I_2 expansions has been thoroughly documented by Kolodney and Amirav.[281] The latter authors conclude that the true He-I_2 collision energies in the experiments of Sulkes et al.[277] could have exceeded the values calculated using the isentropic beam formulas by a factor of 10 or more.

Given the above experimental uncertainties, it is not too surprising that there is also some uncertainty concerning the theoretical interpretation of the low-energy relaxation data. Rice and co-workers[277] have argued that the large vibrational relaxation cross sections are the result of scattering resonances[282] (e.g., orbiting resonances) that lengthen the duration of He–I_2* collisions at specific low values of the collision energy. Numerous theoretical calculations[184,283–287] have been performed in connection with this resonance hypothesis. The close-coupling calculations of Cerjan and Rice,[285] for example, predict that resonances should begin to contribute to He + I_2* vibrational relaxation at collision energies below about 1 cm^{-1}.

Certainly, the resonance hypothesis in itself is not physically unreasonable. (Similar ideas have been used by others[288] to rationalize the efficient relaxation observed in some low-temperature bulb experiments.) However, it is not clear that scattering resonances are really *required* to explain the existing experimental results on He + I_2*. Gentry,[289] in particular, has argued that an "ordinary" mechanism, based on impulsive He-I_2 collisions, might be able to explain the magnitude of the observed vibrational relaxation cross section at low collision energies without invoking resonances. There is also some question (see above discussion) as to whether the experiments performed so far have really probed the region of collision energies below ~ 1 cm^{-1} where the resonances are predicted to occur.

Clearly, much remains to be learned about the relationship between "ordinary" vibrationally inelastic scattering at thermal and hyperthermal collision energies and the special world of van der Waals molecules and low-energy collisions. In our opinion, the case for resonance effects in very-low-energy collisional relaxation has not been conclusively demonstrated *experimentally*. Therefore, the large body of very interesting theoretical work on this topic must stand on its own merits. An important question is whether the vibrational relaxation cross sections increase suddenly once the collision energy drops below a certain critical value (e.g., the He–I_2* van der Waals binding energy), or whether the cross sections increase gradually as the collision energy is lowered from the thermal energy range. The theoretical calculations of Rice and coworkers[184,285–287] clearly favor the first possibility. By extending the crossed beam measurements illustrated in Figure 9 to lower collision energies, it should be possible to give an experimental answer to this question as well.

In closing, we note that experimental evidence for enhanced vibrational relaxation at very low collision energies is not limited to molecular iodine. Similar observations have been reported in several other molecules, most notably glyoxal,[290] aniline,[291] and naphthalene.[292] The glyoxal and naphthalene results appear to be reliable. However, questions have been raised concerning the aniline results. (It appears that at least some of the vibrational relaxation attributed to low-energy He + aniline collisions[291] may instead have been due to vibrational predissociation of aniline···He van der Waals molecules.[293])

IV. Bulb Studies of Vibrational Energy Transfer in Excited Electronic States (S_1)

The information derived from bulb experiments is in principle much reduced from that of crossed beams because of thermal averaging over collision energies and because of the loss of differential scattering cross sections. The constraints are universal with the exception of a few special bulb techniques that attempt to escape

the limitations of thermal averaging.[18] (An example is the use of excimer laser photolysis of precursor molecules to produce hyperthermal H atoms with narrow kinetic energy spreads for studies of T → V processes. A number of interesting studies have been performed at Columbia,[138] Colorado,[139] and Los Alamos.[140])

In compensation, bulb explorations are far more accessible in the laboratory. Accordingly, bulb study of vibrational energy transfer is a venerable[134] experimental endeavor with a large corpus of data. As can be expected, diatomics form a large segment of these efforts. State-resolved polyatomic studies began later with the arrival of infrared lasers,[141] and much information has subsequently accumulated on vibrational energy transfer in the ground electronic state (S_0).[8-14] Complementary data are also available from picosecond time-resolved explorations of V → T,R relaxation of specific states of small polyatomics in liquids[142] and more recently on surfaces.[143]

The limitations of IR technologies have made single-collision state-to-state observations difficult in S_0 studies. With IR pumping of initial levels, historically the challenge has been that of final state detection. The most common final state monitor has been IR fluorescence.[10] The long fluorescence lifetime usually restricts observations to vibrational populations occurring in the extensive collisional sequences associated with the move towards thermal equilibrium. State-to-state inferences must be extracted with kinetic modeling of ensemble populations so that only the dominant energy transfer processes emerge securely.

The spirit of these S_0 studies is particularly well displayed by a paper titled "A Complete Energy Transfer Map for COF_2" by Flynn and co-workers.[144] The study describes the prominent paths of vibrational energy flow in COF_2–COF_2 collisions as the system moves from initial excitation of the C–F stretch towards thermal equilibrium. COF_2 is among the few studied systems in which all modes are IR active so that all final states can in principle be observed.

Four-state double resonance experiments, mostly IR–IR, have played a less important role in the S_0 studies. Those that are CW or without adequate time resolution encounter the same ensemble averaging requirements as experiments with fluorescence probes. Among the advantages of the double resonance technique is the opportunity (in principle) to monitor all possible final states.

The S_0 bulb studies are characterized by experiments sophisticated both in concept and technology. Continuing technological advances are now beginning to expand the four-level double resonance options to encompass a variety of pumping and detection schemes. S_0 level pumping by continuously tunable IR sources,[145] stimulated emission using UV lasers,[146] and stimulated Raman scattering with visible lasers[147] can all involve pulsed initial state preparation. Subsequent final state probing by IR laser absorption,[148] UV or visible laser-induced fluorescence (LIF),[149] coherent anti-Stokes Raman scattering (CARS),[150] or even resonant multiphoton ionization (MPI)[151] can sustain the time resolution that is required to monitor directly single-collision state-to-state processes in S_0 bulb experiments. These approaches are presently tricky to use so that the results, while of high quality with respect to state-to-state detail, are not yet abundant.

As an alternative, researchers have turned to the study of vibrational energy transfer in the S_1 states of polyatomics.[6,7] In S_1 studies, it is much easier to observe single-collision state-resolved V ↔ T transfers in vibrationally complex polyatomics. For this reason, the S_1 studies constitute the set of bulb experiments that is most closely related to beam studies.

The S_1 studies are based on visible or UV S_1 level pumping and $S_1 \rightarrow S_0$ fluorescence detection. The switch to visible/UV radiation eases many of the experimental difficulties that accompany the ground electronic state experiments. S_1 studies have additionally the unique advantage of a natural molecular clock, the fluorescence lifetime, that permits easy control of collisional encounters. By adjustment of collision partner pressure relative to S_1 electronic state lifetimes, one can (usually) insure that the state-to-state processes under study are one-collision transfers, even with CW excitation. There is consequently no need to model the data with assumed transfer paths in order to extract single-collision state-to-state rate constants.

As a consequence of being able to measure many single-collision transfers, detailed collisional "flow patterns" from a given initial S_1 level emerge from the data. A flow pattern is a set of absolute rate constants for vibrational energy transfer from the initial S_1 vibrational level to each of the final S_1 levels that are reached in the collisional interaction. If these rate constants are normalized among themselves, they constitute the branching ratios for collisional vibrational flow from a given initial level. Alternatively, rate constants may be normalized to the measured rate constant for total vibrational energy transfer from the intial level. This procedure gives a flow pattern that shows the percentage of total transfers into each observed final S_1 state. These single-collision flow patterns can be obtained in a given molecule for each of a variety of initial S_1 levels. The ensemble of flow patterns thus provides an encompassing view of state-to-state energy flow in large vibrationally complex molecules. This type of information is so far the unique province of S_1 studies.

Figure 10 shows six molecules for which such S_1 collisional flow patterns have been established for at least one initial level. Flow patterns also exist, so far unpublished, in *s*-tetrazine.[152,153] In the following sections we shall summarize the experimental status of these studies, trying to establish perspective about the extent to which energy flow has been explored and what data exist. In so far as possible, we have endeavored to separate interpretation from the data itself.

It is useful to comment further on experimental techniques that have been used in bulb studies, particularly with respect to their prospects for use with crossed beam experiments. As discussed above, methods of initial state preparation in the ground electronic state include direct IR absorption, stimulated emission pumping (SEP), and stimulated Raman scattering. Methods of final state detection in the ground electronic state include IR absorption (narrow band diode lasers hold particular promise here), spontaneous IR fluorescence, laser-induced fluorescence (LIF), multiphoton ionization (MPI), and coherent anti-Stokes Raman scattering (CARS). In the excited electronic state studies, the initial vibrational level is prepared by direct absorption of the fundamental or doubled output

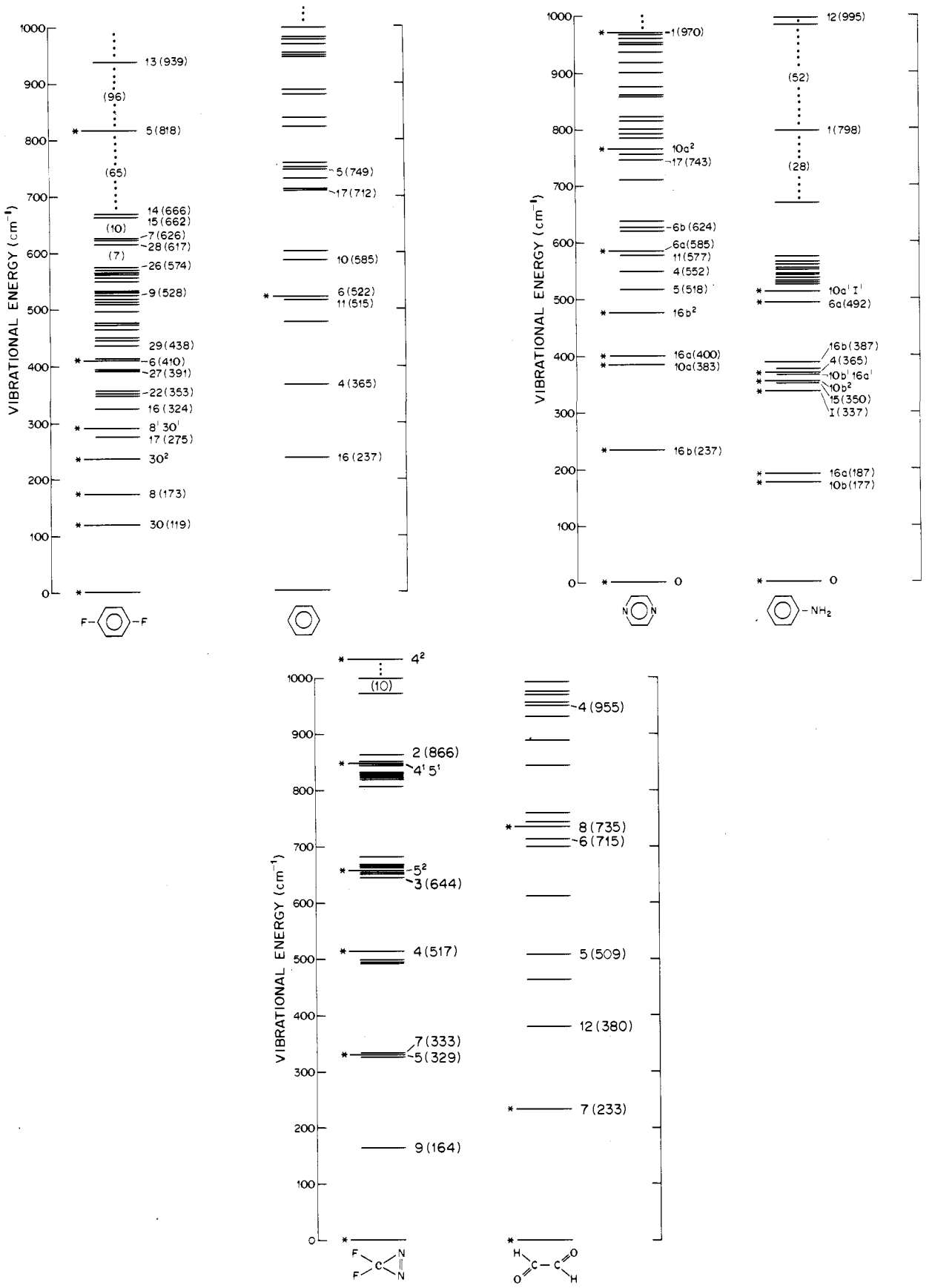

Figure 10. S_1 vibrational energy level diagrams for the six molecules for which collisional flow patterns have been established for at least one initial level. All S_1 levels are shown within the respective energy regions except where dots lie between levels. In those cases, the number of omitted levels is (usually) given in parentheses. Fundamentals are indicated by the mode number followed by the mode frequency (cm^{-1}) in parentheses. Levels pumped to give flow patterns are shown by longer bars and an asterisk, and when other than fundamentals, their mode identity is given to the right.

TABLE I. **Comparisons of Some Aspects of the State-to-State Vibrational Energy Transfer Studies in S_1 "Aromatics"**

	benzene	aniline	pyrazine	*p*DFB
no. of initial levels studied	1	8	8	7
energy of highest initial level (cm^{-1})	522	514	970	818
no. of different modes contained in initial levels	1	4	4	4
no. of fundamentals below highest initial level	4	7	10	15
no. of different modes active in state-to-state changes	2–4	5	7	3
no. of collision partners	10	11	1	4
no. of different state-to-state channels with reported rate constants	4	33	39	40

of a tunable dye laser, and final state identification is accomplished by dispersing the visible or UV fluorescence. Of these techniques, only one of the state preparation methods (visible absorption) and three of the detection methods (LIF, spontaneous IR and visible fluorescence) have been used in crossed beam studies of vibrationally inelastic scattering (see section III.C). Looking to the future, it is doubtful that IR absorption will ever be useful as a *detection* method in a crossed beam experiment. Although stimulated Raman scattering should not be ruled out, it is an inefficient process and may not be able to generate sufficiently high numbers of vibrationally excited molecules to be useful in a crossed beam experiment. On the other hand, we expect that both SEP and direct IR absorption will be used to prepare initial levels for crossed beam studies of vibrationally inelastic scattering. Direct vibrational pumping by IR absorption has been hampered in the past by a lack of tunable IR sources, especially in the 5-20 μm region, but this situation is improving rapidly. We also expect to see MPI become a valuable and routine complement to LIF as a sensitive, state-selective detection method in inelastic scattering studies.

A. Benzene, Aniline, Pyrazine, and *p*-Difluorobenzene

Similarities concerning vibrational energy transfer far outweigh differences in these S_1 molecules and we discuss the molecules as an ensemble. Most of our own *p*DFB work has not been published as of this writing,[126,154] but we take the liberty of including some of its details. Little of an *s*-tetrazine study, involving eight initial levels and six collision partners, has been published.[153] We refer the interested reader to two Ph.D. theses[152] for details. A few results on *s*-tetrazine vibrational relaxation were also obtained by Brumbaugh and Innes[155] in the course of a mainly spectroscopic investigation.

We discuss state-to-state data for benzene, aniline, pyrazine, and *p*DFB. For convenience we shall refer to all as "aromatic" molecules. S_1 vibrational energy level diagrams are shown for each in Figure 10. The vibrational states involved in the transfer experiments are entirely contained within the lowest 1000 cm^{-1} of the S_1 manifold. The majority are out-of-plane modes. The states initially pumped are fundamentals, overtones, or combination levels containing only a few of the modes of each molecule: benzene, one of 20 modes

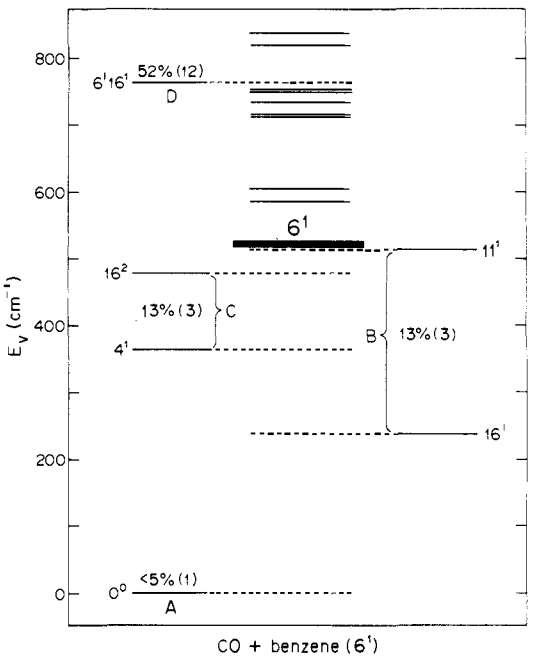

Figure 11. Vibrational flow pattern for CO + benzene collisions after pumping the level 6^1. Those S_1 levels for which energy transfer rate constants are reported are identified. (Brackets show pairs of levels that could not be spectroscopically resolved so that the data refer to the level pair.) The percentages indicate the fraction of total vibrational energy transfer from the initial level 6^1 that goes into the given final state. The transfer efficiencies associated with these state-to-state processes are given in parentheses as the number of effective collisions per 100 gas kinetic collisions, P_{100}. All levels within the energy range of the diagram are shown.

(ten of the 30 vibrational degrees of freedom are double degenerate); aniline, four of 36 modes; pyrazine, four of 24 modes; pDFB, four of 30 modes. Thus the experiments select vibrational domains where the full vibrational complexity is not well developed. On the other hand, the number of levels within, say, kT of the initial level over which new population could be spread is generally very large. In this sense, the vibrational complexity of large polyatomics is present indeed.

Table I lists a number of parameters that provide comparisons among the studies of these S_1 aromatics. The table also reveals the extent to which vibrational energy transfer has been explored. Since the entries refer only to levels and collision partners for which flow patterns involving at least several channels have been established, it is seen that the data are now fairly comprehensive. Roughly 200 state-to-state absolute rate constants have been reported.

A representative flow pattern is shown for each molecule in Figures 11–14 to indicate the spirit of the studies. In benzene and *p*DFB, absolute rate constants are available for both the total transfer out of a pumped level (k_4 in the parlance of all these studies) and the transfer to a specific final state ($k_4(i)$). Thus the data provide experimental measures of the percent of total transfer going to selected states. The k_4 measurements are unavailable for pyrazine, and in aniline they seem unlikely (e.g. the sum of $k_4(i)$ values exceeds k_4 by a factor of two for several levels; in other cases, an individual $k_4(i)$ value exceeds its corresponding k_4 value). The flow patterns for these cases are labeled only with

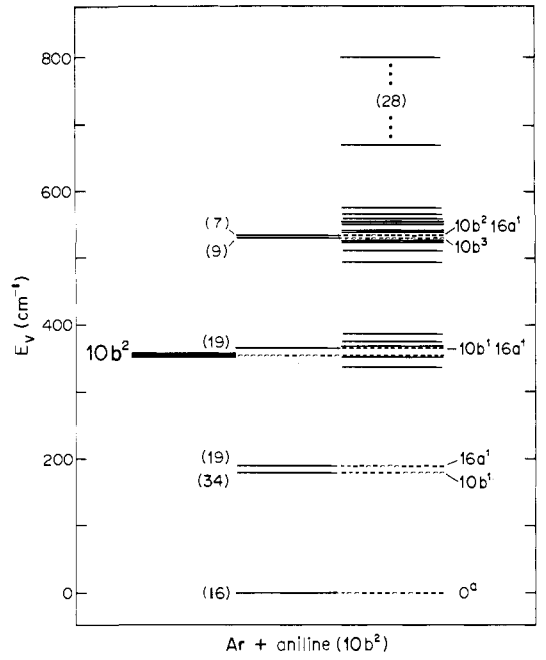

Figure 12. Vibrational flow pattern for Ar + aniline ($10b^2$) collisions. P_{100} values for observed final levels are shown in parentheses. Percentage transfers are not available. (See also Figure 11 caption.)

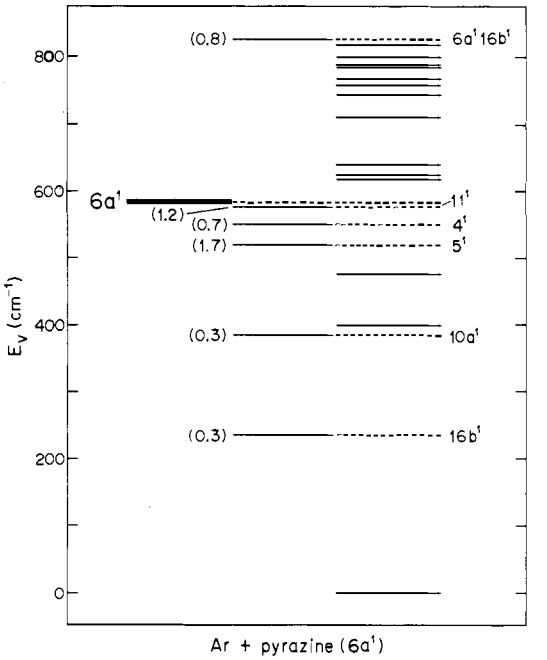

Figure 13. Vibrational flow pattern for Ar + pyrazine ($6a^1$) collisions. P_{100} values for observed final levels are shown in parentheses. Percentage transfers are not available. (See also Figure 11 caption.)

the effective collisions per 100 hard sphere collisions. The relatively large efficiency of these state-to-state transitions as well as the high selectivity among final levels for each example is readily apparent.

1. The Literature

In the paragraphs below, we briefly comment on the vibrational energy transfer literature for each molecule. We follow operatic tradition by listing molecules in order of appearance. In later sections, some of the many issues arising from the studies will be discussed.

Benzene. Tang and Parmenter[156] reported flow patterns after pumping a single in-plane fundamental ($\nu_6' = 522$ cm^{-1}) for nine collision partners ranging from He to vibrationally complex fluorocarbons (n-C_6F_{14}). In a later paper,[157] the role of vibrational degeneracies in the collision partner (using OCS with $\nu_2'' = 520$ cm^{-1}) is discussed. This paper is also concerned with the effect of level degeneracies on transfer rate constants and data checks using microscopic reversibility. A study[158] of state-to-field vibrational energy transfer (i.e., transfer from a selected initial state into the entire field of surrounding levels) with small and large collision partners explored the persistence of high state-to-state selectivity for transfers into higher and denser regions ($\rho_{vib} \approx 10$ per cm^{-1}) of the vibrational manifold as well as the competition between V–T and V–V exchanges with collision partners. The SVL fluorescence spectroscopies[159] and lifetimes[160,161] upon which these studies are based are provided by several groups. Logan et al.[162] have made an extensive experimental survey of state-to-field rate constants for many collision partners operating on one initial level in a region where $\rho_{vib} \approx 1$ per cm^{-1}. Lyman et al.[163] have reported transfer cross sections in S_0 benzene, providing a comparison of transfer in the S_1 and S_0 states.

Benzene has only two fundamentals below 500 cm^{-1} and in terms of level count, it is the least vibrationally complex of the four aromatics. The state-to-state studies were also performed at a time when the available fluorescence resolution was insufficient to resolve some pairs of states participating in vibrational energy transfer. Thus some rate constants concern multistate "channels" as opposed to isolated final states.

Aniline. Chernoff and Rice[164] reported flow patterns from eight S_1 levels with a single collision partner, Ar. The work was extended[165] to the collision partners H_2O and CH_3F on three initial levels in order to study the effect of large dipole interactions and hydrogen bonding on state-to-state transfers. Additional studies were made with He.[166] An explicit study of the sensitivity of flow patterns to collision partner was reported by Struve and co-workers[167] who monitored eight state-to-state transfer channels from the 0^0 level for each of eight collision partners. Gentry and co-workers[122] have studied cross sections for state-to-state transfers from the S_0 0_0 level with He in crossed beam experiments (see section III.C.3). The SVL fluorescence spectroscopy and lifetimes on which the bulb and beam studies are based are given by Rice and co-workers.[124,165]

Among the issues of special interest in aniline is the possible activity of vibrations involving a side group rather than the ring. Only two such "–NH_2" fundamentals lie below 1000 cm^{-1}, however. The inversion mode, $\nu_I' = 337$ cm^{-1}, is well above two out-of-plane ring fundamentals that occur at 177 and 187 cm^{-1}. The first harmonics of ν_I' lie at 760 and 1137 cm^{-1} so that the inversion mode contributes little to the vibrational level structure below 1000 cm^{-1}. The second vibration is an "in-plane" –NH_2 wag $\nu_{15}' = 492$ cm^{-1}.

Pyrazine. McDonald and Rice[168] measured flow patterns for eight S_1 levels using the collision partner Ar. The SVL fluorescence spectroscopy[169] and lifetimes[168] preceding the work are by the same workers.

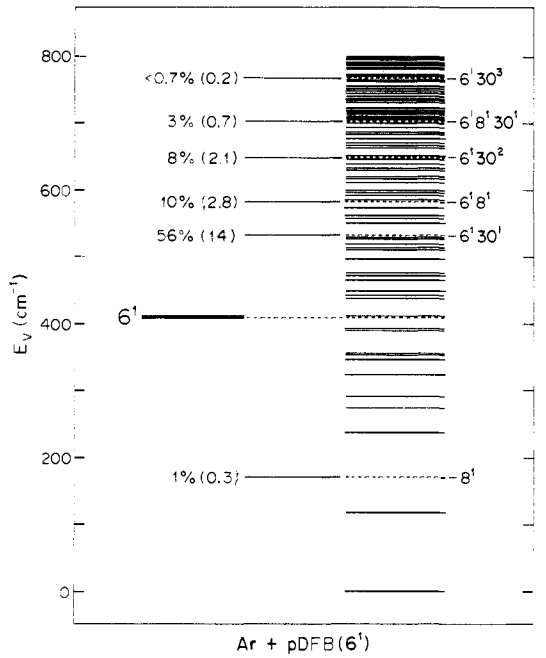

Figure 14. Vibrational flow pattern for Ar + *p*DFB (6^1) collisions. Percentages and P_{100} values are shown for transfers to six final levels. Note that these six levels account for nearly 80% of the total transfer out of 6^1. (See also Figure 11 caption.)

Pyrazine is unique among these aromatics in that its S_1 state is coupled to a triplet state under the so-called intermediate case conditions[170] (the others have statistical case S_1–T coupling). The S_1 state is thus highly sensitive to collisional electronic quenching by all collision partners, (collision-induced intersystem crossing[171]), and the collisional electronic decay channel competes more than favorably with vibrationally inelastic collisional cross sections. Knight and Parmenter[172] have described why the singlet–triplet coupling in pyrazine reduces the vibrational relaxation cross sections relative to those observed in the statistical case molecules.

***p*-Difluorobenzene.** One brief report concerning S_1 transfer characteristics has appeared[126] but most of the results are now being prepared for publication from a Ph.D. thesis.[154] The SVL fluorescence spectroscopy[173] and lifetimes[174] on which the study is based are from several groups. Hall et al.[123] have observed transfer from the S_0 0_0 level using the collision partner He in a crossed beam experiment (section III.C.3). Knight and co-workers[146] have used stimulated emission pumping (SEP) in a three-photon application (pump, dump, probe) to observe state-to-field vibrational transfer in the S_0 electronic state with many collision partners.

The S_1 bulb studies[154] are based primarily on Ar as a collision partner, but make limited flow pattern comparisons with He, N_2, and C_6H_{12} (cyclohexane). They also probe state-to-field transfer with Ar from initial levels ranging as high as 2500 cm^{-1} where the state density exceeds 100 per cm^{-1}. The state-to-field transfers have also been monitored with O_2, an especially interesting collision partner because it also quenches the S_1 electronic state with a cross section similar to that for the vibrational transfers.

*p*DFB has several unique characteristics among these aromatics. One concerns the fact that it has allowed the vibrational flow to be observed also under collision-free conditions[175,176] (the so-called intramolecular vibrational redistribution, IVR) and during vibrational predissociation of S_1 *p*DFB···Ar complexes,[177] a process sometimes considered as a "half-collision". Thus opportunity exists to compare vibrational energy flow within the same molecule under distinctly different interaction Hamiltonians. Second, S_1 *p*DFB has eight fundamentals under 500 cm^{-1} so that it is by a wide margin the most vibrationally complex among the aromatics so far studied. Fourteen fundamentals lie below the highest level pumped for state-to-state studies, that level itself being another fundamental (ν_5' = 818 cm^{-1}). Thus initial level excitation has encompassed half of the 30 modes of S_1 *p*DFB. Third, the studies of Knight and co-workers[146] on S_0 transfer present the best opportunity presently available to compare vibrational energy flow in an excited and ground electronic state of the same molecule.

2. Common Characteristics

The aromatic studies report well over 200 distinct state-to-state rate constants. In this section we are concerned with the forest rather than the trees, and we sort through those data, bringing together those aspects of transfer that appear to be general among the aromatics. We attempt to restrict our discussion to factual observations, that is to the data, as opposed to interpretations which will be treated in a later section. The general energy transfer characteristics described in this section should stand through successive developments of interpretation and should be encompassed by any successful theory.

Large State-to-State Cross Sections. The efficiencies P_{100} listed in the flow patterns of Figures 11–14 give a valid impression of the general magnitude of the V ↔ T,R cross sections commonly found for S_1 state-to-state processes. With the exception of pyrazine (see below) the large cross sections are in the range of a few tenths of hard sphere values. The magnitudes become more impressive when it is realized that a number of those collisional transfers are endoergic T,R → V processes, so that their cross sections have been attenuated by Boltzmann factors from the cross sections that would be found for their exoergic analogues.

Comparisons with Cross Sections for S_0 Transfer. Comments have been made in many of the reports and in other discussions about the *apparent* disparity of magnitudes observed for state-to-state V ↔ T,R cross sections in S_1 electronic states (large) vs. ground electronic states (small). The question is whether some special enhancement mechanism exists for S_1 transfers, an issue of central importance for theoretical discussions of these data.

The answer first requires information about a simpler question. Are S_1 cross sections in fact enhanced at all? Response to this query requires care in the choice of experimental comparisons. As the S_1 aromatic data and many other data show, state-to-state cross sections in a given molecule vary over orders of magnitude among processes that involve different modes, different energy gaps and different quantum number changes. Within this context, it is noted that the S_1 transfers generally involve lower frequency modes and lower energy gaps than those of the S_0 studies. Both effects favor larger S_1 cross sections.

The most valid comparisons of S_1- and S_0-transfer cross sections may derive from the approach by Knight and co-workers[146] who measured state-to-field cross sections in regions of S_1 and S_0 *p*DFB where many state-to-state processes presumably contribute to the cross section. Since these measurements average over many decay channels, there is reduced sensitivity to the parameters that introduce wide variations among transfer cross sections. Knight and co-workers have discussed extensively the subtleties remaining in such comparisons. Within these considerations, they find that their data "provide no evidence to support previous speculations that vibrational relaxation efficiencies in the excited electronic state may be enhanced greatly relative to the ground excited state in the same molecule."[146b] The issue appears settled in *p*DFB.

Lyman et al.[163] have explored vibrational energy flow in S_0 benzene after pumping a level $\nu_{18}'' = 1037$ cm^{-1} with a CO_2 laser followed by a delayed LIF probe of the S_0 vibrational population. The rate constants for state-to-field and state-to-state transfers are extracted from level populations achieved by sequential collisional processes. The extraction uses information theory dependent on model assumptions so that the results are not intrinsically as compelling as those from *p*DFB. The benzene S_0 state-to-field rate constants correspond to about 0.005 of the hard sphere value for Ar collisions[163] whereas one would estimate the number to be about 0.2 from data for a comparable process (with CO) in the S_1 state.[178] It should be noted that 1037 cm^{-1} is a region of quite low level density in S_0 benzene where a few dominant state-to-state processes may well defeat the averaging. Further, the dominant S_1 channels[156-158] involve the lowest frequency S_1 mode $\nu_{16}' = 237$ cm^{-1}. This fundamental nearly doubles in the S_0 state ($\nu_{16}'' = 399$ cm^{-1}). Such a change by itself will have a substantial impact on the transfer cross sections.

High Selectivity among Possible Final States. The selectivity displayed in the four flow patterns of Figures 11–14 is typical of all levels studied with these S_1 molecules. Look, for example, at Figure 14 for transfer from $\nu_6' = 410$ cm^{-1} (an in-plane ring distortion) of S_1 *p*DFB. Transfers to the nearly degenerate levels $8^1 30^2$ (at 411 cm^{-1}), $17^1 30^1$ (394 cm^{-1}), and 27^1 (391 cm^{-1}) are too inefficient to be observed. Instead, the most efficient transfers isolate specific states from comparatively dense fields in regions that are often several hundred cm^{-1} away.

A second common aspect is also displayed in the *p*DFB flow pattern. Endoergic transfers more often than not comprise the dominant channels even though many exoergic channels are available.

Another indicator of high selectivity is found in the experimental parameters $\Sigma k_4(i)/k_4$ reported for three of these studies (pyrazine being the exception). This ratio describes the fraction of total transfer out of a given level that occurs in the *measured* state-to-state channels. (k_4 is the rate constant for transfer into the entire vibrational field and $k_4(i)$ is that for a specific state-to-state process.) In benzene and *p*DFB, for which the k_4 measurements are most secure, most of the transfer (75 percent plus) is generally accounted for by the observed channels, which themselves invariably comprise a small set among the possibilities that lie within one or two kT.

The six listed state-to-state transfers from 6^1 in *p*DFB, for example, account for 80% of the collisional vibrational energy flow, and, in fact, one of those channels alone contains 50% of the total transfer. These numbers become more impressive when it is realized that nearly 160 levels lie within $2kT$ of the initially pumped level. Since $\Sigma k_4(i)/k_4$ ratios are near unity, it is apparent that important decay channels have not been missed due to spectroscopic obfuscation.

TABLE II. A Count of the Reported State-to-State V ↔ T,R Vibrational Energy Transfer Processes with Given Δv Changes in S_1 Polyatomics

	no. of processes with given Δv			
molecule	$\Delta v = 1$	$\Delta v = 2$	$\Delta v = 3$	$\Delta v \geq 4$
benzene	4–9	0–1	0	0
aniline	22	10	1	0
pyrazine	38	1	0	0
*p*DFB	17	17	6	0
CN_2F_2	7	10	4	1

TABLE III. An Ordering by Energy of the Lowest Frequency Modes in Some S_1 Polyatomics Together with a Count of Reported State-to-State Transfers Involving Quantum Changes in These Modes[a]

mode frequency in cm^{-1} (no. of transfers)			
aniline	pyrazine	*p*DFB	CN_2F_2
177 (21)	237 (13)	119 (31)	164 (1)
187 (14)	383 (7)	173 (19)	329 (19)
337 (4)	400 (4)	275 (0)	333 (0)
350[b] (0)	518 (4)	324 (0)	517 (13)
365 (0)	552 (2)	353 (0)	664 (0)
387 (1)	557 (1)	391 (0)	866 (0)
492[b] (2)	558[b] (8)	410[b] (1)	

[a] Only those processes for which absolute rate constants are reported are included. The data are compiled for only a single collision partner, usually Ar. [b] In-plane mode. Unmarked modes in "aromatics" are out-of-plane.

Small Δv Changes. It would be surprising if the high selectivity were not driven by the combined propensities for small change in vibrational quantum number Δv and small energy gaps ΔE between the initial and final states, among other factors. The dominance of small Δv changes among the observed channels is particularly evident in the S_1 aromatic data. Table II makes the point. All reported rate constants turn out to be for processes with $\Delta v \leq 3$.

The ability to see the higher Δv changes is dependent on the ability of the experiments to monitor quantitatively those processes with low cross section. The cutoff at $\Delta v = 3$ thus indicates that high Δv processes have cross sections below the quantitative sensitivity of the experiments. The dynamic range of the experiments as judged by the range in reported rate constants for processes from a given level is commonly less than 10. The range has been expanded for the recent *p*DFB experiments, and this accounts for the exceptional number of $\Delta v = 3$ transitions reported for *p*DFB. They all have (relatively) low cross sections.

Dominant Activity of Low Frequency (Out-of-Plane) Modes. "Low frequency" vs. "out-of-plane" effects cannot be distinguished experimentally since the two are synonomous in these molecules. The dominant activity of the lowest frequency modes is most easily displayed by looking at the modes most frequently undergoing quantum changes in the state-to-state processes. The count is given in Table III which lists

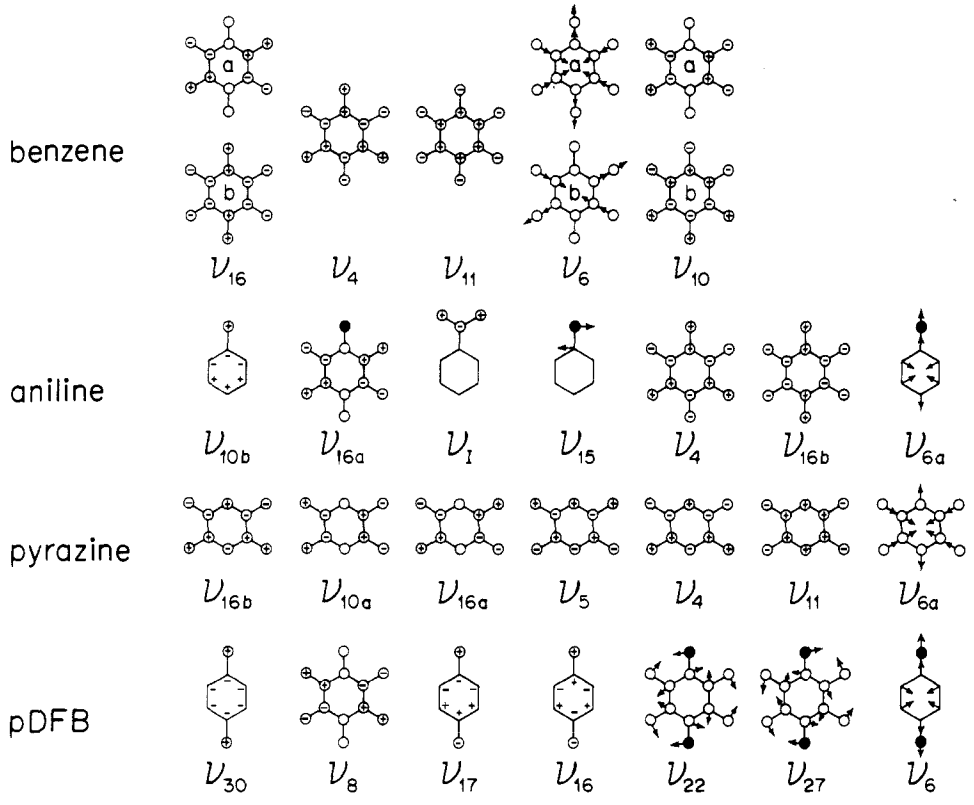

Figure 15. Schematics of the lower frequency S_1 modes in benzene, aniline, pyrazine, and *p*DFB. The schematics are adapted from ref 125 (benzene), ref 124 (aniline), ref 169 (pyrazine), and ref 179 (*p*DFB). The relative displacements are not necessarily to scale. The modes ν_{16}, ν_6, and ν_{10} in benzene are doubly degenerate.

the number of reported rate constants that involve processes with quantum changes in each of the seven lowest frequency modes. Processes involving changes in higher energy modes have not been observed. Diagrams of these vibrational motions are collected in Figure 15.

The role of low frequency modes in aniline and especially in *p*DFB is striking, with the two lowest frequency modes account for more than 85 percent of the reported activity. The pyrazine mode distribution appears more ecumenical by the tabulation in Table III, particularly with respect to activity in the highest mode listed, the in-plane vibration $\nu_{6a}' = 585$ cm^{-1}. All but one of the processes involving that mode are transitions after pumping either $6a^1$ itself or a combination level containing $6a^1$. Thus some of the accumulation of action in ν_{6a} may occur on account of the selection of initial levels. Nevertheless, the largest rate constant reported for any pyrazine process involves a simultaneous change of two "high" frequency modes, $\nu_4' = 522$ cm^{-1} and ν_{6a}'.

Since only one initial level in S_1 benzene was pumped ($\nu_6' = 522$ cm^{-1}), we must look at an indicator other than statistics for an impression of low frequency mode activity. It is found in the flow pattern of Figure 11, where the $\Delta v = +1$ transition in the lowest frequency mode $\nu_{16}' = 237$ cm^{-1} exceeds in efficiency its exoergic competitors by a factor of four and accounts for more than half of the total transfer probability.

On an associated topic, it has been proposed that vibrational levels occur in tightly coupled subsets with respect to energy transfer in benzene and aniline.[164] By this grouping, collisional coupling among levels within subsets would be facile relative to that between levels of different subsets. By reference to the reported data, however, it is difficult to define any such subsets, particularly in the midst of the high activity generally observed for low frequency modes.

Nearly Resonant Levels. Transitions to nearby levels for which ΔE in the V ↔ T,R exchange is small are *not* favored in the competition among state-to-state processes. Numerous examples are found in each molecule where the transition probabilities to nearby levels are too small to allow experimental observation. The example cited above in discussion of the 6^1 *p*DFB flow pattern is typical.

Separated Oscillators. There are now enough data in aniline and in *p*DFB to reveal that cross sections for processes with identical vibration quantum changes are uniform over a wide variety of different initial and final states. As an example consider the S_1 aniline processes

$$0^0 \rightarrow 10b^1$$

$$16a^1 \rightarrow 16a^1 10b^1$$

$$10b^1 \rightarrow 10b^2$$

$$16a^1 10b^1 \rightarrow 16a^1 10b^2$$

In each, the net change is identical, namely $\Delta v = +1$ in the out-of-plane ring deformation ν_{10b}'. In the midst of the wide variation in rate constants for transfer processes, the values for this set are observed to lie within about 25% of their mean. Other $\Delta v_{10b} = +1$ processes also fit this set, and analogous correspondences are found for five other sets of common vibrational mode transfers in S_1 aniline (Table XII of Chernoff and Rice[164]). Extensive data concerning the

lowest frequency mode ν_{30} in S_1 *p*DFB shows uniform rate constants for like Δv_{30} changes between a variety of initial and final states.[154] An explicit exploration of this "independent mode" transfer propensity in S_1 benzene[157] has shown it to be valid for the lowest frequency mode ν_{16} (provided that final level degeneracies are considered!).

This body of data now makes it evident that vibrations can and commonly do operate as independent modes in vibrational transfer processes.

Uniform Flow Patterns among Different Collision Partners. Struve et al.[167] have made an explicit study of the vibrational energy flow patterns established by eight collision partners M effecting T,R → V transfers from 0^0 aniline to 11 final states. When the individual transfer rate constants $k_4(i)$ are normalized by the sum $\Sigma k_4(i)$ of the measured rate constants for a given collision partner, flow patterns emerge where the branching ratios are expressed as the fraction of total measured transfer appearing in each channel. When compared in this way, the flow patterns for all collision partners are similar. Thus, while rate constants for a given process can be sensitive to the identity of the collision partner, the competition among channels is much less so. Similar conclusions have been drawn from data concerning benzene[156] for certain classes of collision partners.

At least one exception occurs to this apparent generality. It concerns intermolecular V–V resonances, that is to say an exchange between a vibrational quantum in the collision partner and a nearly resonant quantum in the pumped molecule. In benzene this exception is seen in several ways. In one case, the flow patterns of small M gases that can exchange V ↔ T,R only are qualitatively different from those in large vibrationally complex M gases that can turn on a large ΔE channel (loss of $\nu_6' = 522$ cm^{-1}), presumably by V–V exchange. This proposition is tested explicitly with the collision partner OCS whose $\nu_2'' = 520$ cm^{-1} is nearly resonant with ν_6' in benzene. The $\Delta v_6 = -1$ channel, which is too small to observe with CO_2 ($\nu_2'' = 667$ cm^{-1}) or with gases permitting only V → T,R exchanges, becomes with one other channel the dominant relaxation process. Struve and co-workers[167] have seen a similar V–V effect in aniline where the S_1 inversion fundamental is nearly resonant with ν_{11}'' of the collision partner allene.

3. Theoretical Modeling

It is probably fair to say that the theoretical efforts directed towards these data have so far been modest. The most successful accounts of the vibrational energy flow, if success is judged by equally modest standards, are based on the atom–diatom model of Schwartz, Slawsky, and Herzfeld[180] as adapted to polyatomics by Tanczos[181] (the SSH-T model). Stretton's early application[182] to ultrasonic relaxation data established its use for polyatomic transfers. All groups reporting the experimental data in aromatics have made some interpretation of flow patterns with constructions related to the SSH-T model. Freed[183] has provided an alternative approach based on an assumed dominant role of intramolecular (isolated molecule) rovibrational couplings. Cerjan, Lipkin, and Rice[184] have considered a special domain of the transfer studies, that of very low energy collisions achieved in expanding supersonic jets (not discussed above), with a theory based on approaches used in neutron scattering. Clary[185–187] has begun an ambitious program of scattering calculations, so far restricted to transfers in ground electronic state polyatomics, that has promise for application to the detailed data on S_1 aromatics (see Section V.A.).

Any theoretical treatment must as a minimum describe the two most blunt generalities of the S_1 transfer data:

(i) large absolute cross sections for the most probable processes, and

(ii) high selectivity among many possible transfers.

In addition, if at least qualitative success is to be achieved, other characteristics must be described:

(iii) propensity for low Δv transitions,

(iv) propensity for activity in low frequency modes,

(v) insensitivity to the molecular point group symmetries of the initial and final vibrational levels (in the isolated molecule),

(vi) insensitivity to V ↔ T,R collision partners, at least to the degree reflected in the data,

(vii) separability of at least some vibrational modes active in transfer processes.

Finally, quantitative success requires as a minimum the reproduction of flow patterns from various initial levels (the competition among state-to-state transfer channels) and as the ultimate achievement, the generation of the correct absolute cross sections that comprise the flow patterns.

Freed[183] has worked out the theory of vibrational energy transfer in large polyatomics under the assumption that intramolecular isolated molecule level couplings, or couplings that become allowed when symmetry is broken in collisions, govern the V ↔ T vibrational flow and establish the flow patterns. The theory is in accord, *at least in principle*, with some of the dominant characteristics of the S_1 aromatic transfers. In particular, it provides a rationale for the large cross sections (a transition between mixed states is dominated by long-range attractive interactions). It also predicts the high final state selectivity that is characteristic of flow patterns since the transfer necessarily selects the set of mixed states. It also contains a ΔE dependence for V ↔ T exchanges of over, say, 100 cm^{-1} that is similar to that often used with applications of the SSH-T approach. The theory would also predict similar flow patterns for various collision partners.

To describe the features of specific flow patterns for given molecules with this theory, one must know the isolated molecule coupling matrix elements between possible levels, at least on a relative basis. It is at this point that a problem occurs. Nothing is known of the values for any of the levels of interest, and no means of estimate is available other than some generalized scaling with coupling order or some other common feature of the interaction. Freed[183] has made comparisons with the aniline and benzene data under the assumption that all coupling matrix elements are identical so that the level interaction for "nonresonant" levels scales as the energy gap between levels, specifically as the ΔE^2 denominator of a squared coupling coefficient. With this severe approximation, the general trend to smaller cross sections for large ΔE transitions is of course reproduced but none of the observed selectivity within this trend is generated.

The promotion of specific collisional vibrational en-

ergy transfers by isolated molecule level couplings has been discussed for several ground electronic state polyatomic molecules.[188-190] A most recent and explicit example occurs, for instance, between Coriolis coupled modes ν_4 and ν_6 in D_2CO.[149a,b]

In contrast to some S_0 state examples, the extent if any to which S_1 aromatic transfer is driven by such couplings remains to be demonstrated. At present there are no reports in which a transfer channel can be associated with an isolated-molecule level mixing. To the contrary, two cases occur in the pyrazine data[168] where tests are possible for efficient transfer between levels known to be in Fermi resonance.[169] Those transfers are not competitive with other channels in either case.

The venerable SSH-T model has been used for most discussions of polyatomic transfer. It is discussed[13,14,182,191] in several monographs and reviews, and numerous authors have commented upon its shortcomings,[192] particularly with respect to its approximations concerning the treatment of collision dynamics and averaging over the intermolecular potential. The model also tends to be used with numerous calibrations to the data so that its a posteriori accounts of energy transfer data are not reliable indicators of its predictive abilities for new systems.

In its application to the S_1 aromatic transfer data, it has completely failed on one basic aspect of the data, namely to account for the large size of the cross sections. On the other hand it has been surprisingly successful in describing the flow patterns, and it is also consistent with other aspects of the data.

The reader is referred to the original papers or monographs listed above for details of the construction of the SSH-T model. We here briefly outline its use with the S_1 aromatic data.

All discussions have dealt with relative transition probabilities expressed as

$$P(\Delta v_a,\Delta v_b) \propto C_{if} V_a^2 V_b^2 I(\Delta E) \qquad (5)$$

$P(\Delta v_a,\Delta v_D)$ is the probability of a state-to-state process in which, for this example, two modes ν_a and ν_b each undergo specified quantum changes. C_{if} is a factor appended to SSH-T by McDonald and Rice[193] to account for aspects of the collision dynamics. V_a^2 and V_b^2 are vibrational coupling matrix elements treating the polyatomic as a collision of uncoupled oscillators ν_a, ν_b, ... $I(\Delta E)$ is an integral over a thermal velocity distribution for colliding pairs under an interaction potential for which the incoming and receding relative velocities reflect the amount of energy ΔE switched between vibrational and translational degrees of freedom (rotations are neglected). Additionally, appropriate multipliers must be used with eq 5 for degenerate final levels.[156,157]

The simplest use of eq 5 concerns its application to the benzene data.[156-158] $I(\Delta E)$ was modeled by a simple function replicating the nearly identical exponential ΔE dependences found by numerical integrations for transfers in several ground electronic state hydrocarbons or halomethanes. The vibrational matrix elements were also set to mimic the results of calculations for these systems. The calculations gave, again rather uniformly, $V^2 \approx 10^{-|\Delta v|}$ for a variety of transfer processes, independent of the frequency, symmetry or other characteristics of the vibrational mode. The factors C_{if} were not used, as this application preceded their introduction.

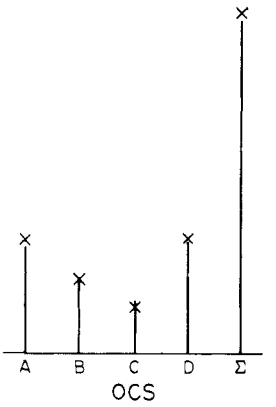

Figure 16. The experimental (bars) and calculated SSH-T (crosses) flow patterns for transfers from 6^1 benzene ($\nu_6' = 522$ cm^{-1}) into the specific state-to-state channels identified in Figure 11. The collision partner is OCS, which has a vibrational resonance ($\nu_2'' = 520$ cm^{-1}) with the S_1 benzene quantum initially pumped.

In this form, such use of SSH-T with parameters modeled entirely for other systems, proves to be remarkably successful in replicating the flow patterns from $\nu_6' = 522$ cm^{-1} for many collision partners. An example (the most successful) is shown in Figure 16 for the collision partner OCS. In the SSH-T calculation, the relative probability of transition to every level within about $2kT$ of the initial level is summed to give a total transition probability out of the initial level 6^1. The flow pattern is then calculated by normalizing the individual channel probabilities to that sum. In the midst of these data lies, presumably, a special V–V resonance with ν_2'' of OCS reflected by a large probability for "channel A", it being the process

$$\text{benzene}(6^1) + \text{OCS}(0_0) \rightarrow \text{benzene}(0^0) + \text{OCS}(2_1)$$

The calculation includes both the V → T ($\Delta v_6 = -1$ only) and the V → V ($\Delta v_6 = -1$, $\Delta v_2 = +1$) processes with the former making negligible contribution because of a small $I(\Delta E)$ factor. Note that here the vibrational matrix element is assumed to be independent even of the molecule in which the quantum change occurs.

The degree to which data and calculations correspond in Figure 16 is not fortuitous since matches of nearly equal quality occur for other collision partners. The simple model also holds in a more stringent test, the state-to-field processes discussed below.

A discussion of benzene, aniline, and pyrazine data within the framework of eq 5 is given by McDonald and Rice[193] where they introduce both the calculation and use of C_{if} factors. These corrections take into consideration aspects of vibrational motions vs. collision trajectories that favor or disfavor specific transfers. The premise is that energy transfer is dominated by those trajectories that produce the largest force on the molecule and that a sampling of trajectories can be converted with symmetry arguments into the C_{if} factors that begin to scale the role of collisional and vibrational dynamics in collisional energy transfer. By this means, some sensitivity to vibrational mode identity is reintroduced into the use of SSH theory. These factors have been combined with the V^2 matrix element from the original benzene application and a similar (but not

identical) $I(\Delta E)$ scaling to calculate some elements of the flow patterns for benzene, aniline, and pyrazine.[193] Predicted relative transfer rates are, with some exceptions, reproduced qualitatively and in some cases quantitatively in these three aromatics.

A further variation in the use of SSH-T procedures has been introduced in the analysis of S_1 *p*DFB data.[194] Attention here turns towards introducing a dependence of the vibrational matrix element V^2 on the mode frequency by using an expression closely related to that in the SSH-T framework derived originally by Stretton.[182] The effect is to boost naturally the matrix elements of low frequency modes relative to others.

When combined with the McDonald–Rice C_{if} factors and an $I(\Delta E)$ dependence similar to that described above, a single set of rules is generated that replicates the dominant aspects of the flow patterns from all seven initial levels for which data exist.

The use of vibrational frequency dependent matrix elements is particular important for *p*DFB because of the high activity associated with an unusually low frequency mode ($\nu_{30}' = 119$ cm^{-1}). Earlier analysis of these data[126] without frequency-sensitive matrix elements required an ad hoc postulate of special activity of this mode, justified in part by its known propensity for facile participation in intramolecular state mixing and intramolecular vibrational redistribution. Within the present SSH-T analysis, however, the "special" character of ν_{30} is entirely due to its low frequency and favorable C_{if} factors.

In summary, the SSH-T model has, in spite of its severe shortcomings of conception, provided a rather useful frame of reference for discussion of the S_1 aromatic data. In application, it has required amendments to fit the data, but all have been steps towards rather than away from improved physics. Most importantly, it has provided a glimpse of the propensity rules that so obviously govern energy transfer and that must be reproduced by the contemporary theoretical approaches. Rice[192] has referred to all of these SSH-T applications with the word "crudities". Perhaps he was making allusion to the French gastronomic term "assiette de crudité", an appetizer exciting the palate for the more serious efforts to follow.

4. *Other Aspects of "Aromatic" Studies*

Several issues concerning transfer do not fall conveniently in the previous sections but are related, in one way or another, to the discussions above.

State-to-Field Transfer. There are now two molecules, benzene and *p*DFB, for which the collisional transfer rate constants have been measured from each of a variety of known initial states into the surrounding field of vibrational levels. The initial states extend well above the regions of the level diagram of Figure 10, occurring in regions with level densities as high as 10 per cm^{-1} (benzene) or 100 per cm^{-1} (*p*DFB). The studies have been instructive in several concerns of vibrational energy transfer.

Logan et al.[162] completed the first extensive work of this type with measurements of transfer induced by many collision partners on a combination level $2\nu_6' + \nu_1'$ of benzene near 1970 cm^{-1}. They demonstrated that all gases ranging from He to complex hydrocarbons relaxed this level with cross sections essentially hard sphere or greater. Furthermore, the range of collisional efficiencies among these diverse collision partners is highly restricted, being less than an order of magnitude. They also monitored the *growth* of three S_1 levels at or near the bottom of the S_1 manifold. Those data demonstrated the stepwise, many-collision nature of reaching these low levels. In contrast to the restricted range of the initial level depopulation efficiencies, large vibrationally complex molecules are by far the more efficient for "full" vibrational relaxation. The efficiencies of initial level depopulation correlate reasonably well with a well depth parameter that reflects primarily the variation of the attractive potential of the colliding pair.[195]

Tang and Parmenter[158] monitored state-to-field rate constants for collisions of S_1 benzene with S_0 benzene, CO, and isopentane for 11 levels ranging from 0^0 up to 2350 cm^{-1}. The rate constants for isopentane remain restricted to a small range for all benzene levels, whereas those for CO are much smaller for low levels but nearly match the constants of isopentane for high levels. This contrast is discussed in terms of the competition between V–T and V–V processes with the two gases (V–V here taken as exchange of vibrational quanta in the collision partner with those of benzene). While the vibrationally stiff partner CO transfers energy only by V–T,R processes, isopentane can additionally take advantage of vibrational "resonances". It is argued that most of the isopentane transfer (ca. 70%) occurs by V–V processes for low levels but that V–T,R takes over at high levels (ca. 90%) where thousands of levels lie within kT.

The CO state-to-field data also comment specifically on state-to-state processes because they can be modeled well on a relative basis with the SSH-T propensity rules that work well for low level transfer. The success of the modeling suggests that the calculations can be examined to reveal the flow patterns into the dense fields. It is concluded that everywhere in these V–T,R studies, energy transfer is dominated by the high selectivity among final levels that has proven to be characteristic of S_1 aromatics. At an initial level energy of 1970 cm^{-1}, where 2200 levels lie within about kT of the initial state, calculations suggest that 58 final levels contribute 70 percent of the total transition probability. Those levels involve $\Delta v = 1$, 2, or 3 transitions only.

State-to-field measurements with Ar in S_1 *p*DFB extend to about 2400 cm^{-1} of vibrational energy where $\rho_{vib} > 100$ per cm^{-1}. They also show the persistence of level selection in these relatively dense regions of the manifold. In this case the demonstration is by the special behavior of state-to-field transfers from combination levels $X^mY^n30^1$ vs. that from their X^mY^n counterparts. In every case studied, transfer rate constants from the levels containing ν_{30}' are higher than those from the corresponding X^mY^n level, and the increase is by an additive amount uniform among all cases. The increase in fact corresponds precisely to that of the known single channel rate constant for the process

$$30^1 \rightarrow 0^0$$

This match implies that the loss of ν_{30} occurs as a distinct quantum change and with a sustained high probability whenever the possibility is present.

E-E Contributions to Vibrational Energy Transfer. S_0 benzene–S_1 benzene collisions are associated with vibrational energy transfer rate constants about twice as large as those for the most efficient vibrationally complex hydrocarbons.[158] One of the contributors to such efficiency could be electronic energy switching without vibrational energy exchange in the interacting molecules. This E-E switch would result in the appearance of an S_1 molecule with different vibrational energy than that in the original vibrationally excited S_1 molecule.

The efficiency of E-E transfer in C_6D_6–C_6H_6 mixtures has been measured[196] with vibrational state selection in the initial state (S_1 C_6D_6, 0^0) and final state (S_1 C_6H_6). E-E switching without change of vibrational quanta,

$$C_6D_6(0^0) + C_6H_6(S_0) \rightarrow C_6D_6(S_0) + C_6H_6(0^0)$$

$$\Delta E = -203 \text{ cm}^{-1}$$

was observed to be more probable than the more nearly resonant process

$$C_6D_6(0^0) + C_6H_6(S_0) \rightarrow C_6D_6(S_0) + C_6H_6(16^1)$$

$$\Delta E = +34 \text{ cm}^{-1}$$

The exchange occurs with a cross section substantially exceeding hard sphere. By implication, E-E transfer provides an efficient special route for vibrational relaxation in $C_6H_6(S_1)$ + $C_6H_6(S_0)$ collisions.

Vibration–Rotation Transfer. Pineault et al.[167] have analyzed their data involving eight collision partners on the 0^0 level of S_1 aniline with a search for evidence of V–R contributions to a state-to-state vibrational change. The test involves a modification by Moore[197] of the SSH-T formulation that obtained a dependence of the V–R transfer probability on the ratio I/d^2. That ratio involves the inertial moment I of a rotor constructed of the peripheral atoms of the collision partner and the separation d of the peripheral atoms from the rotor center of mass. Correlations between collision partner I/d^2 values and the experimental transition probabilities could not be found.

Reduced Transition Probabilities in Molecules with Mixed Electronic States. The V–T,R rate constants for dominant channels in S_1 pyrazine transfers are an order of magnitude less than those in the other S_1 aromatics. Knight and Parmenter[172] have shown that transfer rate constants are similarly reduced in pyrimidine, a pyrazine isomer where the nitrogens are meta. The reduced rate constants are considered to be an example of a general phenomena occurring whenever the fluorescing state displaying vibrational transfer (here S_1) is of mixed electronic character under the strong coupling, intermediate case of radiationless transition theory. In these cases, there is substantial character of a dark, nonfluorescing electronic state mixed with the S_1 state. It is shown that the efficiency of vibrational transfer to another S_1 level is reduced from pure electronic state values by a factor related to the mixing coefficient. The observed reductions of transfer cross sections in pyrazine and pyrimidine are consistent with theoretical predictions that use data concerning the photophysical properties of the S_1 states.

B. Difluorodiazirine

With nine vibrational degrees of freedom, CN_2F_2 is the smallest molecule for which extensive vibrational flow patterns have been established by these S_1 bulb techniques. The energy level schematic in Figure 10 shows the sparse nature of the vibrational manifold below 1000 cm^{-1}, the region of interest for transfer studies. Due to fortuitous ratios of vibrational frequencies for the lowest five modes (approximately 1:2:2:3:4), the levels occur in closely spaced groups separated by about 160 cm^{-1}. Diagrams of the nine vibrational modes have been given.[198]

A comprehensive report of the fluorescence spectroscopy, fluorescence lifetimes, and vibrational energy transfer characteristics has been published by Vandersall and Rice.[198] Flow patterns for Ar collisions derive from measurements of absolute rate constants for 22 state-to-state transfers involving six initially pumped levels. The highest is an overtone at 1034 cm^{-1}.

The vibrational transfers have both similarities and marked departures from the common characteristics of transfer in aromatics. The similarities are most easily described. First, the high selectivity seen among possible final states demonstrates that propensity rules govern the collisional energy flows, and that the rules are as severe as those in aromatics. Second, one of the transfer restrictions would again appear to be the propensity towards processes with small changes in vibrational quantum numbers. The point is made in Table II where the Δv changes are summarized for the 22 processes occurring with large enough probabilities to be characterized by transfer rate constants.

In contrast to the benzene, aniline, and *p*DFB data, the magnitude of transfer rate constants is relatively small. The largest reported constant is only 0.06 of the gas kinetic value. A more striking contrast to the aromatic data appears in the pattern of mode activity that is summarized in Table III. By the criterion of counting the number of distinct processes for which given modes undergo quantum change, a curious pattern of activity emerges. The lowest frequency mode ν_9' = 164 cm^{-1} undergoes quantum change in only one among the 22 processes for which rate constants are reported, in spite of a statement in the report concerning "the ubiquitous presence of mode ....9 in the energy transfer pathways." The next lowest frequencies occur as a close pair, ν_5' = 329 cm^{-1} and ν_7' = 333 cm^{-1}, but only ν_5' is active in the transfers. The remaining reported activity is found in the fourth mode up the ladder at 517 cm^{-1}.

In experiments such as these, there is always hazard that activity in given modes may be obscured by unfortunate coincidences in the spectroscopy. Specific comment in the paper implies that this is not the case for the surprisingly inactive mode ν_7'. The case for ν_9' or other unrecognized activity making substantial contributions to energy flow could be checked easily if the rate constants for total energy transfer out of initial levels were available. These constants would then allow calculation of the fractions of the total energy transfer actually accounted for by the observed transitions.

Two state-to-state transfers are particularly interesting in CN_2F_2 because they seem to be so far outside of the "aromatic" expectations for competitive processes. One is the Δv = 5 transfer $4^2 \rightarrow 5^3$ (ΔE = 47

cm^{-1}). In view of the large Δv change, the size of the rate constant (in midrange among the 22) is as surprising as the fact that it can be observed at all. The second is a $\Delta v = 2$ transfer $4^1 5^1 \rightarrow 1^1 5^1$, also with a midrange rate constant, whose $\Delta E = 920$ cm^{-1} is perhaps the largest for any reported state-to-state transfer among the molecules considered here.

After seeing so many points of departure from the aromatic data, it is not to one's astonishment that the simple propensity rules used to model the benzene flow patterns do not replicate the energy flows observed in CN_2F_2. In an alternative approach, the relative magnitudes of a selection of eight of the 22 rate constants are modeled by a procedure that effectively combines the McDonald–Rice correlation diagram collisional dynamics factors and the ΔE constraint found in the SSH formulation. That constraint occurs in the integral $I(\Delta E)$, and it is approximated by the form used with the S_1 pyrazine data. The model specifically omits any propensity restrictions associated with the magnitude of Δv changes. The success of the modeling is taken as evidence that the collision dynamics propensities with the ΔE dependence are the dominant qualitative factors that control CN_2F_2 transfer dynamics. It might be observed, however, that the remaining 14 processes need to be included in this modeling to obtain a realistic appraisal of the success of such a treatment. Additionally, the modeling would predict that many absent processes involving quantum changes in the low frequency modes ν_9' and ν_7' would have large rate constants, with values matching or in some cases exceeding those of the dominant reported state-to-state changes. Thus, considering the omissions of both observed and nonobserved processes, it is probably most accurate to say that even qualitative success has yet to be demonstrated for modeling of the difluorodiazirine data by any scheme related to the SSH procedures.

Rolfe and Rice[199] have provided a detailed and highly instructive account of their classical trajectory studies of vibrational energy flow in S_1 CN_2F_2 + Ar collisions. Perhaps the most important demonstration of the calculations concerns the issue of selectivity. The studies reveal high mode-to-mode specificity in the midst of the large numbers of near resonances in the system of classical oscillators. In this respect the calculations replicate the most dominant and uniform aspect of the S_1 vibrational energy transfer experiments. On the other hand, the specific flow patterns observed for CN_2F_2 are not reproduced. The authors suggest that part of this problem may be due to the approximate nature of the assumed Ar–CN_2F_2 potential energy surface, and argue also that quantum mechanical simulations will be necessary to account for the specific features of polyatomic mode-to-mode transfers.

C. Glyoxal

Glyoxal, $C_2H_2O_2$, is perhaps supreme among the molecules discussed above with respect to its prospects for informative S_1 vibrational energy transfer studies. To complement theoretical accessibility arising from its relatively small size and high symmetry, it is uniquely suited to the needs of the experimentalist. The $S_1 \leftarrow S_0$ transition is in the visible with a highly detailed absorption spectrum that is relatively free of spectral congestion. The spectrum is well analyzed with respect to both vibrational and rotational structure. Thus excited state levels with selected and known ν, J, and K are readily pumped. Additionally, both glyoxal and glyoxal-d_2 fluoresce with high yields so that state resolved vibrational (and rotational) energy transfer is easily followed.

These assets have generated a relatively rich literature concerning glyoxal photophysics and to a lesser extent photochemistry. The reported vibrational energy transfer picture, on the other hand, is not well developed compared to that for aromatics and difluordiazirine, although substantial unpublished state-to-state data exist in Ph.D. theses.[200,201] In addition the data and discussions are scattered among many papers[172,195,202–207] often appearing as brief ancillary inclusions to other interests.

From the published reports, one can construct to modest quantitative precision flow patterns for the initial levels 0^0, 7^1, and 8^1 of glyoxal-h_2. The lowest frequency mode, $\nu_7' = 233$ cm^{-1}, is a torsional motion of the formyl groups about the C–C bond, while $\nu_8' = 735$ cm^{-1} is a C–H wagging vibration. For all three initial levels, the torsional mode is dominant in activity, particularly when compared to activity in the next lowest fundamental $\nu_{12}' = 380$ cm^{-1}. In transfers from the lowest levels 0^0 and 7^1, $\Delta v_7 = 1$ or 2 are the only quantum changes characterized. With inert gases, the cross sections for the most favorable of these transitions are large, not far below the hard sphere value.

Transfer from the high initial level 8^1 has distinctive elements. For example, Rettschnick and co-workers[202a,204] have published data on glyoxal-$h_2(8^1)$ + glyoxal-$h_2(0_0)$ collisions. They found that the $8^1 \rightarrow 0^0$ channel occurs with a cross section nearly identical with that for the $8^1 \rightarrow 8^1 7^1$ channel. Further, the two quantum change $\Delta v_8 = -1$ with $\Delta v_6 = +1$ to reach the nearly resonant level 6^1 has a cross section nearly 50% *larger* than that for the $\Delta v_7 = +1$ channel.

Unfortunately, it is not clear to what extent the large cross section for $8^1 \rightarrow 0^0$ in glyoxal–glyoxal collisions is due to vibrational energy transfer as opposed to E-E transfer. Rettschnick et al. claim in ref 202a and 204 that the *same* flow pattern was obtained for collisions of glyoxal-$h_2(8^1)$ with CO_2, N_2, CO, Ar, propane, and glyoxal-$h_2(S_0)$. If this statement is correct, it would rule out a large contribution from E-E transfer. However, unpublished results of de Leeuw[201] demonstrate clearly that E-E transfer is mainly responsible for $8^1 \rightarrow 0^0$ transfer in glyoxal-d_2 + glyoxal-h_2 collisions. In collisions of glyoxal-$d_2(8^1)$ with other gases (He, Ne, Ar, Kr, Xe, H_2, D_2, n-C_4H_{10}, CH_3Cl, and OCS), de Leeuw found that $8^1 \rightarrow 8^1 7^1$ was the dominant channel in each case (while the cross section for $8^1 \rightarrow 0^0$ was smaller by a factor of 6 to 20, depending on collision partner). These unpublished results are more in accord with "aromatic" experience. Hopefully, a clearer picture will emerge when these results are presented in detail in the literature.

Glyoxal is also distinctive among the S_1 studies in that it joins benzene as the only polyatomic molecules for which cross sections for rotational energy transfer in an excited electronic state have been reported. They also are among the few studies of rotational transfers in nonpolar polyatomics. The benzene study[208] provided information about the magnitude of the cross

section for total rotational transfer out of an ill-defined distribution of rotational states in the 0^0 level (several times hard sphere for Ar). In glyoxal, however, the open rotational structure in $S_1 \leftrightarrow S_0$ absorption and emission bands allows selection of numerous initial J'K' states. This opportunity has yet to be exploited by tunable excitation with bandwidth narrow enough to pump single rotational states. The published reports describe experiments with either fixed narrow bandwidth lasers that reach simultaneously several known J'K' states,[207] or with tuned excitation with broad (1 cm^{-1}) bandwidth that can only select an ensemble of S_1 levels with uniform K' but dispersion in J'.[202a,b,d] From these studies, it is seen that total rotational relaxation cross sections exceed hard sphere for a variety of collision partners and are of similar magnitude to those reported for many molecules in ground electronic states. It is also established that strong restrictions to small ΔK or small ΔJ transitions do not exist in pure rotational energy transfers.

D. CF_2

The UV spectroscopy of most triatomics is so congested on account of upper electronic state mixing that bulb studies of S_1 vibrational energy flow is not possible. The exception presently concerns the radical triatomic CF_2.

CF_2 can be formed in its ground electronic state by CO_2 laser multiphoton dissociation of CF_2HCl[209] or by KrF laser (248 nm) photolysis of CF_2Br_2.[210] In flowing streams of certain gases, it is sufficiently stable so that selected vibrational levels of the electronically excited $\tilde{A}$ state can be pumped to allow study of V → T vibrational energy flow. Because of the special nature of its preparation and containment, single-collision data are achieved by time-resolved $\tilde{A} \rightarrow \tilde{X}$ UV fluorescence study rather than by simple pressure manipulation as in the cases discussed above.

Akins et al.[209] pumped the bending mode in the $\tilde{A}$ state with a dye laser and were able to reach (0,n,0) levels with $1 < n < 6$. They reported measurements of total vibrational relaxation rate constants for these initial levels; the rate constants increase monotonically and faster than linearly with n, for each of the collision partners He, Ne, N_2, and SF_6.

The state-to-state vibrational energy flow data derive from the study of Dornhofer et al.[210] who used a second 248-nm photon of the KrF laser for $\tilde{A}$ (0,6,0) ← $\tilde{X}$ (0,0,0) pumping. The symmetric and antisymmetric stretches in $\tilde{A}$ CF_2 have similar frequencies and are nearly equal to two quanta of the bend. Thus, two nearly resonant V → T transfer channels involving the stretches,

$$\tilde{A}\ (0,6,0) + M \rightarrow \tilde{A}\ (1,4,0) + M \quad \Delta E = -29\ cm^{-1}$$

$$\tilde{A}\ (0,6,0) + M \rightarrow \tilde{A}\ (0,4,1) + M \quad \Delta E = -16\ cm^{-1}$$

compete with the simple $\Delta v = 1$ process

$$\tilde{A}\ (0,6,0) + M \rightarrow \tilde{A}\ (0,5,0) + M \quad \Delta E = -494\ cm^{-1}$$

With M gases He, Ne, Ar, and N_2, excitation of the infrared active asymmetric stretch is not competitive with the other processes. High selectivity occurs between these $\Delta v = 3$ processes with essentially identical ΔE values (relative to kT). In turn the two remaining channels listed above are competitive, with the rate constant for the nearly resonant channel exceeding that for $\Delta v = 1$ of the bend by only a factor of 2 to 7, depending on the collision partner. The rate constants themselves approach gas kinetic values. The data are consistent with the proposition that these two processes are the principle relaxation channels from (0,6,0).

Dornhofer et al. have also been able to measure the rate constant for a second $\Delta v = 1$ process involving the bend:

$$\tilde{A}\ (1,4,0) + M \rightarrow \tilde{A}\ (1,3,0) + M$$

The rate constants of these two $\Delta v_2 = -1$ state changes are identical within the experimental accuracy. This result is quite reminiscent of an S_1 aromatic characteristic.

DePristo[211] has considered theoretically some of the possible state-to-state processes in $\tilde{A}$ CF_2 relaxation. This study preceded the availability of the quantitative state-to-state data of Dornhofer et al. Some comments about the juxtaposition of that theory with experiment are given by the latter authors.

V. Theoretical Approaches

As in many areas of physical chemistry, there are two aspects to any understanding of energy transfer processes (be they inelastic or reactive). The first has to do with molecular electronic structure, as embodied in the concept of the potential energy surface (PES), while the second has to do with the dynamics of heavy particle motion on the PES. The ability to separate the problem into these two parts is, of course, a consequence of (and only as good as) the Born–Oppenheimer (B.–O.) approximation.[212] Although the assumption of separable electronic and nuclear motions is not always satisfied (leading, for example, to such nonadiabatic processes as electronic predissociation, electronic-to-vibrational energy transfer, etc.), we shall restrict ourselves to systems for which the nuclear motion occurs on a single, well-defined PES.

Despite impressive advances in experimental and theoretical techniques over the past 20 years, determining the form of the full PES remains a very difficult problem, even for three-atom systems. From the experimental side, the problem is that it is usually impossible (or at least infeasible) to directly "invert" even the most detailed inelastic scattering data to obtain the PES. From the theoretical side, the problem is that there is no easy way to calculate the B.–O. potential energy surface. It is an intrinsically quantum mechanical quantity, and the only way to get at it is to solve the electronic Schrödinger equation at a large number of fixed values of the internuclear coordinates.[213]

Since 1970, quantum chemists have succeeded in characterizing the full PES for a handful of light three-atom and four-atom systems using purely ab initio methods. The problem with extending these calculations to more complicated systems is twofold. First, the cost of determining the potential energy for a given configuration of the nuclei increases nonlinearly with the number of electrons in the system. Second, and perhaps more important, the number of points needed to map out the PES increases nonlinearly with the number of nuclei in the system.

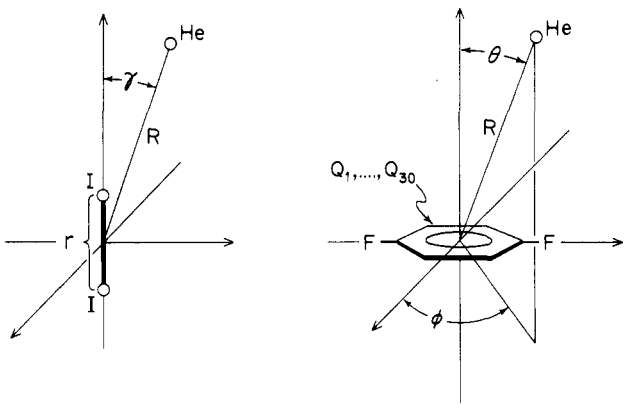

Figure 17. Two systems for which extensive vibrational energy transfer data is available from beam and bulb experiments.

Consider, for example, the two systems shown in Figure 17. These systems are chosen for illustration because extensive data on vibrational energy transfer, from both crossed beam and bulb experiments, exists for each. For the He + I_2 system, the potential energy depends on only three coordinates: the I_2 internuclear separation, r; the distance R between the He atom and the I_2 center-of-mass; and the angle γ between $\vec{r}$ and $\vec{R}$. To map out the ab initio PES one might perform calculations at, say, 10 values each of r, R, and γ, giving a 10 × 10 × 10 grid, or 10^3 points. These points could then be fit to some analytical functional form to represent the full PES. For atom–diatom systems, it is customary to expand the potential in a Legendre series:

$$V(r,R,\gamma) = \sum_n v_n(r,R)P_n(\cos\gamma) \qquad (6)$$

The coupling between r and R leads, in a more or less complicated way, to the experimentally observed vibrationally inelastic scattering. (Of course, for the He–I_2 system, only even values of n would occur in the expansion (6)). Despite the small dimensionality of this system, ab initio calculation of the He + I_2 PES would still be very time consuming due to the fact that there are 108 electrons.

The second system shown in Figure 17, involving the interaction of a He atom with a *p*-difluorobenzene molecule, contains 13 heavy particles and 60 electrons. The potential energy now depends on 33 coordinates, namely the radial distance R between the He atom and the molecular center-of-mass, two angles describing the orientation of the He atom relative to the ring, and 30 internal vibrational coordinates of the molecule. To map out this PES with 10 increments in each coordinate would require 10^{33} separate calculations. Use of the so-called "analytic derivative" methods[213d] might reduce the amount of work substantially, but the number of calculations required to fully characterize the PES would still be astronomical. Because of this dimensionality problem, ab initio theory cannot be expected, either now or in the future, to provide complete potential energy surfaces for complex polyatomic systems. Instead, as Schaefer[213a] wrote in 1979, the best that we can hope for is "a judicious synthesis of theory and experiment to arrive at a complete, working potential surface."

In this regard, it should be emphasized that certain regions of the full PES are usually known quite accurately from spectroscopic measurements on the isolated scattering partners. For example, the one-dimensional potential energy curve of the isolated I_2 molecule is known very accurately (in several electronic states) from electronic absorption and fluorescence studies, and the 30-dimensional vibrational force field of the isolated *p*-difluorobenzene molecule may be determined, at least in principle, using routine spectroscopic methods. By combining this knowledge with selected theoretical calculations describing the perturbation of the isolated molecule by an approaching scattering partner, the hope is to obtain a workable PES while avoiding (theoretically) the full dimensionality of the problem. Since the problem is usually one of determining the interaction between two species whose isolated properties are already understood, the PES is often referred to simply as the "interaction potential."

Ordinarily, the determination of the interaction potential, per se, is not considered to be part of the "theory of vibrationally inelastic scattering." Rather, all theories of vibrationally inelastic scattering assume some form for the interaction potential (be it ab initio, semiempirical, or purely ad hoc) and then proceed to explore various dynamical approximations to the heavy particle scattering. Many of the basic ideas of vibrational energy transfer theory date back to the 1930s. Since then, a wide variety of dynamical approximations has been explored. The richness of this field derives from the fact that (unlike the electronic structure problem, which demands an explicitly quantum mechanical solution) the nuclei are sufficiently massive and move sufficiently slowly that a full quantum mechanical treatment of the nuclear motion is not always necessary, or even desirable.

Unfortunately, we had neither the time nor the energy to comprehensively review the large number of theoretical papers that have appeared, even in just the last few years, on the subject of vibrationally inelastic scattering. This job awaits the efforts of a discriminating theoretician. Nevertheless, we thought it might be useful to some readers (especially newcomers to the field) to try to give an overview of the theory from an experimentalist's point of view, i.e., with an emphasis on theoretical approaches and approximations that have been used to make meaningful comparisons with actual, three-dimensional experimental results. Our discussion is elementary and nonmathematical. References to more sophisticated discussions of various aspects of the theory will be given as we go along.

A. Quantal Scattering Theory

The most rigorous (and in principle exact) theoretical approach involves an explicit, quantum mechanical treatment of all nuclear degrees of freedom, including the relative translational motion. The posing of the quantal scattering problem is not in itself conceptually difficult. For rotationally inelastic scattering of rigid rotor molecules, a succinct statement of the problem is given in eq 1–10 of ref 15a. For rovibrationally inelastic scattering,[15b] more subscripts have to be added to the equations to keep track of the vibrational quantum numbers, but the form of the equations is the same.

In words, the quantum mechanical problem may be formulated in terms of a plane wave incident on a

scattering center. (A time-dependent description involving the scattering of wave packets is also possible and leads to identical results.) Each inelastic transition may be viewed (asymptotically) as the "absorption" of part of the incoming plane wave followed by the "reemission" of a radial scattered wave. The amplitudes of the radial scattered waves determine the state-to-state differential cross sections. To obtain these amplitudes, the total wave function must be expanded in a complete set of basis functions in the internal coordinates (usually the separated system rovibrational eigenfunctions), with an unknown radial function for each internal basis function. By plugging this expansion into the time-independent Schrödinger equation, a coupled set of second-order differential equations involving the unknown radial functions is obtained. The solution of these so-called "close-coupled" equations constitutes the fundamental problem in quantal scattering theory. Once the radial functions are known, it is easy to calculate the amplitudes of the inelastically scattered radial waves, the state-to-state differential cross sections, and any other quantities of interest.

Unfortunately, it is vastly more complicated to solve the close-coupling problem than it is to write it down. Part of the problem has to do with choosing the most convenient coordinate system (or angular momentum representation) and a good set of basis functions in which to expand the total wave function, taking advantage of any symmetry the problem might have. Another problem, of course, is developing efficient and numerically stable methods of solving the coupled differential equations (or an equivalent set of integral equations). An excellent, systematic discussion of the strengths and weaknesses of the various numerical methods that have been developed so far has been given by Secrest.[15a,b] One popular method, due to Gordon,[214] is available as a canned computer program.

Although both the principles and computational tools for tackling the close-coupling problem have been around for some time, most applications have been restricted to pure rotationally inelastic scattering in light systems with widely spaced energy levels and at low collision energies. As far as we know, there have been only two "exact" calculations in atom–diatom systems at collision energies high enough to give a significant probability of vibrational excitation. The first is the study of $Li^+ + H_2$ scattering by Schaefer and Lester;[47] the second is the study of $He + H_2$ scattering by Lin and Secrest.[215]

The problem with extending close-coupling calculations to heavier systems and higher collision energies is reminiscent of the problem we discussed earlier in connection with ab initio calculations of the potential energy surface. Here, the problem has to do with the rapid increase in the number of coupled channels one has to include in the calculation as either the molecular mass or the collision energy increases. Because of the $(2j + 1)$ rotational degeneracy, the number of coupled channels in an atom–diatom system goes roughly as $j_{max}^2 \cdot n_v$, where n_v is the number of vibrational levels included and j_{max} is the maximum value of the rotational quantum number j, assumed to be the same for each vibrational level. (In practice, it is usually necessary to include some vibrational and rotational levels beyond those which are energetically accessible in order to obtain converged solutions, but it may not be necessary to include the same number of rotational levels for each vibrational channel.) Since, using presently available algorithms, the time required to solve N close-coupled equations scales roughly as N^3, the total cost of a close-coupling calculation on an atom–diatom system increases roughly as j_{max}^5.

The implications of this result were recognized from early on: for quantal scattering theory to have any practical utility in vibrationally inelastic scattering problems, approximations had to be devised to simplify the treatment of the rotational part of the problem. The most dramatic simplification occurs if one ignores the rotations entirely, either by reducing the problem to one dimension or, in three dimensions, by assuming that the vibrational transition probabilities can be calculated using just the spherical average of the interaction potential (the "breathing sphere" approximation). The one-dimensional approximation presumes that a single collision orientation is mainly responsible for the vibrationally inelastic scattering, while the breathing sphere approximation presumes that all collision orientations are equally likely. Neither of these approximations is expected to hold very well for any real physical system. Both should be appreciated in the spirit in which they were originally offered, that is, as model problems whose primary purpose is to provide qualitative insight into the vibrational energy transfer process. (A few model problems will be discussed in part D below.)

For a quantitative description of vibrationally inelastic scattering, more realistic approximations are required. Since 1972, a variety of so-called "angular momentum decoupling approximations" have been proposed. These approximations have been discussed in a systematic way by several authors.[216–218] The two most important are: the coupled-states (CS) approximation (also referred to in the literature as the "centrifugal-sudden," the "j_z-conserving," the "helicity-conserving," and the "spherical rotor" approximation); and the infinite-order sudden (IOS) approximation (also known as the "oriented rotor" approximation). Since both the CS and especially the IOS approximations have played a crucial role in extending quantal scattering theory to vibrationally inelastic problems, it is important even for experimentalists to gain at least a qualitative understanding of what is involved in each approximation.

For concreteness, consider the problem of calculating cross sections for the rovibrationally inelastic transition

$$A + BC(v_i = 0, j_i = 0) \rightarrow A + BC(v_f = 1, j_f = 3) \quad (7)$$

As stated earlier, the relative motion of A and BC before the collision may be represented by a plane wave. In quantal scattering theory, the incident plane wave may be expanded as a sum of partial waves, one for each initial (integer) value of the orbital angular momentum, l_i. (Recall that, classically, the orbital angular momentum is given by $l = \mu v b$, where μ and v are the reduced mass and relative velocity of the collision pair, and b is the classical impact parameter). Consider first a close-coupling treatment of process 7. To obtain converged solutions for the $(v = 0, \theta = 0) \rightarrow (v = 1, j = 3)$ transition, it might be necessary, say, to include four vibrational levels (v = 0–3) and rotational levels up to $j_{max} = 5$ in the calculation. (We choose these values only for illustration.) Since the total angular

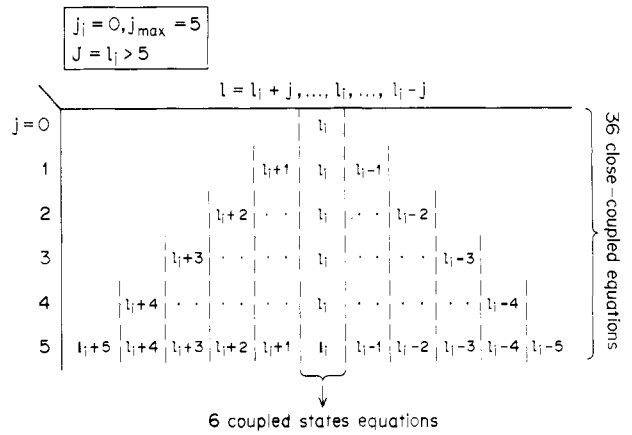

Figure 18. Schematic representation of the rotational channels involved (for each vibrational level and for a typical partial wave with $l_i > j_{max}$) in a quantal treatment of the sample problem (7) described in the text. In the exact close-coupling treatment, all 36 rotational channels are coupled together. In the coupled-states approximation, rotational channels are coupled only to other channels in the same column with the same value of l. In the infinite-order sudden approximation, rotational channel coupling is eliminated entirely. But rotational information is recovered by solving the uncoupled problem for various fixed orientations of the colliding molecules.

momentum J must be conserved, the close-coupled equations may be solved for each value of J independently. Since $j_i = 0$ in our example, $J = l_i$. The number of close-coupled equations that must be solved for each value of l_i is determined by the coupling between the rotor angular momentum j and the orbital angular momentum l. The number of equations is different depending on whether $l_i < j_{max}$ or $l_i > j_{max}$. Usually, the number of partial waves that contribute to the scattering is much larger than j_{max}, so we can consider ($l_i > j_{max}$) as the typical case.

In the close-coupling treatment, all (v,j,l) channels that conserve total angular momentum are coupled. For each of the n_v vibrational levels included in the calculation, and for each value of j from 0 to j_{max}, there will be $(2j + 1)$ values of l, ranging from $(l_i + j)$ down to $(l_i - j)$, that conserve total angular momentum (see Figure 18). Therefore, the total number of close-coupled equations for each partial wave with $l_i > j_{max}$ will be

$$N = n_v \sum_{j=0}^{j_{max}} (2j + 1) = n_v(j_{max} + 1)^2$$

In our example, $n_v = 4$, $j_{max} = 5$, and $N = 4 \times 36 = 144$. This number is comparable to the number of channels included in the largest close-coupling calculations performed to date.

The big problem with the full close-coupling treatment is the proliferation of channels caused by the coupling of j and l. The coupled states (CS) approximation uncouples j and l by appealing to the following physical argument. The coupling between (v,j,l) states of different l (but the same total angular momentum) basically originates in the centrifugal potential, $l(l + 1)/2\mu R^2$, *not* the interaction potential V. (Recall that the centrifugal potential pops up when the kinetic energy operator in the Schrödinger equation is transformed from Cartesian to center-of-mass coordinates). Therefore, while the l-channel coupling through the centrifugal potential "looks" like a potential coupling, it is really a kinematic coupling that does not depend on the details of the physical interaction potential. The basic idea behind the CS approximation, then, is that the kinematic coupling can be neglected whenever the centrifugal potential is small compared to the interaction potential in the region of strong interaction (i.e., in the vicinity of the classical turning point for the collision). This approximation is expected to break down for weak, long-range attractive interactions, but should be excellent for the kinds of short-range repulsive interactions believed to be responsible for most T ↔ V inelastic scattering.

The computational savings afforded by the CS approximation can be illustrated (at least heuristically) by using our sample problem 7 and Figure 18. For each partial wave, the total number of channels is the same in the CS approximation as in the close-coupling problem. But now, instead of a single set of 144 coupled equations, we have 11 smaller sets of coupled equations (one set for each value of l), with $n_v(j_{max}+1) = 4 \times 6 = 24$ in the single largest set, $4 \times 5 = 20$ in the two next largest sets, etc. An additional simplification occurs because it is only necessary to solve those sets of equations that "sample" both the initial and final j-levels for the transition of interest. Our sample problem involves a transition from the initial level $j_i = 0$. Since only the largest set of 24 equations samples $j = 0$, this is the only set that needs to be solved in the CS approximation. Remembering that the cost of solving N coupled equations scales as N^3, it is easy to see that a coupled states treatment of process 7 would be around 200× cheaper than a full close-coupling treatment.

In the infinite-order sudden (IOS) approximation, a second assumption is made in addition to the one implied in the CS approximation. The second assumption is that, at high collision energies, the energy differences between the various rotational levels (within each vibrational level) can be ignored. Remarkably, these assumptions reduce the close-coupling problem to a continuous set of "fixed orientation" problems, each involving the collision of molecules *whose orientations remain fixed throughout the collision.*[216] Each fixed orientation problem bears a superficial resemblance to the breathing sphere problem, in that the number of coupled equations to be solved for each partial wave is equal to the number of vibrational channels (i.e., no rotational coupling). But the resemblance stops there. Unlike the breathing sphere model, *the IOS approximation retains the full, anisotropic interaction potential in the calculation.* And while the breathing sphere model neglects rotational-channel coupling entirely, the IOS approximation only appears to neglect this coupling. In fact, the rotational information is hidden in the parametric dependence of the solutions to the fixed orientation problem on the orientation angles. By suitably averaging the results of many oriented collisions, it is possible to obtain amplitudes and cross sections for specific rovibrational transitions. The IOS approximation, like the CS approximation, is expected to work best for systems where short-range, repulsive interactions dominate. Both the IOS and CS approximations should improve with increasing collision energy.

As applied to our sample problem, the IOS approx-

imation would involve solving four coupled vibrational equations at each of a dozen or so fixed orientation angles. (Pathological cases may arise where the solutions to the fixed orientation problem depend sensitively on small changes in the orientation angles. In such problems, it might be necessary to solve a much larger number of fixed orientation problems, and the IOS approximation would not be so useful. See, for example, the discussion of Li^+-N_2 scattering in ref 15b and 64c.) Even with 20 orientation angles, the work required would be 10× less than for a CS calculation, and 2000× less than for a close-coupling calculation. For problems involving larger numbers of rotational and vibrational channels, the disparity in computation times between the three approaches would become even greater. For many vibrational problems, only the IOS approximation is currently feasible. (We should emphasize again that an IOS calculation is a big improvement over a breathing sphere calculation on physical grounds and often involves only a factor of 10 or so more work.) The combination of an infinite-order sudden approximation for rotation and a close-coupling treatment for vibration, as discussed above, has become quite popular, and is often referred to in the literature as VCC/IOS.

Not surprisingly, most applications of quantal scattering theory (at the VCC/IOS level or better) have involved atom–diatom systems. Among the questions that arise in extending the theory to polyatomics are (1) Can the relevant part of the multidimensional interaction potential be identified and represented in an accurate and economical way? (2) How do vibrational anharmonicity, anharmonic interactions (e.g., Fermi resonance), and rotation–vibration interactions (e.g. Coriolis coupling) affect the outcome of a scattering event? Is it satisfactory to consider just the harmonic part of the vibrational force field? (3) Is it necessary to consider all vibrational modes simultaneously to obtain accurate results for a transition involving just one or two vibrational modes? Or is it a good approximation to include only those vibrational modes that are excited before and after the collision?

While most of these questions remain to be explored, some very important "first steps" have already been taken. In particular we would like to mention Clary's recent work on the scattering of He atoms from ethene[185] and cyclopropane[186] molecules. In these calculations, several simplifying assumptions were made (in addition to the IOS approximation). First, the interaction potential was approximated by a sum of pair-wise exponential repulsions between the He atom and each atom in the polyatomic molecule. By symmetry, there are only two exponential pair functions (He–H and He–C) for both ethene and cyclopropane. The parameters of the pair functions were obtained by fitting to a few dozen ab initio (SCF) points. Attractive forces were neglected. (Helium was chosen as the scattering partner to minimize the consequences of this assumption.) Second, the intramolecular part of the PES was represented by the harmonic vibrational force field, as obtained from experiment. That is, vibrational anharmonicity and anharmonic interactions were neglected. Third, rotation–vibration interactions were neglected. Fourth, vibrational energy transfer was assumed to occur independently in each vibrational mode.

Using these assumptions, Clary set up the VCC/IOS problem independently for each of several vibrational modes, ν_k, of the polyatomic molecule. He then solved the equations at several values of the collision energy, E_T^i, to obtain $v = 0 \rightarrow 1$ and $v = 1 \rightarrow 0$ integral state-to-state cross sections (as a function of E_T^i) and rate constants (as a function of T). The results showed that, for both molecules, the lowest frequency vibrational mode was most easily excited (or deexcited) in thermal energy collisions. But some interesting differences were also predicted between vibrational modes of similar frequency but differing vibrational character. For example, in cyclopropane,[186] the ν_7 CH_2 rocking mode (854 cm^{-1}) was predicted to be 3–4 times more active than the nearly degenerate ν_{11} ring deformation mode (869 cm^{-1}). Unfortunately, no experimental state-to-state cross sections or rate constants were available to test Clary's predictions.[219]

It is clear that more detailed experimental work and theoretical comparisons will be needed to test the assumptions that went into these two early calculations. But it is rather remarkable and exciting that quantal scattering theory and the associated computational tools have advanced to the point where such complicated polyatomic scattering processes can be attacked from first principles with a fair degree of realism.

B. Classical Trajectory Methods

Even if quantal scattering calculations could be performed cheaply and exactly on any system of interest, most chemists would *still* not be satisfied. It is hard for most of us to rise above the mathematical complexities of the quantal scattering theory and actually "see" what is going on. Fortunately, many aspects of molecular collision processes at high energies can be understood using classical mechanics. If all nuclear degrees of freedom, including the rotational and vibrational motions, are assumed to obey the laws of classical mechanics, then it is a straightforward task (at least for three-atom systems) to numerically integrate the classical equations of motion on a computer to obtain the "trajectories" of the nuclei on the PES. By properly sampling the distribution of initial conditions (e.g., using Monte Carlo techniques), the classical outcome of a complicated 3-D scattering experiment on a given PES can be obtained with modest effort. The big attraction of this approach is that, since it is easy to visualize what the trajectories are doing, the effects of changes in the PES can be explored in a straightforward and "physical" way.[220] The question is, when is this approach valid?

A classical description of a molecular scattering process is expected to be appropriate whenever the wavelike character of the nuclear motion can be neglected. The three most striking consequences of this wavelike character in quantum mechanics are: interference (superposition of wave amplitudes), tunneling through "classically forbidden" regions (i.e., regions where the potential energy exceeds the total energy), and quantization of energy levels. Interference and tunneling can never be handled in a purely classical framework. Quantization can be accounted for in an approximate way by (i) starting out the trajectories with rotational and vibrational energies characteristic of the initial quantized energy level(s); (ii) assigning the trajectories, after scattering, to quantized "bins" depending on the

final classical values of the rotational and vibrational energies. This binning procedure is usually referred to as the "quasiclassical histogram method." (Actually, to get state-to-state results that satisfy microscopic reversibility, the initial rotational and vibrational energies should also be chosen randomly from quantized bins.)

The usefulness of the quasiclassical histogram method depends on how much energy is transferred in a typical collision. If the classical energy transfer is large enough to populate at least a few quantized energy levels, then most of the "state-to-state" transfers are classically allowed and the quasiclassical procedure should work well. This condition is almost always satisfied for rotational energy transfer,[221] since the rotational energy levels lie so close together, but is frequently violated for vibrational energy transfer in nonreactive collisions. For example, in our sample problem (7), it may turn out that there are *no* classical trajectories whatsoever that involve the transfer of a full quantum of vibrational energy, or even half a quantum, between A and BC, even when such transfers are energetically allowed. The quasiclassical procedure, then, would predict no $v = 0 \rightarrow 1$ excitation, whereas quantum mechanically such excitation does occur because of tunneling. In general, tunneling effects will be important and the quasiclassical histogram method will break down whenever the vibrational transition probabilities are very small. In such cases, resort must be made to a full quantal treatment or to one of the semiclassical approaches described in part C below. However, we might mention in advance the following remarkable fact: even when tunneling is important, the *average* vibrational energy transfer calculated classically usually agrees rather well (in some cases exactly) with the average quantal vibrational energy transfer. The problem with classical mechanics is not that it gets the average energy transfer wrong, but that it doesn't know how to assign transition probabilities when the energy transfer is small. The semiclassical theories address this deficiency.

Summarizing, purely classical calculations can sometimes be useful if all one is interested in is the average amount of vibrational energy transferred in a collision. (Recent examples of this type of application include: two studies of collisional deactivation of highly vibrationally excited CH_4 molecules by Date et al.[222] and by Grinchak et al.[223]; and a study of the effects of attractive potential wells on vibrational energy transfer in A + BC ($v = 1$) collisions, by Osborn and Smith.[224]) If state-to-state cross sections are desired, one is restricted to situations where the classical energy transfer is at least comparable to the vibrational level spacings. This usually means working at hyperthermal collision energies, or with molecules initially in high vibrational levels, or both. A few examples are a quasiclassical study of Ar and Br collisions with vibrationally hot Br_2 molecules by Koshi et al.[225], a study of Ar + OH ($v = 9$) collisions by Thompson[226], and a study of high-energy Ar + H_2 collisions by Blais and Truhlar.[227] None of these studies allowed a direct comparison with experimental results, partly because the conditions that validate a quasiclassical treatment are hard to achieve in the laboratory. (In this respect, nonreactive collisions are very different from their reactive cousins.) An exception to this statement is provided by the recent experimental results on $T \rightarrow V$ transfer in hyperthermal collisions of H atoms with diatomic and polyatomic molecules. Some interesting quasiclassical trajectory calculations have been performed in connection with these experiments by Schatz and co-workers[228] and by Blais and Truhlar.[229]

We close this section with a few remarks concerning the status of classical trajectory methods. For A + BC systems, 3-D quasiclassical trajectory calculations are truly routine (even on a minicomputer), and several "black box" computer programs are available for this purpose.[230] A QCPE program is also available for polyatomic problems.[231] This program, due to Hase, assumes harmonic normal mode vibrations and ignores rotation–vibration interaction. If it is necessary to include anharmonic and rotation–vibration interactions, then the quasiclassical specifications of initial conditions and the "binning" of final trajectories become much more difficult problems. The difficulties are related to the general problem of finding the correct "semiclassical" description of quantized energy levels in coupled anharmonic oscillator systems. An interesting discussion of this problem, as it pertains to trajectory calculations, has been given recently by Schatz.[16b]

C. Semiclassical Approaches

Most semiclassical theories of vibrational energy transfer can be divided into three classes: "classical path" approximations, classical S-matrix theory, and classical–quantal correspondence methods. The purpose of this section is to give an overview of these three classes of semiclassical theories, without a lot of formulas and with only selected literature references. For a more detailed survey of semiclassical methods and an extensive reference list, see ref 15c.

1. "Classical Path" Approximations

The "classical path" concept was first introduced by Zener in his pioneering work on the vibrational energy transfer problem[232] and the electronic curve-crossing problem.[233] Many variations of the classical path approach have been tried since then, but the basic idea behind all of them is the same. The translational motion is always treated classically, using some effective interaction potential that does not depend on the vibrational coordinates. (The latter are normally just "frozen" at their equilibrium values.) Usually, in 3-D applications, the rotational motion is also treated classically. The solution of the classical problem is a set of time-dependent trajectories, or "classical paths." The second step is to evaluate the driving force on each vibrational coordinate along each classical path, and then solve the time-dependent Schrödinger equation to obtain vibrational transition probabilities.

Most early applications of the classical path approximation were restricted to 1-D model problems for which the classical path could be derived analytically; then, vibrational transition probabilities were calculated using perturbation approximations to the time-dependent Schrödinger equation. These additional approximations were made for computational convenience and they add little or no physical insight to the problem. Nowadays, these additional approximations can and should be avoided.[17] The classical part of the problem

can be treated exactly in three dimensions using classical trajectory methods, and the quantum mechanical part of the problem can also be treated exactly by numerically solving the coupled set of first-order differential equations that fall out of the time-dependent Schrödinger equation. Therefore, the only approximation left is the basic classical path assumption itself, namely, that the translational and vibrational motions can be treated on different dynamical footings.

The crudest classical path approximation in three dimensions is to assume that the relative translational motion continues on in a straight line for each classical impact parameter. This so-called "impact parameter" approximation is only applicable to very long-range interactions, or at very high collision energies. Surprisingly, differential cross sections can still be calculated using the impact parameter approximation[37] if the anisotropic interaction potential is used. (The trick is similar to the one used in the IOS approximation. Namely, the angular information is recovered after solving the "straight-line" problem for various fixed values of the molecular orientation angles.) A much better approximation is to actually calculate the classical paths in three dimensions using the anisotropic potential, assuming that the same classical paths apply to all vibrationally elastic and inelastic channels. This procedure is satisfactory as long as the collision energy is large compared to the amount of energy transferred, but it does not satisfy the principle of detailed balance. The "best" classical path approximation is to evaluate the classical paths at a different collision energy for each vibrationally inelastic channel, with the collision energies chosen in such a way as to ensure detailed balance. When this is done, good results can be obtained even at low collision energies.

A detailed discussion of the methodology involved in classical path calculations on A + BC, AB + CD, and A + BCD collision systems has been given recently by Billing.[17] General computer programs for dealing with vibrationally inelastic A + BC and AB + CD collisions are obtainable from the CPC Program Library, Queen's University of Belfast, N. Ireland.[234]

2. Classical S-Matrix Theory

While the classical path approach is physically reasonable and has led to many useful results, there is still something a bit arbitrary and awkward about using classical mechanics to treat half of the problem and then switching to quantum mechanics to treat the other half. The classical S-matrix theory and the correspondence methods both avoid this dynamical inconsistency by treating all of the dynamics classically. Both give detailed prescriptions for calculating quantum mechanical transition probabilities from classical trajectory results. The classical S-matrix theory is unquestionably the most elegant of the semiclassical approaches. It provides simple and illuminating physical interpretations of the quantum mechanical effects that arise in inelastic scattering, and for this reason alone it is worthwhile spending some time getting acquainted with the theory. Practical applications of the classical S-matrix theory to 3-D scattering problems are, however, difficult, for reasons to be discussed below. In this regard, the more approximate classical path and correspondence methods have been more generally useful.

The classical S-matrix theory was developed independently by Miller[235] and by Marcus[236] and their coworkers in the early 1970's. The goal was to extend the very successful Ford and Wheeler[237] semiclassical theory of atom–atom elastic scattering to inelastic processes. In these theories, formulas are derived for transition amplitudes (or S-matrix elements) in the classical limit of quantum mechanics (i.e., in the limit of short wavelengths). But while the description of the process in terms of transition amplitudes is quantum mechanical, all of the information required to evaluate the transition amplitudes is obtained classically. Marcus' derivation of the theory is probably easier for most people to follow in detail, since he starts with the familiar Schrödinger equation and its semiclassical relationship to the continuity equation and the Hamilton–Jacobi equation of classical mechanics. A good introduction to this approach may be found in ref 24. An alternative approach based on Feynmann's path integral formulation of quantum mechanics[238] was used by Miller. Although the path integral formalism is less familiar to most chemists, it illustrates most clearly the qualitative relationship between quantum mechanics, classical S-matrix theory, and classical mechanics. Of course, the final results come out the same using either the Schrödinger equation or the path integral approach. (In fact, the basic formulas can be derived from general transformation relations). The general theory of classical-limit quantum mechanics was reviewed by Miller[239a] in 1974. Specific applications of the theory to molecular collision problems were discussed in a follow-up review article[239b] in 1975. These reviews are probably still the best place to go for a detailed discussion of the subject. Here, we only want to indicate qualitatively how the classical S-matrix theory "fits in" between quantum and classical mechanics, and basically how it works.

In the path integral formulation of quantum mechanics, one thinks of a system making a transition from state A to state B as "exploring" all possible paths in space and time connecting the initial and final states. Each path from A to B has a probability amplitude associated with it that depends on the classical action. The quantum mechanical transition probability is obtained by superposing the amplitudes for all paths and squaring. In the classical limit, only one or a few "important" paths survive the superposition step; the rest cancel each other out through destructive interference. If the transition from A to B is classically allowed, then the "important" paths are just the classical paths (which satisfy the principle of least action[240]). Therefore, in classical-limit quantum mechanics, the dynamics of classically allowed processes can be treated entirely using classical mechanics; quantum effects enter only through the principle of superposition.

What if the transition from A to B is classically forbidden? In the path integral description, when the system encounters a classically impassable (but energetically passable) potential barrier, the system tends to surmount (or penetrate) the barrier by following real but nonclassical paths in space and time. An exciting breakthrough in the classical S-matrix theory was the realization[235e,236e] that these nonclassical paths could be handled, *without abandoning classical mechanics*, by allowing time to become a complex variable. At first this might sound like a strange idea or a desperate

attempt to "fix" the theory, but in fact the procedure is very well defined, thanks to the special properties of analytic functions of a complex variable. The net result, then, is that all processes can be described in the classical limit of quantum mechanics using only classical dynamics and the quantum principle of superposition.

The application of classical S-matrix theory to an inelastic scattering process involves three steps: (i) finding all of the "important" paths (real or complex) that connect the initial and final states; (ii) evaluating the probability amplitude associated with each important path; (iii) superposing the probability amplitudes to obtain S-matrix elements and squaring to obtain transition probabilities. The simplest application is to vibrational excitation in a collinear A + BC collision. Suppose that the BC oscillator starts out in its zero-point vibrational level, and that the collision energy is high so that the $v = 0 \rightarrow 1$ transition is classically allowed. Then step (i) involves finding real classical trajectories that satisfy the $v = 0 \rightarrow 1$ "double-ended" boundary conditions. At a given total energy, the only variable in the starting conditions is the phase of the oscillator. Classically, the final vibrational energy will be a smooth and periodic function of the initial phase of the oscillator. In the principal phase interval 0 to 2π, there will be, in general, an even number of trajectories that give a final vibrational energy equal to the desired quantized value. In the classical S-matrix theory, the $v = 0 \rightarrow 1$ transition probability depends only on these "special" trajectories. The rest are irrelevant.

While this result is fascinating from a physical point of view, it also reveals one reason why classical S-matrix calculations are much more difficult to carry out than quasiclassical calculations. In the latter, initial conditions such as the vibrational phase can be randomly sampled, and only enough trajectories run to reduce the statistical sampling error to some acceptable level. But in classical S-matrix theory, the vibrational phase must be varied in a systematic way so that all of the "roots" of the double-ended boundary value problem can be found. This root-search problem becomes much more troublesome in three dimensions. One way to simplify 3-D problems is to implement classical versions[241] of the angular momentum decoupling approximations discussed earlier. An even greater simplification occurs if it is possible to use a "partially averaged" version of the theory,[48,242] in which the vibrational degrees of freedom are treated using double-ended boundary conditions while the rotational degrees of freedom are treated quasiclassically.

Besides the root-search problem, there are two other problems that have hampered practical applications of classical S-matrix theory to systems with more than one internal degree of freedom. One has to do with the numerical integration of complex-valued classical trajectories. Since the oscillatory time-dependence of the vibrational coordinates acquires some exponential character when time is allowed to become a complex variable, special stabilization methods are needed to prevent the trajectories from "wandering" unphysically far into the complex coordinate plane during the numerical integration of the equations of motion. The other problem is developing so-called "uniform approximations" to handle situations where two or more roots of the boundary value problem lie close together. In such cases the "primitive" semiclassical expressions for the S-matrix elements break down.

Because of these problems, there have been only a few 3-D applications of classical S-matrix theory so far,[48,242,243] and most of these have involved either the "partially averaged" theory or the calculation of a few selected S-matrix elements using the full theory (to allow comparison with exact quantal values). These tests have shown that whenever the theory can be executed, it gives results that are in superb agreement with exact quantum mechanics, even for classically forbidden transitions. As far as we know, there have been no applications of classical S-matrix theory to 3-D vibrationally inelastic scattering problems in the past 5 years, and no applications whatsoever to polyatomic problems. Significant progress toward solving two of the basic technical problems (the multidimensional root search and the stable integration of complex trajectories) was reported by McCurdy and Miller[243] in 1980. The latter authors concluded that the lack of suitable uniform approximations was the main bottleneck in trying to extend the theory to more complicated collision systems, but that this problem was "one clearly meriting further research effort."

3. Classical–Quantal Correspondence Methods

Finally, we turn to the classical–quantal correspondence methods. These methods exploit the special relationship that exists between the forced harmonic oscillator problem in quantum and classical mechanics. The most important correspondence may be stated as follows: If the perturbing force on a harmonic oscillator is *independent of the oscillator displacement*, but is otherwise an *arbitrary function of time*, then: (i) the average vibrational energy transfer is exactly the same classically as it is quantum mechanically; (ii) it is possible to derive explicit formulas for the quantum mechanical vibrational transition probabilities in terms of the exact classical energy transfer.

Bartlett and Moyal[244] were the first to derive an explicit formula for the vibrational transition probabilities. (Their result is quoted in Takayanagi's 1963 review.[245]) Many other derivations have been given since then. The derivations of Kerner[246] and of Pechukas and Light[247] are probably the easiest to follow. The exact result for the $n \rightarrow n'$ vibrational transition probability is

$$P(n \rightarrow n') = n!\, n'!\, e^{-\epsilon}\, \epsilon^{|n-n'|} \left| \sum_{k=0}^{n_<} \frac{(-\epsilon)^k}{(n_< - k)!(n_> - n_< + k)!\, k!} \right|^2 \quad (8a)$$

where $n_<$ ($n_>$) is the lesser (greater) of n and n', and where ϵ is the reduced classical energy transfer *to an initially stationary oscillator* (in units of $\hbar\omega$). This formula is sometimes rewritten as

$$P(n \rightarrow n') = n!\, n'!\, e^{-\epsilon}\, \epsilon^{n+n'} \left| \sum_{j=0}^{n_<} \frac{(-1)^j\, \epsilon^{-j}}{(n-j)!(n'-j)!\, j!} \right|^2 \quad (8b)$$

where again the sum extends only to the lesser of n and n'. For the special case of vibrational excitation out of the zero point vibrational level, the formulas reduce to a simple Poisson distribution:

$$P(0 \rightarrow n') = \frac{\epsilon^{n'}\, e^{-\epsilon}}{n'!} \quad (9)$$

The "picture" behind the classical–quantal correspondence method is very simple and is clearly illustrated in Kerner's derivation.[246] The initial stationary state n of the quantum oscillator (it doesn't matter which one) always corresponds to a classical oscillator at rest. During the collision, the classical oscillator gets excited and starts moving back and forth. The initial stationary state wave function of the quantum oscillator, as a whole, starts moving back and forth in precisely the same way. It doesn't change its shape. In Kerner's words, it "dances a classical dance centered at the instantaneous classical position..., moving *in toto* classically." This oscillating quantum mechanical wave function represents a nonstationary superposition of the final vibrational states n'. Formula (8) for the vibrational transition probabilities is obtained by decomposing the oscillating wave function into its component parts.

It should perhaps be emphasized that the correspondence method is really just a "special case" of the general classical path approach discussed earlier. For any problem involving harmonic oscillators and a linear interaction potential, the most general two-step classical path treatment (à la Billing[17]) and the correspondence method should give identical results. The important point is that, for this special class of problems, it is not *necessary* to grind through the second step of the classical path treatment (the numerical solution of the time-dependent Schrödinger equation), since this part of the problem can be solved analytically. What's left is the much simpler problem of calculating the reduced classical energy transfer to use in eq 8.

Unfortunately, real collision problems do not involve harmonic oscillators or linear interaction potentials. But if the deviations from the idealized problem are not too severe, the simple classical–quantal correspondence method, as outlined above, can still give good results. (In other words, an approximate correspondence still holds in more general problems.) Two popular correspondence models were proposed in the early 1970's: the ITFITS model[248] of Heidrich, Wilson, and Rapp, and the DECENT/INDECENT models[27,249] of Gentry and Giese. The acronyms evidently were chosen to emphasize how well the correspondence method works! However, the philosophy of the two models is different. ITFITS represents the "impulsive limit" of a popular 1-D collision model, for which the reduced classical energy transfer can be calculated analytically. Although attempts have been made to extend ITFITS to three dimensions,[135f,250] and even to polyatomic collisions,[251] the model was mainly intended for back-of-the-envelope calculations.

The philosophy behind the DECENT model[27] is more general, in that ϵ is obtained from numerically integrated classical trajectories. Therefore, it is possible to apply the model in three dimensions without making any assumptions about the interaction potential. The model can also be applied to polyatomic molecules if the vibrational modes of the polyatomic are assumed to be separable. In 3-D problems, of course, it is necessary to run classical trajectories for various initial values of the impact parameter and molecular orientation angles. But since the initial vibrational energy must be zero to satisfy the classical–quantal correspondence relationship, there is no averaging to perform over the vibrational phase. (Again, setting the initial vibrational energy to zero is the correct correspondence procedure, even if the molecules in the *physical* problem are vibrationally excited before the collision. The quantity ϵ is *not* the same as the classical energy transfer that would be calculated quasiclassically.) Each classical trajectory, then, gives its own value of ϵ and its own set of vibrational transition probabilities. (In polyatomic problems, each trajectory would give a value of ϵ and a set of transition probabilities for each vibrational mode.) If desired, the trajectories may be separated according to final scattering angle to obtain vibrationally inelastic differential cross sections. Rotational energy transfer can be handled quasiclassically.

In the DECENT model, all classical trajectories are run, and all vibrational transition probabilities are calculated, using one value of the initial collision energy. As with all classical path methods, this procedure does not satisfy the principle of detailed balance. In the INDECENT model,[249] a different collision energy is used for each vibrationally inelastic channel, with the collision energies chosen in such a way as to ensure detailed balance. (The same fix is used in the ITFITS model.[248]) Once this is done, accurate transition probabilities are often obtained, even for classically forbidden transitions near threshold, and with much less effort than with any other semiclassical or quantal approach. There have been many applications of these correspondence methods to 1-D model problems.[15c,249,252] A few 3-D experimental applications[27,46,77] were discussed in section III.

An interesting extension of the DECENT model has been proposed by Meyer.[253] The DECENT model works best when the linear term in the interaction potential dominates the inelastic scattering. Meyer has shown how to include the effects of the quadratic term in the interaction potential. (Note that the quadratic term essentially modulates the oscillator force constant or frequency during the collision.) When both the linear and quadratic perturbations are included, it is possible to generalize the formula for the vibrational transition probabilities $P(n \rightarrow n')$. The new formula depends on three parameters, ϵ, $|B|$, and φ, where ϵ is as before, $|B|$ is a measure of the strength of the quadratic perturbation, and φ is the relative phase of the two perturbations. In principle, all three parameters can be obtained from certain types of classical trajectories. Meyer[253] treats the case of $v = 0 \rightarrow n'$ excitation in some detail. For small $|B|$, the main effect of the quadratic perturbation is to enhance the vibrational energy transfer; the shape of the vibrational state distribution hardly changes. However, large quadratic perturbations can cause significant deviations from the simple Poisson distribution predicted by eq 9. It would be very interesting to see how this theory handles a model problem treated by Gordon,[254] in which a failure of the INDECENT model at high collision energies was attributed to large changes in the molecular force constant during the collision.

D. Model Problems

In 1969, Rapp and Kassal[255] reviewed the theory of vibrational energy transfer in this journal. They wrote: "No existing calculation is based on a collision model that is sufficiently realistic so that accurate results can be expected." Their review is filled with theoretical

treatments of A + BC model problems, mostly in one dimension. In contrast, all of the theoretical approaches we have discussed in this section (quantal scattering theory, quasiclassical trajectory calculations, the classical path approximation, classical S-matrix theory, and the correspondence method) have been applied to realistic A + BC scattering problems in three dimensions. With the exception of the classical S-matrix theory, all of the approaches have also been applied (in a more approximate way) to polyatomic problems in three dimensions.

The increasing sophistication of theoretical calculations is obviously connected to the dramatic and continuing improvements in the performance-to-cost ratio of digital computers. The mainframe computers of the 1960's are now on every lab bench and tabletop. The mainframes of the 1980's allow calculations to be performed that could only be dreamed of 15 years ago. The greatest impact of this increased computational capability is that it has helped to extend the range of fully quantal scattering calculations. But the quasiclassical and semiclassical approaches have benefited as well, since they all depend on the numerical integration of large numbers of classical trajectories for practical applications. While integrating trajectories is straightforward enough, the amount of computer time required can still add up fast, especially in polyatomic problems. So any increases in speed are helpful here, too.

In the field of vibrational energy transfer (as in any field where the fundamental equations of motion are known but are hard to solve), the question arises as to how much reliance should be placed on numerical calculations as opposed to analytic developments of the theory. Most people would agree that expressing results in analytical form is not an end in itself. Sometimes an analytical solution or approximation can provide useful physical insight. But if a lot of assumptions or bad approximations must be made to force an analytical solution, then it is probably better just to solve the problem on a computer (if possible).

Historically, the first model used to study vibrational energy transfer involved collinear collisions between an atom A and a harmonic oscillator BC, with exponential repulsion between A and B (and no interaction between A and C). This problem was first studied quantum mechanically by Zener[256] and by Jackson and Mott.[257] A related problem was treated classically by Landau and Teller.[258] These old papers are still fun to read. Actually, Jackson and Mott were interested in the accomodation of atoms on solid surfaces, but their model of an atom impinging on a harmonically bound surface oscillator is mathematically equivalent to the A + BC problem. Jackson and Mott were able to solve the quantum mechanical problem analytically by making a first-order distorted wave approximation. This approximation is expected to be valid if the vibrational transition probabilities are small. (For a simple explanation of the relationship between the usual Born approximation, the distorted wave approximation, and the exponential distorted wave approximation, see chapter 7 of ref 24.) The Jackson–Mott result later formed the basis for the well-known SSH theory[180,259] of vibrational energy transfer in polyatomic molecules. In SSH theory, the polyatomic problem is "reduced" to a one-dimensional A + BC problem by assuming a spherically averaged interaction potential (the "breathing sphere" approximation), and by assuming that only "head-on" collisions are important; there is no new physics in the theory beyond the Jackson–Mott result. In spite of its severe approximations (or because nothing better was available), SSH theory soon became entrenched as the "standard" theory for making comparisons with experimental results. Even today, frequent references to the theory may be found in the experimental literature. It is probably fair to say that, in many applications, the theory has been taken too literally. There are many ambiguous parameters in the SSH formulas.[259,260] The theory is best regarded as a semiempirical model.

The 1960s brought an explosion of interest in the Jackson–Mott problem. Much of this work is discussed in the Rapp and Kassal review,[255] and much of it can now be safely ignored. However, the papers by Kelley and Wolfsberg,[261] Secrest and Johnson,[262] Secrest,[263] and Roberts and Diestler[264] are still highly recommended. These papers contain exact classical and quantal solutions to the Jackson–Mott problem for a variety of collision energies and A, B, C mass combinations. A surprising result emerged from these studies: for certain mass combinations, the first-order solution obtained by Jackson and Mott is always poor, even at low collision energies where the transition probabilities are small. The reason is that the BC oscillator may undergo large displacements *during* the collision even when the net vibrational energy transfer is small.[265] Similar effects probably occur in polyatomic collisions. This is an interesting but also a troublesome result, since it implies that all perturbative solutions to the problem will break down (including SSH). It also suggests that the neglect of anharmonicity might be a bad approximation even for vibrational transitions between low-lying levels that are nearly harmonic.

Many variations of the Jackson–Mott problem have been studied, using quantal, classical, and semiclassical techniques. The next simplest model problem, collinear AB + CD, has also been extensively studied.[266] For examples and references, see the reviews by Secrest[267] and Gentry.[15c] It is amusing to note that not all 1-D studies have succumbed to the historical prejudice for a collinear collision geometry. Faubel and Toennies[268] and Schinke and Toennies[269] have studied 1-D perpendicular A + BB collisions. When BB is a harmonic oscillator, more energy is usually transferred in the collinear geometry than in the perpendicular geometry, but when BB is a Morse oscillator, the reverse can be true!

Of course, work on model problems continues unabated in the 1980's. As simple models become well understood and are extended to three dimensions, more complicated 1-D models come to take their place. This has something in common with the relationship between the beam and bulb worlds experimentally; complicated problems are usually tackled first using the easier theoretical models and experimental techniques. Of the many theoretical questions that have been explored since 1980 using 1-D models, we mention three that we find particularly interesting.

The Effect of the Molecular Continuum on the Convergence of Quantal Scattering Calculations. The convergence of a quantal scattering calculation involving a harmonic oscillator is readily assessed. When the problem involves an anharmonic oscillator

with a dissociative continuum, the question arises: is it necessary to include continuum functions in the basis set to obtain converged solutions? Or is the discrete molecular basis set sufficient (as long as the collision energy is well below the dissociation energy of the oscillator)? This intriguing question was first addressed explicitly by Scherzinger and Secrest[270] in 1980 using a collinear A + BC model and a BC Morse oscillator. They found that, in general, the discrete Morse oscillator basis functions did not provide an adequate basis for the close-coupling calculations. In some cases, the results using the discrete basis set appeared to converge as more basis functions were added, when in fact the correct result was significantly different.

Scaling Laws. There is substantial practical and theoretical interest in trying to find simple rules to describe how various quantities (e.g., the first moment of the vibrational energy transfer) scale with vibrational quantum number in a given collision system. The hope is that, by making just a few measurements (or calculations) low in the vibrational well, it might be possible to extrapolate reliably up to experimentally inaccessible states close to the dissociation limit. Two recent classical trajectory studies[271,272] of prototype collinear rare gas–$I_2(v)$ collisions provide evidence for such simple scaling laws. More fundamental rationales for scaling behavior also exist, and references to this theoretical work may be found in ref 272.

Collision Dynamics of Nonintegrable Systems. A fundamental difficulty in applying any of the scattering theories to realistic polyatomic vibrational energy transfer problems is how to deal with anharmonic interactions between vibrational modes. It may turn out that the only way to handle this problem accurately is to do the whole thing quantum mechanically. The simplest model problem of this type would involve the collinear collision of an atom with an anharmonically coupled triatomic molecule. An exact close-coupling solution for such a model problem would become an extremely useful benchmark for testing various quasiclassical and semiclassical approximations. As far as we know, no such calculation has been done yet, but such a calculation appears feasible and is probably just around the corner. The problem in all of the quasiclassical and semiclassical approaches is how to assign vibrational quantum numbers before and after the collision when there is anharmonic coupling between vibrational modes.

This problem was mentioned briefly in part B. We refer the reader again to Schatz's review.[16b] At low energies, the usual semiclassical procedures for assigning vibrational quantum numbers can be extended to deal with anharmonically coupled oscillators. At high energies, when the classical vibrational motion becomes very irregular, these semiclassical procedures break down. Purely classical studies of 1-D atom–triatomic collisions with anharmonic coupling have been reported by Noid and Koszykowski,[273] Nalewajski and Wyatt,[274] and Ramaswamy.[275] These studies examined what happens to the classical energy transfer when the triatomic motion becomes "chaotic," in the mathematical sense. The relationship of these classical models to the equivalent quantum mechanical problem is not yet understood.

Acknowledgments. We are grateful to the National Science Foundation and to the Donors of the Petroleum Research Fund administered by the American Chemical Society for the financial support that made the writing of this review possible. We thank the American Institute of Physics, the Institute of Physics, and North-Holland Publishing Company for permission to reproduce Figures 1–8. C.S.P. greatly appreciates a Senior U.S. Scientist Award from the Alexander von Humboldt-Stiftung and interactions with Prof. E. W. Schlag during the writing of part of this review. D.J.K. acknowledges helpful conversation or correspondence with Dr. M. Faubel, Prof. W. R. Gentry, Prof. W. A. Lester, Jr., and Prof. D. Secrest on a number of topics related to this review. Last, but not least, we thank Cherie Becker for her enormous help in the preparation of the manuscript, and Roger Purcell for drafting a number of original figures.

References

(1) Faubel, M. "Low Energy Atom Collisions". In *Fundamental Processes in Atomic Collision Physics*, Kleinpoppen, H., Briggs, J. S., Lutz, H. O., Eds.; Plenum: New York, 1985. A brief survey of the current state-of-the-art of molecular beam inelastic scattering experiments, with examples chosen to illustrate rotational and vibrational excitation in gas-phase collisions, as well as phonon excitation in gas–surface collisions.

(2) Faubel, M. "Vibrational and Rotational Excitation in Molecular Collisions". *Adv. At. Mol. Phys.* **1983**, *19*, 345. The most recent detailed review of crossed beam work. Emphasis is on rotationally inelastic scattering.

(3) Toennies, J. P. "Rotational and Vibrational Transitions in Molecular Collisions". *Aust. J. Phys.* **1982**, *35*, 593. A good introduction to the crossed beam world that can be read in less than an hour.

(4) Faubel, M.; Toennies, J. P. "Scattering Studies of Rotational and Vibrational Excitation of Molecules". *Adv. At. Mol. Phys.* **1977**, *13*, 229. A detailed discussion of experimental and theoretical methods and early experimental results.

(5) Toennies, J. P. "The Calculation and Measurement of Cross Sections for Rotational and Vibrational Excitation". *Annu. Rev. Phys. Chem.* **1976**, *27*, 225. Includes some discussion of bulb work and extensive references to the earlier review literature.

(6) Rice, S. A. "Collision-Induced Intramolecular Energy Transfer in Electronically Excited Molecules". *Adv. Chem. Phys.* **1981**, *47 (Part 2)*, 237. A collection of early experimental results on S_1 vibrational energy transfer, including some results on very-low-energy collisional relaxation.

(7) Parmenter, C. S. "Vibrational Energy Flow Within Excited Electronic States of Large Molecules". *J. Phys. Chem.* **1982**, *86*, 1735. An introduction to the study of both collision-induced and collision-free vibrational energy flow in the S_1 states of large polyatomic molecules.

(8) Smith, I. W. M. "Lasers and Vibrational Relaxation in Small Molecules". In *Lasers as Reactants and Probes in Chemistry*, Jackson, W. M., Harvey, A. B., Eds.; Howard University: Washington, DC, 1985; p 373. A review of recent progress in S_0 bulb studies made possible by pulsed, tunable IR sources.

(9) Smith, I. W. M. "The Collision Dynamics of Vibrationally Excited Molecules". *Chem. Soc. Rev.* **1985**, *14*, 141. An interesting discussion of both reactive and nonreactive collisions of vibrationally excited molecules and free radicals in the ground electronic state.

(10) Weitz, E.; Flynn, G. "Vibrational Energy Flow in the Ground Electronic States of Polyatomic Molecules". *Adv. Chem. Phys.* **1981**, *47 (Part 2)*, 185. An in-depth review of S_0 bulb studies on methane and substituted methane molecules, including a detailed discussion of the techniques used to unravel sequential energy transfer pathways in IR fluorescence experiments. References to most earlier bulb reviews are given in this paper.

(11) Flynn, G. W. "Collision-Induced Energy Flow Between Vibrational Modes of Small Polyatomic Molecules". *Acc. Chem. Res.* **1981**, *14*, 334. A brief introduction to the S_0 bulb world.

(12) For reviews of recent work on the relaxation of highly vibrationally excited molecules in the ground electronic state, see: (a) Barker, J. R. *J. Phys. Chem.* **1984**, *88*, 11. (b) Hippler, H. *Ber. Bunsenges. Phys. Chem.* **1985**, *89*, 303.

(13) Yardley, J. T. *Introduction to Molecular Energy Transfer*; Academic: New York, 1980.

(14) Lambert, J. D. *Vibrational and Rotational Relaxation in Gases*; Oxford University: London, 1977.
(15) *Atom-Molecule Collision Theory—A Guide for the Experimentalist*; Bernstein, R. B., Ed.; Plenum: New York, 1979. (a) Secrest, D. "Rotational Excitation I: The Quantal Treatment". p 265. (b) Secrest, D. "Vibrational Excitation I: The Quantal Treatment". p 377. (c) Gentry, W. R. "Vibrational Excitation II: Classical and Semiclassical Methods". p 391.
(16) *Molecular Collision Dynamics* (Vol. 33 of *Topics in Current Physics*); Bowman, J. M., Ed.; Springer-Verlag: New York, 1983. (a) Secrest, D. "Inelastic Vibrational and Rotational Quantum Collisions". p 7. (b) Schatz, G. C. "Quasiclassical Trajectory Studies of State to State Collisional Energy Transfer in Polyatomic Molecules". p 25.
(17) Billing, G. D. "The Semiclassical Treatment of Molecular Roto-Vibrational Energy Transfer". *Comput. Phys. Rep.* **1984**, *1*, 237.
(18) Information on the collision energy dependence of integral state-to-state cross sections may be obtained in a bulb by using sub-Doppler laser techniques. Such techniques have been used already to study rotationally inelastic transitions in excited electronic states of diatomic molecules. (See, for example: (a) Smith, N.; Scott, T. P.; Pritchard, D. E. *J. Chem. Phys.* **1984**, *81*, 1229. (b) Smith, N.; Brunner, T. A.; Pritchard, D. E. *Ibid.* **1981**, *74*, 467. (c) Gottscho, R. A.; Field, R. W.; Bacis, R.; Silvers, S. J. *Ibid.* **1980**, *73*, 599). In principle, it might even be possible to reconstruct full differential cross sections in a bulb using sub-Doppler techniques. But in any practical case it would probably be easier to perform the same measurements using a combination of crossed molecular beam and laser techniques.
(19) Bernstein, R. B. *Chemical Dynamics via Molecular Beam and Laser Techniques*; Oxford University: New York, 1982.
(20) Lee, Y. T.; McDonald, J. D.; LeBreton, P. R.; Herschbach, D. R. *Rev. Sci. Instrum.* **1969**, *40*, 1402.
(21) (a) See, for example: Petty, F.; Moran, T. F. *Phys. Rev. A* **1972**, *5*, 266. Cosby, P. C.; Moran, T. F. *J. Chem. Phys.* **1970**, *52*, 6157. (b) Baer, T. "State Selection by Photoion–Photoelectron Coincidence". In *Gas Phase Ion Chemistry*; Bowers, M. T., Ed.; Academic: New York, 1979; Vol. 1, p 153.
(22) Fluendy, M. A. D.; Lawley, K. P. *Chemical Applications of Molecular Beam Scattering*; Chapman and Hall: London, 1973.
(23) Levine, R. D.; Bernstein, R. B. *Molecular Reaction Dynamics*; Oxford University: New York, 1974.
(24) Child, M. S. *Molecular Collision Theory*; Academic: New York, 1974.
(25) (a) Moore, J. H., Jr.; Doering, J. P. *Phys. Rev. Lett.* **1969**, *23*, 564. (b) Herrero, F. A.; Doering, J. P. *Phys. Rev. A* **1972**, *5*, 702.
(26) Udseth, H.; Giese, C. F.; Gentry, W. R. *Phys. Rev. A* **1973**, *8*, 2483.
(27) Giese, C. F.; Gentry, W. R. *Phys. Rev. A* **1974**, *10*, 2156.
(28) Schmidt, H.; Hermann, V.; Linder, F. *Chem. Phys. Lett.* **1976**, *41*, 365.
(29) McGuire, P.; Schmidt, H.; Hermann, V.; Linder, F. *J. Chem. Phys.* **1977**, *66*, 4243.
(30) Schmidt, H.; Hermann, V.; Linder, F. *J. Chem. Phys.* **1978**, *69*, 2734.
(31) Hermann, V.; Schmidt, H.; Linder, F. *J. Phys. B* **1978**, *11*, 493.
(32) Schinke, R.; Kruger, H.; Hermann, V.; Schmidt, H.; Linder, F. *J. Chem. Phys.* **1977**, *67*, 1187.
(33) A detailed study of pure rotational excitation (at E_{cm} = 3.7 eV) has also been performed by the Goettingen group using time-of-flight methods. See: (a) Rudolph, K.; Toennies, J. P. *J. Chem. Phys.* **1976**, *65*, 4483. (b) McGuire, P.; Rudolph, K.; Toennies, J. P. *Ibid.* **1977**, *65*, 5522.
(34) Schinke, R.; McGuire, P. *Chem. Phys.* **1978**, *31*, 391.
(35) Schinke, R.; Dupuis, M.; Lester, W. A., Jr. *J. Chem. Phys.* **1980**, *72*, 3909.
(36) Schinke, R. *J. Chem. Phys.* **1980**, *72*, 3916.
(37) Schinke, R. *Chem. Phys.* **1977**, *24*, 379.
(38) Krutein, J.; Bischof, G.; Linder, F.; Schinke, R. *J. Phys. B.* **1979**, *12*, L57.
(39) David, R.; Faubel, M.; Toennies, J. P. *Chem. Phys. Lett.* **1973**, *18*, 87.
(40) For a review dealing almost exclusively with the early work on Li^+–H_2 scattering, see: Toennies, J. P. *Chem. Soc. Rev.* **1974**, *3*, 407.
(41) van den Bergh, H. E.; Faubel, M.; Toennies, J. P. *Faraday Discuss. Chem. Soc.* **1973**, *73*, 203.
(42) Faubel, M.; Toennies, J. P. *J. Chem. Phys.* **1979**, *71*, 3770.
(43) Faubel, M. Ph.D. Thesis, Bericht 29/1976, Max-Planck-Institut für Strömungsforschung, Göttingen, West Germany, 1976.
(44) Lester, W. A., Jr. *J. Chem. Phys.* **1971**, *54*, 3171.
(45) Kutzelnigg, W.; Staemmler, V.; Hoheisel, K. *Chem. Phys.* **1973**, *1*, 27.
(46) Gentry, W. R.; Giese, C. F. *J. Chem. Phys.* **1975**, *62*, 1364.
(47) (a) Schaefer, J.; Lester, W. A., Jr. *J. Chem. Phys.* **1975**, *62*, 1913. (b) Schaefer, J.; Lester, W. A., Jr.; Kouri, D.; Wells, C. A. *Chem. Phys. Lett.* **1974**, *24*, 185. (c) Schaefer, J.; Lester, W. A., Jr. *Ibid.* **1973**, *20*, 575.
(48) Raczkowski, A. W.; Miller, W. H. *J. Chem. Phys.* **1975**, *61*, 5413.
(49) The close-coupling calculations of Schaefer and Lester at 3.6 eV are referred to by Barg et al. in ref 52.
(50) Schinke, R. *Chem. Phys.* **1978**, *34*, 65.
(51) "Breathing sphere" model calculations have also been performed on the Li^+–H_2 system (Drolshagen, G.; Toennies, J. P.; Baer, M. *Chem. Phys. Lett.* **1983**, *102*, 354. Drolshagen, G.; Toennies, J. P. *Chem. Phys.* **1983**, *79*, 159). These calcualtions evidently refer to a hypothetical Li^+–H_2 system, since the results in ref 46 and 50 demonstrate clearly that vibrational excitation in the physical Li^+–H_2 system depends sensitively on the rotational motion of H_2 during the collision.
(52) Barg, G. D.; Kendall, G. M.; Toennies, J. P. *Chem. Phys.* **1976**, *16*, 243.
(53) There has been some confusion over the absolute magnitude of the differential cross section for Li^+–H_2 backward scattering. David et al. obtained the approximate experimental value 0.13 Å^2/sr (±50%) for the $v = 0 \rightarrow 1$ differential cross section in the *laboratory* coordinate system at E_{cm} = 3.6 eV (ref 39 and M. Faubel, private communication). At the same energy, Gentry and Giese (ref 46) and Barg et al. (ref 52) calculated the values 0.021 Å^2/sr and 0.007 Å^2/sr, respectively, for the $v = 0 \rightarrow 1$ differential cross section in the *center-of-mass* coordinate system. The difference between the two calculated values (both obtained classically using the same potential surface) is not understood. However, there is really no discrepancy between the experimental and calculated cross sections, since the laboratory differential cross section for Li^+–H_2 backward scattering should be roughly 6 times larger than the c.m. differential cross section. (The factor of 6 comes from the c.m. → lab transformation Jacobian.)
(54) Udseth, H.; Giese, C. F.; Gentry, W. R. *J. Chem. Phys.* **1974**, *60*, 3051.
(55) Krutein, J.; Linder, F. *J. Chem. Phys.* **1979**, *71*, 599; *Chem. Phys. Lett.* **1977**, *51*, 597.
(56) Gianturco, F. A.; Gierz, U.; Toennies, J. P. *J. Phys. B.* **1981**, *14*, 667.
(57) For recent theoretical and experimental studies of charge transfer effects in the H^+–O_2 system, see: (a) Staemmler, V.; Gianturco, F. A. *Int. J. Quantum Chem.* **1985**, *28*, 553. (b) Noll, M.; Toennies, J. P. *J. Chem. Phys.*, in press.
(58) Huber, K. P.; Herzberg, G. *Constants of Diatomic Molecules*; Van Nostrand: New York, 1979.
(59) Szanto, P. G.; Anderson, T. G.; Saykally, R. J.; Piltch, N. D.; Dixon, T. A.; Woods, R. C. *J. Chem. Phys.* **1981**, *75*, 4261.
(60) Woods, R. C.; Saykally, R. J.; Anderson, T. G.; Dixon, T. A.; Szanto, P. G. *J. Chem. Phys.* **1981**, *75*, 4256.
(61) Richards, D. *J. Phys. B.* **1982**, *15*, 1499. See also: Iwamatsu, M.; Onodera, Y.; Itoh, Y.; Kobayashi, N.; Kaneko, Y. *Chem. Phys. Lett.* **1981**, *77*, 585.
(62) Staemmler, V. *Chem. Phys.* **1975**, *7*, 17; *Ibid.* **1976**, *17*, 187.
(63) Böttner, R.; Ross, U.; Toennies, J. P. *J. Chem. Phys.* **1976**, *65*, 733.
(64) Many theoretical studies of Li^+–N_2,CO inelastic scattering have appeared. Some workers attempted to "explain" the original misinterpreted experimental results, while others concluded that the agreement between theory and experiment was poor. Here we mention three of the more interesting scattering calculations: (a) Thomas, L. D.; *J. Chem. Phys.* **1977**, *67*, 5224. (b) Thomas, L. D.; Kraemer, W. P.; Diercksen, G. H. F. *Chem. Phys.* **1978**, *30*, 33. (c) Pfeffer, G. A.; Secrest, D. *J. Chem. Phys.* **1983**, *78*, 3052. (References to other theoretical studies are given in the paper by Pfeffer and Secrest and in ref 65).
(65) Gierz, U.; Toennies, J. P.; Wilde, M. *Chem. Phys. Lett.* **1984**, *110*, 115.
(66) For an excellent review of rotational rainbow theory, see the article by R. Schinke and J. M. Bowman in ref 16.
(67) Hege, U.; Linder, F. *Z. Phys. A* **1985**, *320*, 95.
(68) Li^+–H_2O scattering has also been studied, but without vibrational state resolution. [Siskind, B.; Alexander, M. H.; Coplan, M. A. *J. Chem. Phys.* **1976**, *65*, 1063].
(69) Krutein, J.; Linder, F. *J. Phys. B.* **1977**, *10*, 1363.
(70) Bischof, G.; Hermann, V.; Krutein, J.; Linder, F. *J. Phys. B.* **1982**, *15*, 249.
(71) Green, S.; Schor, H.; Siegbahn, P.; Thaddeus, P. *Chem. Phys.* **1976**, *17*, 479. See also: Gianturco, F. A.; Semprini, E.; Stefani, F. *Chem. Phys. Lett.* **1986**, *126*, 81.
(72) Eastes, W.; Ross, U.; Toennies, J. P. *J. Chem. Phys.* **1977**, *66*, 1919.
(73) Eastes, W.; Ross, U.; Toennies, J. P. *J. Chem. Phys.* **1979**, *70*, 1652.

(74) Ellenbroek, T.; Gierz, U.; Toennies, J. P. *Chem. Phys. Lett.* **1980**, *70*, 459.
(75) Ellenbroek, T.; Gierz, U.; Noll, M.; Toennies, J. P. *J. Phys. Chem.* **1982**, *86*, 1153.
(76) Gentry, W. R.; Udseth, H.; Giese, C. F. *Chem. Phys. Lett.* **1975**, *36*, 671.
(77) Ellenbroek, T.; Toennies, J. P. *Chem. Phys.* **1982**, *71*, 309.
(78) Noll, M.; Toennies, J. P. *Chem. Phys. Lett.* **1984**, *108*, 297.
(79) Gierz, U.; Noll, M.; Toennies, J. P. *J. Chem. Phys.* **1985**, *83*, 2259.
(80) Gierz, U.; Toennies, J. P.; Wilde, M. *Chem. Phys. Lett.* **1983**, *95*, 517.
(81) Gierz, U.; Noll, M.; Toennies, J. P. *J. Chem. Phys.* **1985**, *82*, 217.
(82) He + HD: Gentry, W. R.; Giese, C. F. *J. Chem. Phys.* **1977**, *67*, 5389.
(83) Ne + HD: Buck, U.; Huisken, F.; Schleusener, J.; Pauly, H. *Phys. Rev. Lett.* **1977**, *38*, 680. Buck, U.; Huisken, F.; Schleusener, J.; Schaefer, J. *J. Chem. Phys.* **1980**, *72*, 1512.
(84) Ne + D_2: Andres, J.; Buck, U.; Huisken, F.; Schleusener, J.; Torello, F. *J. Chem. Phys.* **1980**, *73*, 5620. Gerber, R. B.; Buch, V.; Buck, U.; Maneke, G.; Schleusener, J. *Phys. Rev. Lett.* **1980**, *44*, 1397.
(85) Ar + D_2: Buck, U.; Meyer, H.; LeRoy, R. J. *J. Chem. Phys.* **1984**, *80*, 5589.
(86) HD + HD: Gentry, W. R.; Giese, C. F. *Phys. Rev. Lett.* **1977**, *39*, 1259.
(87) HD + D_2: Buck, U.; Huisken, F.; Schleusener, J. *J. Chem. Phys.* **1978**, *68*, 5654. Buck, U.; Huisken, F.; Maneke, G.; Schaefer, J. *Ibid.* **1983**, *78*, 4430.
(88) H_2 + D_2: Buck, U.; Huisken, F.; Kohlhase, A.; Otten, D.; Schaefer, J. *J. Chem. Phys.* **1983**, *78*, 4439.
(89) He + N_2, CO, CH_4: Faubel, M.; Kohl, K. H.; Toennies, J. P. *J. Chem. Phys.* **1980**, *73*, 2506. See also: Faubel, M. *Ibid.* **1984**, *81*, 5559.
(90) He + N_2: Faubel, M.; Kohl, K. H.; Toennies, J. P.; Tang, K. T.; Yung, Y. Y. *Faraday Discuss. Chem. Soc.* **1982**, *73*, 205.
(91) He + O_2: Faubel, M.; Kohl, K. H.; Toennies, J. P.; Gianturco, F. A. *J. Chem. Phys.* **1983**, *78*, 5629.
(92) He + CH_4: Buck, U.; Kohl, K. H.; Kohlhase, A.; Faubel, M.; Staemmler, V. *Mol. Phys.* **1985**, *55*, 1255.
(93) Loesch, H. *Adv. Chem. Phys.* **1980**, *42*, 421.
(94) Ar + CO, O_2: Preliminary results are discussed in ref 1.
(95) Ar + Cl_2: Hoffbauer, M. A.; Burdenski, S.; Giese, C. F.; Gentry, W. R. *J. Chem. Phys.* **1983**, *78*, 3832.
(96) D_2 + CO: Andres, J.; Buck, U.; Meyer, H.; Launay, J. M. *J. Chem. Phys.* **1982**, *76*, 1417. Schinke, R.; Meyer, H.; Buck, U.; Diercksen, G. H. F. *Ibid.* **1984**, *80*, 5518.
(97) Xe + CO_2: Buck, U.; Huisken, F.; Otten, D.; Schinke, R. *Chem. Phys. Lett.* **1983**, *101*, 126. Buck, U.; Otten, F.; Schinke, R.; Poppe, D. *J. Chem. Phys.* **1985**, *82*, 202.
(98) Ne + CH_4: Buck, U.; Kohlhase, A.; Secrest, D.; Phillips, T.; Scoles, G.; Grein, F. *Mol. Phys.* **1985**, *55*, 1233.
(99) Ar + CH_4: Buck, U.; Schleusener, J.; Malik, D. J.; Secrest, D. *J. Chem. Phys.* **1981**, *74*, 1707. Buck, U.; Kohlhase, A.; Phillips, T.; Secrest, D. *Chem. Phys. Lett.* **1983**, *98*, 199.
(100) He + NH_3: Buck, U. "Rotational Excitation in Molecular Beam Experiments". In *Molecular Astrophysics—State of the Art* and *Future Directions*, Diercksen, G. H. F., Huebner, W. F., Langhoff, P. W., Eds.; Reidel: Dordrecht, 1984.
(101) Ar, Kr + SF_6: Pack, R. T.; Valentini, J. J.; Cross, J. B. *J. Chem. Phys.* **1982**, *77*, 5486.
(102) For a review of the "triple-beam" work, see: Fisk, G. A.; Crim, F. F. *Acc. Chem. Res.* **1977**, *10*, 73.
(103) The alkali halide work is discussed in detail in ref 93.
(104) For a fascinating study of collision-induced dissociation of alkali halide molecules, including differential cross section measurements, see: Tully, F. P.; Cheung, N. H.; Haberland, N.; Lee, Y. T. *J. Chem. Phys.* **1980**, *73*, 4460.
(105) Eccles, J.; Pfeffer, G.; Piper, E.; Ringer, G.; Toennies, J. P. *Chem. Phys.* **1984**, *89*, 1.
(106) Billing, G. D. *Chem. Phys.* **1983**, *79*, 179.
(107) Mariella, R. P., Jr.; Herschbach, D. R.; Klemperer, W. *J. Chem. Phys.* **1974**, *61*, 4575.
(108) Dagdigian, P. J. *Chem. Phys.* **1980**, *52*, 279.
(109) Dagdigian, P. J.; Wilcomb, B. E. *J. Chem. Phys.* **1980**, *72*, 6462.
(110) Ryali, S. B.; Fenn, J. B.; Kolb, C. E.; Silver, J. A. *J. Chem. Phys.* **1982**, *76*, 5878.
(111) Venkateshan, S. P.; Ryali, S. B.; Fenn, J. B. *Chem. Phys. Lett.* **1982**, *92*, 606.
(112) Rahbee, A. *J. Phys. Chem.* **1984**, *88*, 4488.
(113) Billing, G. D.; Clary, D. C. *Chem. Phys.* **1983**, *80*, 213.
(114) Billing, G. D. *Chem. Phys.* **1984**, *91*, 327; *Chem. Phys. Lett.* **1985**, *117*, 145.
(115) Gentry, W. R. "State-to-State Energy Transfer in Collisions of Neutral Molecules". In *Electronic and Atomic Collisions—Invited Papers of ICPEAC XIV*, Lorents, D. C., Meyerhof, W. E., Peterson, J. R., Eds.; North-Holland: Amsterdam, 1986; p 13.
(116) Gentry, W. R.; Giese, C. F. *Rev. Sci. Instrum.* **1978**, *49*, 595.
(117) Hall, G.; Liu, K.; McAuliffe, M. J.; Giese, C. F.; Gentry, W. R. *J. Chem. Phys.* **1983**, *78*, 5260.
(118) Hall, G.; Liu, K.; McAuliffe, M. J.; Giese, C. F.; Gentry, W. R. *J. Chem. Phys.* **1984**, *81*, 5577. (A factor of ϵ^{m+n} is missing from eq 12 of this paper.)
(119) See, for example: Mahan, B. H. *J. Chem. Phys.* **1970**, *52*, 5221.
(120) Hall, G.; Liu, K.; McAuliffe, M. J.; Giese, C. F.; Gentry, W. R. *J. Chem. Phys.* **1986**, *84*, 1402.
(121) Schwenke, D. W.; Truhlar, D. G. *J. Chem. Phys.* **1984**, *81*, 5586.
(122) Liu, K.; Hall, G.; McAuliffe, M. J.; Giese, C. F.; Gentry, W. R. *J. Chem. Phys.* **1984**, *80*, 3494.
(123) Hall, G.; Giese, C. F.; Gentry, W. R. *J. Chem. Phys.* **1985**, *83*, 5343.
(124) For details of aniline S_1–S_0 spectroscopy, see: Chernoff, D. A.; Rice, S. A. *J. Chem. Phys.* **1979**, *70*, 2511.
(125) Varsanyi, G. *Assignments for Vibrational Spectra of Seven Hundred Benzene Derivatives*; Wiley: New York, 1974; Vol. 1.
(126) Catlett, D. L., Jr.; Holtzclaw, K. W.; Krajnovich, D.; Moss, D. B.; Parmenter, C. S.; Lawrance, W. D.; Knight, A. E. W. *J. Phys. Chem.* **1985**, *89*, 1577.
(127) Serri, J. A.; Becker, C. H.; Elbel, M. B.; Kinsey, J. L.; Moskowitz, W. P.; Pritchard, D. E. *J. Chem. Phys.* **1981**, *74*, 5116.
(128) Serri, J. A.; Bilotta, R. M.; Pritchard, D. E. *J. Chem. Phys.* **1982**, *77*, 2940.
(129) Serri, J. A.; Kinsey, J. L.; Pritchard, D. E. *J. Chem. Phys.* **1981**, *75*, 663.
(130) Moskowitz, W. P.; Stewart, B.; Bilotta, R. M.; Kinsey, J. L.; Pritchard, D. E. *J. Chem. Phys.* **1984**, *80*, 5496.
(131) For a detailed description of the rotatable LIF detector, see: Bergmann, K.; Hefter, U.; Witt, J. *J. Chem. Phys.* **1980**, *72*, 4777.
(132) Gottwald, E.; Mattheus, A.; Bergmann, K.; Schinke, R. *J. Chem. Phys.* **1986**, *84*, 756.
(133) Barnes, J. A.; Keil, M.; Kutina, R. E.; Polanyi, J. C. *J. Chem. Phys.* **1982**, *76*, 913.
(134) Wood, R. W. *Philos. Mag.* (*Ser. 6*) **1911**, *21*, 309. Franck, J.; Wood, R. W. *Ibid.* **1911**, *21*, 314.
(135) (a) Brown, R. L.; Klemperer, W. *J. Chem. Phys.* **1964**, *41*, 3072. (b) Steinfeld, J. I.; Klemperer, W. *Ibid.* **1965**, *42*, 3475. (c) Kurzel, R. B.; Steinfeld, J. I. *Ibid.* **1970**, *53*, 3293. (d) Steinfeld, J. I.; Schweid, A. N. *Ibid.* **1970**, *53*, 3304. (e) Kurzel, R. B.; Degenkolb, E. O.; Steinfeld, J. I. *Ibid.* **1972**, *56*, 1784. (f) Rubinson, M.; Garetz, B.; Steinfeld, J. I. *Ibid.* **1974**, *60*, 3082.
(136) Since the dispersed fluorescence signal is normalized to the total fluorescence signal on a shot-by-shot basis, electronic quenching does *not* contribute to the dip in the subtracted spectrum in Figure 9. Only inelastic transitions to other fluorescing levels contribute to the dip.
(137) Some preliminary results have been obtained on the inelastic scattering of He and H_2 from S_1 *trans*-glyoxal molecules. (Butz, K.; Du, H.; Krajnovich, D.; Parmenter, C. S., unpublished).
(138) (a) O'Neill, J. A.; Cai, J. Y.; Flynn, G. W.; Weston, R. E., Jr. *J. Chem. Phys.* **1986**, *84*, 50. (b) McGee, T. H.; Weston, R. E., Jr.; Flynn, G. W. *Ibid.* **1985**, *82*, 3607. (c) Chu, J. O.; Wood, C. F.; Flynn, G. W.; Weston, R. E., Jr. *Ibid.* **1984**, *81*, 5533. (d) Datta, S.; Weston, R. E., Jr.; Flynn, G. W. *Ibid.* **1984**, *80*, 4071. (e) Chu, J. O.; Wood, C. F.; Flynn, G. W.; Weston, R. E., Jr. *Ibid.* **1984**, *80*, 1703. (f) Chu, J. O.; Flynn, G. W.; Weston, R. E., Jr. *Ibid.* **1983**, *78*, 2990. (g) Wood, C. F.; Flynn, G. W.; Weston, R. E., Jr. *Ibid.* **1982**, *77*, 4776. (h) Quick, C. R., Jr.; Weston, R. E., Jr.; Flynn, G. W. *Chem. Phys. Lett.* **1981**, *83*, 15.
(139) (a) Wight, C. A.; Donaldson, D. J.; Leone, S. R. *J. Chem. Phys.* **1985**, *83*, 660. (b) Wight, C. A.; Magnotta, F.; Leone, S. R. *Ibid.* **1984**, *81*, 3951. (c) Wight, C. A.; Leone, S. R. *Ibid.* **1983**, *79*, 4823. (d) Wight, C. A.; Leone, S. R. *Ibid.* **1983**, *78*, 4875. (e) Magnotta, F.; Nesbitt, D. J.; Leone, S. R. *Chem. Phys. Lett.* **1981**, *83*, 21.
(140) (a) Gerrity, D. P.; Valentini, J. J. *J. Chem. Phys.* **1985**, *83*, 2207. (b) Quick, C. R., Jr.; Moore, D. S. *Ibid.* **1983**, *79*, 759.
(141) (a) Yardley, J. T.; Moore, C. B. *J. Chem. Phys.* **1966**, *45*, 1066. (b) Hocker, L. O.; Kovacs, M. A.; Rhodes, C. K.; Flynn, G. W.; Javan, A. *Phys. Rev. Lett.* **1966**, *17*, 233.
(142) See, for example: (a) Laubereau, A.; Kaiser, W. *Rev. Mod. Phys.* **1978**, *50*, 607. (b) Zinth, W.; Kolmeder, C.; Benna, B.; Irgens-Defregger, A.; Fischer, S. F.; Kaiser, W. *J. Chem. Phys.* **1983**, *78*, 3916.
(143) See, for example: (a) Casassa, M. P.; Heilweil, E. J.; Stephenson, J. C.; Cavanagh, R. R. *J. Electron Spectrosc. Relat. Phenom.* **1986**, *38*, 257; (b) *J. Chem. Phys.* **1986**, *84*, 2361.
(144) Ahl, J. L.; Bohn, R. K.; Casleton, K. H.; Rao, Y. V. C.; Flynn, G. W. *J. Chem. Phys.* **1983**, *78*, 3899.
(145) For examples of the use of optical parametric oscillators and Raman-shifted dye lasers for initial state preparation in S_0

bulb studies, see: (a) Canon, B. D.; Francisco, J. S.; Smith, I. W. M. *Chem. Phys.* **1984**, *89*, 141. (b) Hastings, P. W.; Osborn, M. K.; Sadowski, C. M.; Smith, I. W. M. *J. Chem. Phys.* **1983**, *78*, 3893. (c) Hess, P.; Kung, A. H.; Moore, C. B. *Ibid.* **1980**, *72*, 5525. (d) Robinson, J. M.; Pearson, D. J.; Copeland, R. A.; Crim, F. F. *Ibid.* **1985**, *82*, 780.

(146) For examples of initial state preparation in S_0 using stimulate emission pumping (SEP), see: (a) Lawrance, W. D.; Knight, A. E. W. *J. Chem. Phys.* **1982**, *77*, 570. (b) Muller, D. J.; Lawrance, W. D.; Knight, A. E. W. *J. Phys. Chem.* **1983**, *87*, 4952. (c) Thoman, J. W., Jr.; Kable, S. H.; Rock, A. B.; Knight, A. E. W. *J. Chem. Phys.* **1986**, *85*, 6234.

(147) Stimulated Raman scattering is still in an early stage of development with respect to energy transfer studies. For recent developments, see: (a) Duval, A. B.; King, D. A.; Haines, R.; Isenor, N. R.; Orr, B. J. *J. Opt. Soc. Am. B: Opt. Phys.* **1985**, *2*, 1570. (b) King, D. A.; Haines, R.; Isenor, N. R.; Orr, B. J. *Opt. Lett.* **1983**, *8*, 629. (c) Brodnikovsky, A. M.; Gladkov, S. M.; Koroteev, N. I. *Opt. Commun.* **1982**, *40*, 312.

(148) For examples of the use of F-center lasers and diode lasers as final state probes in bulb studies of vibrational energy transfer, see: Haugen, H. K.; Pence, W. H.; Leone, S. R. *J. Chem. Phys.* **1984**, *80*, 1839 and ref 138c,e.

(149) Visible/UV LIF has been used as a final state probe in a number of S_0 bulb studies of vibrational energy transfer. See, for example: (a) Bewick, C. P.; Duval, A. B.; Orr, B. J. *J. Chem. Phys.* **1985**, *82*, 3470. (b) Haub, J. G.; Orr, B. J. *Chem. Phys. Lett.* **1984**, *107*, 162; and ref 139a and 146a,b,c.

(150) CARS was used as a final state probe in ref 140a,b and 147c.

(151) MPI has been used in bulbs to study rotational energy transfer in two electronic states of NO. See: (a) Sudbø Aa. S. Loy, M. M. T. *J. Chem. Phys.* **1982**, *76*, 3646. (b) Ebata, T.; Anezaki, Y.; Fuji, M.; Mikami, N.; Ito, M. *Chem. Phys.* **1984**, *84*, 151. Applications to vibrational energy trnasfer have yet to appear.

(152) (a) Leeuw, M. W. "Collision-Induced Energy Transfer in s-Tetrazine". Ph.D. Thesis, University of Amsterdam, 1981. (b) Ramaekers, J. J. F. "Energy Conversion in s-Tetrazine and in van der Waals Complexes of s-Tetrazine and Argon". Ph.D. Thesis, University of Amsterdam, 1983.

(153) Langelaar, J.; Bebelaar, D.; Leeuw, M. W.; Ramaekers, J. J. F.; Rettschnick, R. P. H. In *Picosecond Phenomena II*, Hochstrasser, R. M. et al., Eds.; Springer Series in Chemical Physics; Springer: Berlin, 1980; Vol. 14, p 171.

(154) Catlett, D. L., Jr. "Vibrational Energy Transfer in the S_1 State of *p*-Difluorobenzene". Ph.D. Thesis, Indiana University, 1986.

(155) Brumbaugh, D. V.; Innes, K. K. *Chem. Phys.* **1981**, *59*, 413.

(156) Parmenter, C. S.; Tang, K. Y. *Chem. Phys.* **1978**, *27*, 127.

(157) Atkinson, G. H.; Parmenter, C. S.; Tang, K. Y. *J. Chem. Phys.* **1979**, *71*, 68.

(158) Tang, K. Y.; Parmenter, C. S. *J. Chem. Phys.* **1983**, *78*, 3922.

(159) See: Knight, A. E. W.; Parmenter, C. S.; Schuyler, M. W. *J. Am. Chem. Soc.* **1975**, *97*, 1993, 2005, and references cited therein.

(160) Spears, K. G.; Rice, S. A. *J. Chem. Phys.* **1971**, *55*, 5561.

(161) Ware, W. R.; Garcia, A. M.; Parmenter, C. S.; Schuh, M. D.; Tang, K. Y. *Chem. Phys.* **1976**, *17*, 377.

(162) Logan, L. M.; Buduls, I.; Knight, A. E. W.; Ross, I. G. *J. Chem. Phys.* **1980**, *72*, 5667.

(163) Lyman, J. L.; Muller, G.; Houston, P. L.; Piltch, M.; Schmid, W. E.; Kompa, K. L. *J. Chem. Phys.* **1985**, *82*, 810.

(164) Chernoff, D. A.; Rice, S. A. *J. Chem. Phys.* **1979**, *70*, 2521.

(165) Vandersall, M.; Chernoff, D. A.; Rice, S. A. *J. Chem. Phys.* **1981**, *74*, 4888.

(166) Cameron, S. M.; Vandersall, M.; Rice, S. A. *J. Chem. Phys.* **1981**, *75*, 1046.

(167) Pineault, R. L.; Crackel, R. L.; Hedstrom, J. F.; Struve, W. S. *J. Chem. Phys.* **1984**, *80*, 5545.

(168) McDonald, D. B.; Rice, S. A. *J. Chem. Phys.* **1981**, *74*, 4907.

(169) McDonald, D. B.; Rice, S. A. *J. Chem. Phys.* **1981**, *74*, 4893.

(170) For a discussion of intermediate case S_1–T coupling in pyrazine, see: (a) Frad, A.; Lahmani, F.; Tramer, A.; Tric, C. *J. Chem. Phys.* **1974**, *60*, 4419. (b) van der Meer, B. J.; Jonkman, H. Th.; Kommandeur, J. *Laser Chem.* **1983**, *2*, 77.

(171) Knight, A. E. W.; Jones, J. T.; Parmenter, C. S. *J. Phys. Chem.* **1983**, *87*, 973.

(172) Knight, A. E. W.; Parmenter, C. S. *J. Phys. Chem.* **1983**, *87*, 417.

(173) Coveleskie, R. A.; Parmenter, C. S. *J. Mol. Spectrosc.* **1981**, *86*, 86.

(174) (a) Volk, L. J.; Lee, E. K. C. *J. Chem. Phys.* **1977**, *67*, 236. (b) Guttman, C.; Rice, S. A. *Ibid.* **1974**, *61*, 661.

(175) See: Holtzclaw, K. W.; Parmenter, C. S. *J. Chem. Phys.* **1986**, *84*, 1099 and references cited therein.

(176) Dolson, D. A.; Holtzclaw, K. W.; Moss, D. B.; Parmenter, C. S. *J. Chem. Phys.* **1986**, *84*, 1119.

(177) Butz, K. W.; Catlett, D. L., Jr.; Ewing, G. E.; Krajnovich, D.; Parmenter, C. S. *J. Phys. Chem.* **1986**, *90*, 3533.

(178) From Figure 2 of ref 158.

(179) Schmid, E. W.; Brandmuller, J.; Nonnenmacher, G. *Z. Elektrochem.* **1960**, *64*, 940.

(180) (a) Schwartz, R. N.; Slawsky, Z. I.; Herzfeld, K. F. *J. Chem. Phys.* **1952**, *20*, 1591. (b) Schwartz, R. N.; Herzfeld, K. F. *Ibid.* **1954**, *22*, 767.

(181) Tanczos, F. I. *J. Chem. Phys.* **1956**, *25*, 439.

(182) (a) Stretton, J. L. *Trans. Faraday Soc.* **1965**, *61*, 1053. (b) Stretton, J. L. In *Transfer and Storage of Energy in Molecules*, Wiley: London, 1969; Vol. 2, p 58.

(183) Freed, K. F. *Chem. Phys. Lett.* **1984**, *106*, 1.

(184) Cerjan, C.; Lipkin, M.; Rice, S. A. *J. Chem. Phys.* **1983**, *78*, 4929.

(185) (a) Clary, D. C. *J. Chem. Phys.* **1984**, *81*, 4466; (b) *Mol. Phys.* **1984**, *51*, 1299.

(186) Clary, D. C. *J. Am. Chem. Soc.* **1984**, *106*, 970.

(187) Clary, D. C. *J. Chem. Phys.* **1981**, *75*, 2899.

(188) (a) Sheorey, R. S.; Flynn, G. *J. Chem. Phys.* **1980**, *72*, 1175. (b) Ahl, J. L.; Flynn, G. W. *J. Phys. Chem.* **1983**, *87*, 2172.

(189) Brenner, D. M. *J. Chem. Phys.* **1981**, *74*, 494.

(190) (a) Fischer, S. F.; Irgens-Defregger, A. *J. Phys. Chem.* **1983**, *87*, 2054. (b) Fischer, S. F. In *Intramolecular Dynamics*; Reidel: Amsterdam, 1982; p 205.

(191) Cottrell, T. L.; McCoubrey, J. C. *Molecular Energy Transfer in Gases*; Butterworths: London, 1961.

(192) See, for example: ref 193 and Rice, S. A. *J. Phys. Chem.* **1986**, *90*, 3063.

(193) McDonald, D. B.; Rice, S. A. *J. Chem. Phys.* **1981**, *74*, 4918.

(194) Catlett, D. L., Jr.; Parmenter, C. S. unpublished results.

(195) Lin, H.-M.; Seaver, M.; Tang, K. Y.; Knight, A. E. W.; Parmenter, C. S. *J. Chem. Phys.* **1979**, *70*, 5442.

(196) Parmenter, C. S.; Setzer, B.; Tang, K. Y. *J. Chem. Phys.* **1977**, *66*, 1317.

(197) Moore, C. B. *J. Chem. Phys.* **1965**, *43*, 2979.

(198) Vandersall, M.; Rice, S. A. *J. Chem. Phys.* **1983**, *79*, 4845.

(199) Rolfe, T. J.; Rice, S. A. *J. Chem. Phys.* **1983**, *79*, 4863.

(200) ten Brink, H. M. "Vibrational Deactivation Pathways in Glyoxal ^1A_u". Ph.D. Thesis, University of Amsterdam, 1979.

(201) de Leeuw, G. "Energy Conversion in *trans*-Glyoxal". Ph.D. Thesis, University of Amsterdam, 1981.

(202) (a) Rettschnick, R. P. H.; ten Brink, H. M.; Langelaar, J. *J. Mol. Struct.* **1978**, *47*, 261. (b) ten Brink, H. M.; Langelaar, J.; Rettschnick, R. P. H. *Chem. Phys. Lett.* **1979**, *62*, 263. (c) de Leeuw, G.; Langelaar, J.; Rettschnick, R. P. H. *J. Mol. Struct.* **1980**, *61*, 101. (d) ten Brink, H. M.; Langelaar, J.; Rettschnick, R. P. H. *Chem. Phys. Lett.* **1980**, *75*, 115.

(203) Rettschnick, R. P. H. In *Radiationless Transitions*; Lin, S. H., Ed.; Academic: New York, 1980; p 185.

(204) ten Brink, H. M.; Rettschnick, R. P. H.; Langelaar, J.; van Voorst, J. D. W. In *Conference Proceedings, Lasers in Chemistry*, West, M. A., Ed.; Elsevier: Amsterdam, 1977; p 330.

(205) (a) Beyer, R. A.; Zittel, P. F.; Lineberger, W. C. *J. Chem. Phys.* **1975**, *62*, 4016. (b) Beyer, R. A.; Lineberger, W. C. *Ibid.* **1975**, *62*, 4024. (c) Zittel, P. F.; Lineberger, W. C. *Ibid.* **1977**, *66*, 2972.

(206) Anderson, L. G.; Parmenter, C. S.; Poland, H. M. *Chem. Phys.* **1973**, *1*, 401.

(207) Rordorf, B. F.; Knight, A. E. W.; Parmenter, C. S. *Chem. Phys.* **1978**, *27*, 11.

(208) Coveleskie, R. A.; Parmenter, C. S. *J. Chem. Phys.* **1978**, *69*, 1044.

(209) Akins, D. L.; King, D. S.; Stephenson, J. C. *Chem. Phys. Lett.* **1979**, *65*, 257.

(210) Dornhofer, G.; Hack, W.; Langel, W. *J. Phys. Chem.* **1983**, *87*, 3456.

(211) DePristo, A. E. *J. Chem. Phys.* **1980**, *73*, 4329.

(212) For an intermediate-level discussion of the B.-O. approximation and the potential energy surface, see: Hirst, D. M. *Potential Energy Surfaces*; Taylor and Francis: London, 1985.

(213) For reviews of ab initio and semiempirical methods of determining potential energy surfaces, see: (a) Schaefer, H. F., III. "Atom-Molecule Potentials". In ref 15, p 45. (b) Kuntz, P. J. "Semiempirical Atom–Molecule Potentials for Collision Theory". In ref 15, p 79. (c) Tully, J. C. "Semiempirical Diatomics-in-Molecules Potential Energy Surfaces". *Adv. Chem. Phys.* **1980**, *42*, 63. (d) Fogarasi, G.; Pulay, P. "Ab Initio Vibrational Force Fields". *Annu. Rev. Phys. Chem.* **1984**, *35*, 191.

(214) Gordon, R. G. "Coupled Channel Scattering Matrices". *QCPE* **1971**, *11*, 187. (Available through the Quantum Chemistry Program Exchange, Indiana University Chemistry Department, Bloomington, IN 47405).

(215) Lin, C. S.; Secrest, D. *J. Chem. Phys.* **1979**, *70*, 199. (See, however: Lin, C. S. *Ibid.* **1981**, *74*, 5928.)

(216) Secrest, D. *J. Chem. Phys.* **1975**, *62*, 710.

(217) Kouri, D. J. In ref 15, p 301.

(218) Kouri, D. J.; Fitz, D. E. *J. Phys. Chem.* **1982**, *86*, 2224.

(219) The humble comparison in Figure 5 of ref 186 between a highly averaged theoretical curve and a single, highly aver-

aged experimental V → T rate constant dramatically points up the need for more detailed experimental measurements.
(220) For a good introduction to both the philosophy and technology of classical trajectory methods, see: Bunker, D. L. *Methods Comput. Phys.* **1971**, *10*, 287.
(221) See, for example: Pattengill, M. D. In ref 15, p 359.
(222) Date, N.; Hase, W. L.; Gilbert, R. G. *J. Phys. Chem.* **1984**, *88*, 5135.
(223) Grinchak, M. B.; Levitsky, A. A.; Polak, L. S.; Umanskii, S. Ya. *Chem. Phys.* **1984**, *88*, 365.
(224) Osborn, M. K.; Smith, I. W. M. *Chem. Phys.* **1984**, *91*, 13.
(225) Koshi, M.; Itoh, H.; Matsui, H. *J. Chem. Phys.* **1985**, *82*, 4903.
(226) Thompson, D. L. *Chem. Phys. Lett.* **1982**, *92*, 383.
(227) Blais, N. C.; Truhlar, D. G. *J. Phys. Chem.* **1982**, *86*, 638.
(228) (a) Colton, M. C.; Schatz, G. C. *J. Chem. Phys.* **1985**, *83*, 3413. (b) Geiger, L. C.; Schatz, G. C.; Harding, L. B. *Chem. Phys. Lett.* **1985**, *114*, 520. (c) Geiger, L. C.; Schatz, G. C. *J. Phys. Chem.* **1984**, *88* 214.
(229) Blais, N. C.; Truhlar, D. G. *J. Chem. Phys.* **1985**, *83*, 2201.
(230) (a) Muckerman, J. T. "CLASTR: Monte Carlo Quasi-Classical Trajectory Program". QCPE **1973**, *11*, 229. (b) Chapman, S.; Bunker, D. L.; Gelb, A. "A + BC: General Trajectory Program". *QCPE* **1975**, *11*, 273. (c) Chapman, S.; Wright, K. R.; Bunker, D. L.; Gelb, A.; Santamaria, J. "Mini A + BC: Minicomputer-Adapted Version of the QCPE 273 General Trajectory Program". *QCPE* **1976**, *11*, 316. (All programs are available through the Quantum Chemistry Program Exchange, Indiana University, Chemistry Department, Bloomington, IN 47405. The programs in ref 230b and 230c follow closely the description in ref 220.)
(231) Hase, W. L. "MERCURY: A General Monte Carlo Trajectory Program", QCPE Program No. 453. (Available through the Quantum Chemistry Program Exchange, Indiana University Chemistry Department, Bloomington, IN 47405.)
(232) Zener, C. *Phys. Rev.* **1931**, *38*, 277; *Proc. Cambridge Philos. Soc.* **1932**, *29*, 136.
(233) Zener, C. *Proc. R. Soc. London A* **1932**, *137*, 696.
(234) For information on the classical path approximation computer programs, see: Billing, G. D. *Comput. Phys. Commun.* **1984**, *32*, 45.
(235) (a) Miller, W. H. *J. Chem. Phys.* **1970**, *53*, 1949; (b) *Ibid.* **1970**, *53*, 3578; (c) *Chem. Phys. Lett.* **1970**, *7*, 431; (d) *J. Chem. Phys.* **1971**, *54*, 5386. (e) Miller, W. H.; George, T. F. *Ibid.* **1972**, *56*, 5668.
(236) (a) Marcus, R. A. *Chem. Phys. Lett.* **1970**, *7*, 525; (b) *J. Chem. Phys.* **1971**, *54*, 3965. (c) Connor, J. N. L.; Marcus, R. A. *Ibid.* **1971**, *55*, 5636. (d) Marcus, R. A. *Ibid.* **1972**, *56*, 311. (e) Stine, J.; Marcus, R. A. *Chem. Phys. Lett.* **1972**, *15*, 536.
(237) Ford, K. W.; Wheeler, J. A. *Ann. Phys.* **1959**, *7*, 259,287.
(238) Feynmann, R. P.; Hibbs, A. R. *Quantum Mechanics and Path Integrals*; McGraw-Hill: New York, 1965.
(239) (a) Miller, W. H. *Adv. Chem. Phys.* **1974**, *25*, 69; (b) *Ibid.* **1975**, *30*, 77.
(240) For an intriguing discussion of the least-action principle in classical and quantum mechanics, see: Feynman, R. P.; Leighton, R. B.; Sands, M. *The Feynman Lectures on Physics*, Addison-Wesley: Reading, 1964; Vol. II, Chapter 19.
(241) McCurdy, C. W.; Miller, W. H. *J. Chem. Phys.* **1977**, *67*, 463.
(242) (a) Doll, J. D.; Miller, W. H. *J. Chem. Phys.* **1972**, *57*, 5019. (b) Miller, W. H.; Raczkowski, A. W. *Faraday Discuss. Chem. Soc.* **1973**, *55*, 45.
(243) McCurdy, C. W.; Miller, W. H. *J. Chem. Phys.* **1980**, *73*, 3191.
(244) Bartlett, M. S.; Moyal, J. E. *Proc. Cambridge Philos. Soc.* **1949**, *45*, 545.
(245) Takayanagi, K. *Suppl. Prog. Theor. Phys.* **1963**, *25*, 1.
(246) Kerner, E. H. *Can. J. Phys.* **1958**, *36*, 371. (Evidently, in Kerner's formula for P_{mn} on p. 373, $L_{\nu}^{r-\mu}$ should read $L_{\mu}^{r-\mu}$. Then his formula reduces to eq 8a of the text.)
(247) Pechukas, P.; Light, J. C. *J. Chem. Phys.* **1966**, *44*, 3897.
(248) Heidrich, F. E.; Wilson, K. R.; Rapp, D. *J. Chem. Phys.* **1971**, *54*, 3885.
(249) Gentry, W. R.; Giese, C. F. *J. Chem. Phys.* **1975**, *63*, 3144.
(250) Morse, R. I. *J. Chem. Phys.* **1971**, *54*, 4138.
(251) Shobatake, K.; Rice, S. A.; Lee, Y. T. *J. Chem. Phys.* **1973**, *59*, 2483.
(252) Skodje, R. T.; Gentry, W. R.; Giese, C. F. *J. Chem. Phys.* **1977**, *66*, 160; *Chem. Phys.* **1983**, *74*, 347.
(253) Meyer, H.-D. *Chem. Phys.* **1981**, *61*, 365.
(254) Gordon, R. J. *J. Chem. Phys.* **1979**, *71*, 4720.
(255) Rapp, D.; Kassal, T. *Chem. Rev.* **1969**, *69*, 61.
(256) Zener, C. *Phys. Rev.* **1931**, *37*, 556.
(257) Jackson, J. M.; Mott, N. F. *Proc. R. Soc. London A* **1932**, *137*, 703.
(258) For the original Landau–Teller paper in English translation, see: *Collected Papers of L. D. Landau*, Ter Haar, D., Ed.; Gordon and Breach: New York, 1965; p 147.
(259) The SSH theory was developed independently by K. Takayanagi. An excellent historical discussion of the work leading up to SSH theory, and the shortcomings of the theory, may be found in ref 245.
(260) See, for example: Widom, B. *Faraday Discuss. Chem. Soc.* **1962**, *33*, 37.
(261) Kelley, J. D.; Wolfsberg, M. *J. Chem. Phys.* **1966**, *44*, 324.
(262) Secrest, D.; Johnson, B. R. *J. Chem. Phys.* **1966**, *45*, 4556.
(263) Secrest, D. *J. Chem. Phys.* **1969**, *51*, 421.
(264) Roberts, R. E.; Diestler, D. J. *J. Chem. Phys.* **1972**, *56*, 2482.
(265) See Figure 4 of ref 261.
(266) For a very recent model study of collinear AB + CD collisions, see: Page, M.; Oran, E. S.; Boris, J. P.; Miller, D.; Wyatt, R. E.; Rabitz, H.; Waite, B. A. *J. Chem. Phys.* **1985**, *83*, 5635.
(267) Secrest, D. *Annu. Rev. Phys. Chem.* **1973**, *24*, 379.
(268) Faubel, M.; Toennies, J. P. *Chem. Phys.* **1974**, *4*, 36.
(269) Schinke, R.; Toennies, J. P. *J. Chem. Phys.* **1975**, *62*, 4871.
(270) Scherzinger, A. L.; Secrest, D. *J. Chem. Phys.* **1980**, *73*, 1706.
(271) Nesbitt, D. J.; Hynes, J. T. *J. Chem. Phys.* **1982**, *76*, 6002.
(272) Ramaswamy, R.; Bhargava, R. *J. Chem. Phys.* **1984**, *80*, 1095.
(273) Noid, D. W.; Koszykowski, M. L. *Chem. Phys. Lett.* **1981**, *79*, 485.
(274) Nalewajski, R. F.; Wyatt, R. E. *Chem. Phys.* **1983**, *81*, 357.
(275) Ramaswamy, R. *Chem. Phys.* **1984**, *88*, 17.
(276) Russell, T. D.; DeKoven, B. M.; Blazy, J. A.; Levy, D. H. *J. Chem. Phys.* **1980**, *72*, 3001.
(277) Sulkes, M.; Tusa, J.; Rice, S. A. *J. Chem. Phys.* **1980**, *72*, 5733.
(278) Baba, H.; Sakurai, K. *J. Chem. Phys.* **1985**, *82*, 4977.
(279) See, for example: (a) Abuaf, N.; Anderson, J. B.; Andres, R. P.; Fenn, J. B.; Marsen, D. G. H. *Science* **1967**, *155*, 997. (b) Anderson, J. B. In *Molecular Beams and Low Density Gasdynamics*, Wegener, P. P., Ed.; Marcel Dekker: New York, 1974.
(280) The issue of mass separation, or "heavy particle focusing", in free jet expansions of gas mixtures has been a matter of some debate. See, for example: (a) Reis, V. H.; Fenn, J. B. *J. Chem. Phys.* **1963**, *39*, 3240. (b) Sherman, F. S. *Phys. Fluids* 1965 *8*, 773. See also ref 279b.
(281) Kolodney, E.; Amirav, A. *Chem. Phys.* **1983**, *82*, 269.
(282) For a review of both the theory and the experimental determination of resonances in the scattering of atoms and molecules, see: (a) Toennies, J. P.; *Adv. At. Mol. Phys.* **1979**, *8*, 137. (b) Toennies, J. P.; Welz, W.; Wolf, G. *J. Chem. Phys.* **1979**, *71*, 614. (See if you can find two little men hiding in one of the figures of the latter paper.)
(283) Sethuraman, V.; Rice, S. A. *J. Phys. Chem.* **1981**, *85*, 3187.
(284) Villarreal, P.; Delgado-Barrio, G.; Mareca, P. *J. Chem. Phys.* **1982**, *76*, 4445.
(285) Cerjan, C.; Rice, S. A. *J. Chem. Phys.* **1983**, *78*, 4952.
(286) Rice, S. A.; Cerjan, C. *Laser Chem.* **1983**, *2*, 137.
(287) Gray, S. K.; Rice, S. A. *J. Chem. Phys.* **1985**, *83*, 2818.
(288) Ewing, G. *Chem. Phys.* **1978**, *29*, 253.
(289) Gentry, W. R. *J. Chem. Phys.* **1984**, *81*, 5737.
(290) (a) Jouvet, C.; Sulkes, M.; Rice, S. A. *J. Chem. Phys.* **1983**, *78*, 3935. (b) Sulkes, M.; Jouvet, C.; Rice, S. A. *Chem. Phys. Lett.* **1982**, *93*, 1.
(291) Tusa, J.; Sulkes, M.; Rice, S. A.; Jouvet, C. *J. Chem. Phys.* **1982**, *76*, 3513.
(292) Moss, D. B.; Kable, S. H.; Knight, A. E. W. *J. Chem. Phys.* **1983**, *79*, 2869.
(293) Bernstein, E. R.; Law, K.; Schauer, M. *J. Chem. Phys.* **1984**, *80*, 207; *Ibid.* **1984**, *80*, 634.